University of Kentucky

UKnowledge

Theses and Dissertations--Molecular and
Cellular Biochemistry

Molecular and Cellular Biochemistry

2013

HETEROGENEITY IN PLATELET EXOCYTOSIS

Deepa Jonnalagadda
University of Kentucky, DJONN2@uky.edu

Right click to open a feedback form in a new tab to let us know how this document benefits you.

STUDENT AGREEMENT:

I represent that my thesis or dissertation and abstract are my original work. Proper attribution has been given to all outside sources. I understand that I am solely responsible for obtaining any needed copyright permissions. I have obtained and attached hereto needed written permission statements(s) from the owner(s) of each third-party copyrighted matter to be included in my work, allowing electronic distribution (if such use is not permitted by the fair use doctrine).

I hereby grant to The University of Kentucky and its agents the non-exclusive license to archive and make accessible my work in whole or in part in all forms of media, now or hereafter known. I agree that the document mentioned above may be made available immediately for worldwide access unless a preapproved embargo applies.

I retain all other ownership rights to the copyright of my work. I also retain the right to use in future works (such as articles or books) all or part of my work. I understand that I am free to register the copyright to my work.

REVIEW, APPROVAL AND ACCEPTANCE

The document mentioned above has been reviewed and accepted by the student's advisor, on behalf of the advisory committee, and by the Director of Graduate Studies (DGS), on behalf of the program; we verify that this is the final, approved version of the student's dissertation including all changes required by the advisory committee. The undersigned agree to abide by the statements above.

Deepa Jonnalagadda, Student

Dr. Sidney W. Whiteheart, Major Professor

Dr. Michael Mendenhall, Director of Graduate Studies

HETEROGENEITY IN PLATELET EXOCYTOSIS

DISSERTATION

A dissertation submitted in partial fulfillment of the requirements for the degree of
Doctor of Philosophy in the College of Medicine at the University of Kentucky

By
Deepa Jonnalagadda

Lexington, Kentucky

Director: Dr. Sidney W. Whiteheart, Professor of Molecular and Cellular Biochemistry

Lexington, Kentucky

2013

HETEROGENEITY IN PLATELET EXOCYTOSIS

DISSERTATION

A dissertation submitted in partial fulfillment of the requirements for the degree of Doctor of Philosophy in the College of Medicine at the University of Kentucky

By
Deepa Jonnalagadda

Lexington, Kentucky

Director: Dr. Sidney W. Whiteheart, Professor of Molecular and Cellular Biochemistry

Lexington, Kentucky

2013

ABSTRACT OF DISSERTATION

HETEROGENEITY IN PLATELET EXOCYTOSIS

Platelet exocytosis is essential for hemostasis and for many of its *sequelae*. Platelets release numerous bioactive molecules stored in their granules enabling them to exert a wide range of effects on the vascular microenvironment. Are these granule cargo released thematically in a context-specific pattern or *via* a stochastic, kinetically-controlled process? My work describes platelet exocytosis using a systematic examination of platelet secretion kinetics. Platelets were stimulated for increasing times with different agonists (*i.e.* thrombin, PAR1-agonist, PAR4-agonist, and convulxin) and micro-ELISA arrays were used to quantify the release of 28 distinct α-granule cargo molecules. Agonist potency directly correlated with the speed and extent of release. PAR4-agonist induced slower release of fewer molecules while thrombin rapidly induced the greatest release. Cargo with opposing actions (*e.g.* pro- and anti-angiogenic) had similar release profiles, suggesting limited thematic response to specific agonists. From the release time-course data, rate constants were calculated and used to probe for underlying patterns. Probability density function and operator variance analyses were consistent with three classes of release events, differing in their rates. The distribution of cargo into these three classes was heterogeneous suggesting that platelet secretion is a stochastic process potentially controlled by several factors such as cargo solubility, granule shape, and/or granule-plasma membrane fusion routes.

Sphingosine 1 phosphate (S1P) is a bioactive lipid that is stored in platelets. S1P is essential for embryonic development, vascular integrity, and inflammation. Platelets are an abundant source of S1P due to the absence of the enzymes that degrade it. Platelets release S1P upon stimulation. My work attempts to determine how this bioactive lipid is released from platelets. Washed platelets were stimulated with agonists for defined periods of time and the supernatant and pellet fractions were separated by centrifugation. Lipids were separated by liquid phase extraction and S1P was quantified with a triple quadrapole mass spectrometer. A carrier molecule (BSA) is

required to detect release of S1P. Further, there is a dose-dependent increase in total S1P with increasing BSA. S1P release shows characteristics similar to other platelet granule cargo *e.g.* platelet factor IV (PF4). Platelets from *Unc13-d* ^{Jinx} mice and VAMP8$^{-/-}$ mice, which are secretion-deficient (dense granule, alpha granule and lysosome), were utilized to understand the process of S1P release. S1P release was more affected in *Unc13-d* ^{Jinx} mice mirroring their dense granule secretion defect. Fluorescence microscopy and sub-cellular fractionation were used to examine localization of S1P in platelets. S1P was observed to be enriched in a granule population. These studies indicate the existence of two pools of S1P, a readily extractable agranular pool, sensitive to BSA, and a granular pool that requires the secretion machinery for release. The secretion machinery of platelets in addition to being involved in the release of normal granule cargo is thus proved to be involved in the release of bioactive lipid molecules like S1P.

KEYWORDS: Platelet Exocytosis, Agonist-Potency, Micro-ELISA arrays, S1P, BSA

Deepa Jonnalagadda

_____

04/30/2013

_____

HETEROGENEITY IN PLATELET EXOCYTOSIS

By

Deepa Jonnalagadda

<u>Dr. Sidney W. Whiteheart</u>

Director of Dissertation

<u>Dr. Michael Mendenhall</u>

Director of Graduate Studies

<u>04/30/2013</u>

To my parents

ACKNOWLEDGEMENTS

I would start my long list of acknowledgements by thanking my parents for their unconditional love and support in raising me into what I am today. If not for my mentor, Dr. Sidney W. Whiteheart, I could not imagine myself completing this pre-doctoral training program successfully. I joined his research group envisioning a challenging yet, ambient environment for my graduate career. Major part of my thesis entailed mathematical modeling. Dealing with such subject by a person trained as a Biochemist is certainly challenging. I did not fear these new concepts being introduced, but was enthusiastic in knowing them and I'm positive that this was possible only due to encouraging atmosphere in the laboratory. Both of my aforementioned goals for my graduate career were already fulfilled. In spite of a terrible unexpected car accident that disturbed my life, my mentor's support and encouragement helped me believe that I am doing okay. Designing a good experiment and being a good scientist are the two things I attempted to learn from him. The second part of my thesis stood as an example for this. He encouraged me to pursue future research in my field of interest. Many of my friends are envious of me having such an intelligent, kind and reasonable human being as my mentor. It is certainly a sign of me being fortunate. I owe him my successful and peaceful graduate training, so I thank him a ton. Not to make him sound old, but he is a father-like figure to me.

Dr. Matveeva (Elena), originally from Russia, was very organized, helpful, encouraging and above all, she was always concerned of my well-being. Dr. Qiensheng Ren (Jason), a past member of the Whiteheart lab has been my teacher following my mentor. He was very helpful and encouraging. I was also fortunate to have him as my bench-mate. I used to enjoy all the scientific conversations we had. Also, he donated blood for most of my experiments. Dr. Michael C. Chicka (Mike), another past member, helped me train in protein work. Even though, this piece of work was not successful and did not end up in my thesis, this phase of my graduate training allowed me to learn planning a meaningful experiment. Not only did he enjoy the Indian accent that I had but also used to teach me the slang used here. Dr. Choi (Wangsun) is a former Korean member of our lab. He was a clear scientific thinker and a good organizer. I enjoyed the lunch time, as people used to share the table with him and he used to speak about a new entertaining topic daily. Dr. Zhao (Chunxia) has been very helpful and encouraging irrespective of her leaving the lab for a post-doc position after graduation. Both Jason and Chunxia were from China. Dr. Al-Hawas (Rania) helped me maintain my spirits high all through and have always enjoyed her bubbly personality. I thank all of them, who are geographically from five different parts of the world to expose me to different cultures and could learn at least one good quality from each of them, if not more.

Table of Contents

LIST OF TABLES

LIST OF FIGURES

Chapter One

Introduction

Platelet overview

Platelets are natural band-aids circulating in the blood stream forming hemostatic plug to stop bleeding upon vascular injury. They are 2.0-5.0 μm in diameter, discoid, anucleate cells, at 150-400 × 10^9 per liter of whole blood, and surviving for 7-10 days. Electron-dense, dense granules, mostly peptide/protein rich alpha (α-) granules, acid hydrolase-rich lysosomes, mitochondria and peroxisomes constitute the most obvious organelles of platelets. A closed calcium rich network, dense tubular system (DTS), invaginations of surface plasma membrane referred to as open canalicular system (OCS), spectrin membrane cytoskeleton, actin cytoskeleton and peripheral microtubules complete the structural entities of platelets (**Figure. 1.1**).

Accumulating evidence suggests that platelet functions are not restricted to maintain hemostasis but are potentially important for inflammation, angiogenesis, and maintenance of vascular permeability barrier (*Ho-Tin-Noé et al.*, 2011). Recruitment of fewer leukocytes to the inflamed organs in thrombocytopenic mice provided the first mechanistic clue for the involvement of platelets in exacerbating inflammation (*Devi et al.*, 2010; *Iannacone et al.*, 2008; *Kuligowski et al.*, 2006). Regulation of tumor angiogenesis by platelets is not surprising given the presence of both pro- and anti-angiogenic factors in α-granules of platelets (*Pinedo et al.*, 1998). The importance of platelets in the maintenance of the vascular permeability barrier has been appreciated for quite some time. Excessive leakage of radiolabelled albumin into the lungs and ears of experimentally induced thrombocytopenic sheep (*Lo et al.*, 1988) and rabbits (*Aursnes*, 1974) provides evidence. Thrombocytopenic mice though do not show spontaneous bleeding, but are more susceptible to vascular injury upon a localized inflammatory stimulation (*Goerge et al.*, 2008), further supporting a role for platelets as vascular guardians (*Ho-Tin-Noé et al.*, 2011). The pleiotropic functions of platelets are

1

enabled by the secretion of hundreds of granule cargo molecules. Therefore, understanding the mode of platelet secretion is important and significant.

The origin of platelets in circulation from megakaryocytes (MKs) and the overall importance of platelet secretion in health and disease are highlighted in this chapter. Platelet activation and the exocytotic machinery involved in platelet secretion are also discussed. Additionally, this chapter also provides a summary of the present knowledge on an important bioactive sphingolipid, S1P, which is stored in platelets and released upon activation. The following commentary aims to synopsize the accruing roles of platelet secretion.

Platelet biogenesis

Platelets are generated from MKs, which are 30-100 μm in diameter. These are myeloid cells constituting less than 0.1% of total bone marrow cell population. MKs undergo multiple rounds of mitosis without cell division; a process called endomitosis which yields a multinucleate structure. The production of proteins and lipids is proportional to their ploidy. During maturation, MKs migrate from the osteoblastic niche to the vascular niche, a region proximal to the blood vessels of bone marrow cavity. Long branching processes emanate from them, called pro-platelets and continue to mature in the vasculature, eventually releasing individual platelets (*Italiano et al.*, 1999).

Commitment of stem cells of megakaryocytic lineage, proliferation of the progenitors, and final differentiation of MKs lead to the formation of platelets. The megakaryocytic lineage arises from a common erythrocyte-MK progenitor derived from a common myeloid progenitor in the bone marrow. The proliferating diploid MK progenitors retain the capacity to duplicate DNA and form new cytoplasm, even though they lose their ability to divide. MK maturation results in the formation of megakaryoblast which ranges < 50-100 μm in cell size with a ploidy up to 128N (*Tomer et al.*, 1987; *Tomer et al.*, 1988). With an increased nucleus to cytoplasm ratio these structures do have all the organelles that are eventually seen in an individual platelet. As the maturation process progresses, the polyploid nucleus acquires horse-shoe shape;

the cytoplasm, the demarcation membrane system expand and, the platelet organelles increase in number. This is followed by the formation of pro-platelet projections that finally result in 2000-5000 platelets per megakaryocyte (*Deutsch and Tomer*, 2006; *Italiano et al.*, 1999; *Italiano and Shivdasani*, 2003; *Long*, 1998).

Platelet activation

Platelets in circulation are maintained in a quiescent state by 'passivators' like nitric oxide (NO) and prostaglandin I_2 (PGI$_2$). The premature activation of platelets is prevented by intact endothelial cell monolayer which enables concealment of potential platelet agonists like collagen and von Willebrand Factor (vWF). This is also achieved by restricted accumulation of platelet stimulators like thrombin, ADP, thromboxane A_2 (TxA$_2$) and epinephrine (*Brass*, 2003). This is the first indication for platelet activation to be a highly regulated process. To release their granular contents, platelets must be activated. This occurs upon a vascular disturbance – injury, trauma, rupture of a plaque – conditions that disrupt the vascular barrier resulting in local generation of thrombin and/or exposure of collagen. The role played by NO and PGI$_2$ in maintaining platelets in a resting state in circulation is incumbent upon their ability to maintain high cyclic nucleotide levels (cAMP or cGMP). The importance of PGI$_2$ and NO is not only indicated by PGI$_2$ mimetics, acting as anti-platelet agents but also, by pro-thrombotic effects seen in platelet specific PGI$_2$ receptor null mice (*Murata et al.*, 1997).

Platelet plug formation upon sensing a vascular injury occurs in three stages – initiation, extension and perpetuation (*Brass*, 2003). Initiation phase includes the events that culminate in the formation of focal point for the formation of platelet plug. Platelets in circulation roll onto the ruptured vascular endothelial layer with exposed collagen. The brake in the movement of platelets is potentiated by the interaction of GPVI receptors present on platelet surface and collagen. This further leads to clustering of GPVI receptors on the platelet surface ultimately leading to the mobilization of intracellular calcium ($[Ca^{2+}]_i$) pools by the activation of PLCγ2. These events lead to the successful formation of platelet monolayer. The extension phase relies on the presence

of platelet surface receptors which can bind to accumulating soluble agonists like thrombin, ADP and TxA$_2$. This facilitates recruitment and lodging of more platelets even without direct contact with collagen. The interplatelet contacts in this phase are mediated by the activated α$_{IIb}$β$_3$. Perpetuation phase includes the events that maintain the platelet plug preventing premature disaggregation.

Platelet activation is mediated by an array of cell surface receptors that sense components produced at the site of vascular damage. Thrombin is a serine protease that acts through PAR family receptors – PAR1/3/4 (*Coughlin et al.*, 1992). The structure of PARs is similar to other G-Protein-Coupled Receptors (GPCRs). Thrombin acts on PARs, cleaving their N-termini, resulting in the exposure of a new N-terminus (SFLLRN for PAR1 and AYPGKF for PAR4) that acts as a tethered ligand (*Chen et al.*, 1994; *Vu et al.*, 1991). This imparts a very high local concentration of ligand to bind to its receptor, and thus thrombin is one of the potent platelet agonists. PAR1 is more immediately responsive to thrombin at low concentrations, while PAR4 requires 10-100 fold more and is probably responsible for the sustained activation of platelets (*Covic et al.*, 2000; *Shapiro et al.*, 2000). The distribution of PARs on platelets varies across species. PAR1 and PAR4 are expressed on human platelets (*Kahn et al.*, 1999), while PAR3 and PAR4 are present on mouse platelets. TxA$_2$ through TP receptor and ADP through P$_2$Y$_1$ receptor – result in increasing [Ca^{2+}]$_i$ levels by activating G$_q$ (*Offermanns et al.*, 1997). ADP receptor P$_2$Y$_{12}$ and epinephrine receptor α$_{2A}$ act through Gi$_2$ (*Yang et al.*, 2002) or G$_z$ (*Yang et al.*, 2000) to inhibit adenylyl cyclase and, to activate PI3K and a Ras family member, RapI (*Woulfe et al.*, 2002). The importance of ADP-Gi$_2$ coupled P$_2$Y$_{12}$ receptor is confirmed by the phenotypes of the receptor knockout mice and the effectiveness of P$_2$Y$_{12}$ antagonists, clopidogrel and ticlopidine (*Foster et al.*, 2001; *Hollopeter et al.*, 2001; *Jantzen et al.*, 2001). Irrespective of the receptor type, an activated platelet typically exhibits increase in [Ca^{2+}]$_i$. This is an important trigger for platelet exocytosis. PARs and TP receptors by coupling guanine nucleotide exchange factors with Rho, can also result in cytoskeletal rearrangements responsible for platelet shape change and potentially secretion (*Offermanns et al.*, 1994).

Platelet granules

Platelets broadly have three distinct types of granules – dense granules, α-granules and lysosomes. The salient features of each kind of granule are described here.

Dense granules

The dense granules are 250 nm, electron dense structures, first identified from electron micrographs. There are typically three to eight dense granules per normal human platelet (*Israels et al.*, 1990; *White*, 1968). Their relatively acidic internal pH is maintained by a H^+ pumping ATPase located on the granule membrane (*Carty et al.*, 1981). Dense granules contain some P-selectin (*Israels et al.*, 1992) which was initially identified as α-granule protein (*Stenberg et al.*, 1985), is essential for platelet-leukocyte interaction. Similarly CD63 and LAMP2 originally identified as components of lysosomal granule membrane are also present on the dense granule membrane (*Metzelaar and Nieuwenhuis*, 1991, Silverstein, 1992 #42). The origin of various granule types from MKs *via* multi vesicular bodies (MVBs) is therefore thought to be defined by the specific distribution of contents.

These granules house a number of bioactive small molecules such as serotonin, catecholamine, calcium, a non-metabolic pool of ADP and ATP and, pyrophosphate (*Holmsen and Weiss*, 1979). Serotonin, though not synthesized by platelets, is taken up from plasma and stored in dense granules where it is complexed with ATP or calcium (*De Clerck et al.*, 1984). Upon platelet activation serotonin is released from dense granules and recruits more platelets to form an aggregate (*Gerrard*, 1988). Serotonin limits the blood flow at the injury site by vasoconstriction, thus controlling the blood loss (*De Clerck et al.*, 1984). Calcium and polyphosphates stored in dense granules constitute 60-70% of total calcium stored in platelets and are likely responsible for the electron density seen in EM (*Holmsen and Weiss*, 1979; *White*, 1969). Hemansky-Pudlak syndrome (HPS) and Chediak-Higashi syndrome (CHS) are genetic, dense granule storage pool disorders (SPDs) which will be discussed further in the later section.

Alpha granules

Alpha (α-) granules form the major granule population in platelets, ranging from 200-500 nm in size and 40-80 per platelet. Immunogold electron microscopy studies of MKs suggest the development of α-granules and MVBs from budding vesicles off the Golgi (*Blair and Flaumenhaft*, 2009; *Heijnen et al.*, 1998; *Jones*, 1960). The studies by *Heijnen et al.* have shown that there are two kinds of MVBs – type I, which have only internal vesicles and type II, which have both internal vesicles and an electron dense matrix (*Blair and Flaumenhaft*, 2009; *Heijnen et al.*, 1998). MVBs form an intermediate stage not only in the formation of α-granules (*Heijnen et al.*, 1998) but also, dense granules (*Nishibori et al.*, 1993). This conclusion is based on the presence of lysosomal/dense granule protein, CD63 also on MVBs (*Nishibori et al.*, 1993).

There are hundreds of stored peptides and proteins (*Qureshi et al.*, 2009) which differ in their origin. The stored cargo can either be synthesized by the megakaryocyte (*e.g.* vWF, platelet factor 4 (PF4) and β-thromboglobulin (β-TG)), *de novo* synthesized in the platelet (*e.g.* IL8). Some α-granule cargo (*e.g.* fibrinogen and Factor V) are not made by megakaryocytes but are thought to be endocytosed by circulating platelets (*Louache et al.*, 1991). They are then transported to α-granules (*Harrison et al.*, 1989; *Heijnen et al.*, 1998). α-Granules contain hemostatic factors (*e.g.* Factor V, fibrinogen), angiogenic factors (*e.g.* angiogenin, VEGF), anti-angiogenic factors (*e.g.* angiostatin, PF4), growth factors (*e.g.* PDGF, SDF1α), proteases (*e.g.* MMP2, MMP9), necrosis factors (*e.g.* TNFα, TNFβ) and other cytokines (*Coppinger et al.*, 2004). Around 30 angiogenesis regulators have been identified to be stored in platelets and are reported to be distributed to different subclasses of α-granules depending on their biological function (*Italiano et al.*, 2008). Membrane proteins important for platelet function, like $α_{IIb}β_3$ (*Coller et al.*, 1991), CD62P (P-selectin) and CD36 (*Blair and Flaumenhaft*, 2009) are present in α-granule membranes. Patients with Gray Platelet Syndrome (GPS) lack recognizable α-granules and presumably have a defect in their biosynthesis (*Mori et al.*, 1984). GPS represents α-granule defect in platelets and is discussed in detail later.

Lysosomes

Lysosomes constitute a sparse granule type in platelets (0-1 per platelet), and they appear similar to α-granules in electron micrographs. Lysosomes store cathepsins, carboxypeptidases, β-hexosaminidase, acid phosphatases, enzymes for hydrolyzing various sugars and aryl sulfatases (*McNicol and Israels*, 1999; *Thon and Italiano*, 2012). CD63 and LAMP2 serve as markers for lysosomes. Apart from platelets, secretory lysosomes are also found in other hematopoietic cells like neutrophils, eosinophils, mast cells, macrophages, and cytotoxic T lymphocytes (CTLs) (*Andrews*, 2000). Though the exact function of lysosomes in platelets is not known, they are thought to be involved in clot remodeling. CHS, Griscelli syndrome, and HPS are some of the autosomal recessive disorders that exhibit impaired lysosomal biogenesis and exocytosis. These are further described in the following section.

Platelet defects

The complications associated with platelet defects result in mild to severe bleeding. They can be related to a defect in one of the receptors required for platelet activation, or defective platelet biogenesis, or related to impaired cytoskeletal changes. Some of such defects are discussed below.

Platelet biogenetic defects

These are the defects that result in the production of morphologically abnormal platelets. Bernard-Soulier syndrome (BSS), MYH9 related disorders (MYH9RD) and GPS – the common characteristic associated with all these disorders is macrothrombocytopenia (decreased platelet number with increased platelet volume) (*Patel et al.*, 2005). BSS is autosomal dominant disorder with increased bleeding time and impaired platelet aggregation. Deficiency or absence of glycoprotein GP-Ib/IX/V, which is a receptor for vWF, is responsible for this disorder (*Balduini et al.*, 2002). MYH9 related disorders have a defect in MYH9 gene which encodes for myosin heavy chain. Though a defect in GP-Ib/IX/V has been reported, this disorder causes cytoskeletal rearrangement anomalies upon platelet activation (*Franke et al.*, 2005). GPS is another

autosomal dominant disorder which in addition to macrothrombocytopenia has a defect in the production of α-granules. Granule contents leak from most of the organelles during platelet development in MK leaving behind the empty α-granule vacuoles, which are later on filled with cytoplasm of circulating platelets (*Cramer et al.*, 1985; *Stenberg et al.*, 1998).

Dense granule SPDs

These disorders appear due to congenital deficiency of dense granules and present as a moderate bleeding diathesis, manifested in a minority population as a more severe life-threatening bleeding disorder. HPS (*Hermansky and PUDLAK*, 1959) and CHS (*Higashi*, 1954), both autosomal recessive disorders characterized by hypopigmentation, are representative of numerous dense granule SPDs. HPS patients have profound dense granule deficiency and severe mucocutaneous bleeding and postoperative bleeding necessitating repeated red cell and platelet transfusions (*Gahl et al.*, 1998). *HPS1, AP3B1, HPS3-6, DTNBP1, BLOC1S3, BLOC1S6* genes (*Masliah-Planchon et al.*, 2013) have been identified to contribute to HPS (*Di Pietro and Dell'Angelica*, 2005; *Gunay-Aygun et al.*, 2004; *Li et al.*, 2004). Many of these gene products make up the sorting complexes that mediate the transfer of molecules to the granules. Histological analyses on CHS patients reveal gigantic inclusion bodies in leukocytes, lysosomes and melanosomes in melanocytes. While their platelets lack these abnormal granules, they also lack dense granules (*White and Gerrard*, 1976).

α-Granule SPDs

GPS is an inherited α-granule formation disorder (*Nurden and Nurden*, 2007). Patients with GPS exhibit moderate but, progressive thrombocytopenia (*Nurden and Nurden*, 2011). The defective gene reported to be responsible for this disorder has been localized to chromosome 3p (*Fabbro et al.*, 2011). Moreover, mutation in *Hzf*, a zinc finger transcription factor, results in the normal number of megakaryocytes and platelets, but with reduced number of α-granules in platelets, mimicking GPS in *Hzf* [-/-] mice (*Kimura et al.*, 2002). Two proteins have been identified to be important for α-

granule biogenesis: BEACH domain containing protein (NBEAL2 – deficient in GPS patients) (*Gunay-Aygun et al.*, 2011; *Kahr et al.*, 2011) and Sec1/Munc18 protein (VPS33B – deficient in arthrogryposis-renal dysfunction-cholestasis (ARC) syndrome patients) (*Gissen et al.*, 2004; *Lo et al.*, 2005). Though the mechanism of action of NBEAL2 is unknown, VPS33B has been shown to facilitate membrane docking and fusion during vesicle trafficking and α-granule formation (*Lo et al.*, 2005). Loss of VPS33B, at least in humans (but not in mice, *unpublished communication*), is responsible for a defect in incorporation of endogenous and endocytosed proteins in α-granules of platelets (*Lo et al.*, 2005).

Platelet exocytosis machinery

Activated platelets release their granular contents into the extra-platelet space by fusion of the granular membrane with the plasma membrane. This is facilitated by the machinery that was initially identified in neurons (*Sollner et al.*, 1993). It includes vesicle-soluble N-ethylmaleimide sensitive fusion proteins (v-SNAREs), target-SNAREs (t-SNAREs) and a number of regulatory proteins. The minimal requirement for fusion is the pairing of cognate v- and heterodimeric/trimeric t-SNAREs to form a transmembrane fusion complex (*Weber et al.*, 1998). v-SNAREs (also known as Vesicle Associated Membrane Proteins, VAMPs) are type II membrane proteins characterized by a 60-70 amino acid conserved SNARE motif and a transmembrane domain (*Jahn and Südhof*, 1999). t-SNAREs are of two types – syntaxin type and synaptosomal-associated protein type (SNAP type). Syntaxins are type II integral membrane proteins with a characteristic SNARE motif and an N-terminal regulatory domain (*Dietrich et al.*, 2003). SNAP-23/25 family members contain two SNARE motifs and lack transmembrane domains. They are anchored to the membrane by thioester-linked acyl groups (*Dietrich et al.*, 2003). Platelets (human and mouse) contain VAMP-2 (synaptobrevin), VAMP-3 (cellubrevin), VAMP-5 (*Burkhart et al.*, 2012), VAMP-7 (TI-VAMP), and VAMP-8 (endobrevin) (*Bernstein and Whiteheart*, 1999; *Polgár et al.*, 2002; *Ren et al.*, 2007; *Schraw et al.*, 2003). Human platelets contain syntaxins - 1, 2, 4, 6, 7, 8, and 11 (*Burkhart et al.*, 2012; *Chen et al.*, 2000a; *Chen et al.*, 2000b; *Coppinger et al.*, 2004; *Lemons et al.*, 1997; *Lemons et al.*,

2000), SNAP-23 (*Flaumenhaft et al.*, 1999), SNAP-29 (*Polgár et al.*, 2003), and SNAP-25 (*Redondo et al.*, 2004). The representative SNAREs found in platelets leading to exocytosis are represented in the **Figure 1.2**. The conserved SNARE motifs form a coiled-coil, four-helix bundle that is stabilized by the core hydrophobic interactions (*Sutton et al.*, 1998). The complex is sufficient to mediate membrane fusion in proteoliposomes (*Weber et al.*, 1998).

Tetanus toxin, a neurotoxin, is a heterodimeric zinc-dependent endopeptidase specific for VAMP-1/2/3 (*Schiavo et al.*, 2000). Initial studies of v-SNAREs in platelets utilized this toxin and showed that α-granule release was inhibited (*Flaumenhaft et al.*, 1999). α-Granule secretion was also affected when antibody directed against the N-terminus of VAMP-3 was added to permeabilized platelets (*Feng et al.*, 2002). The results obtained in the previous studies did not correlate with the lack of secretion defect in VAMP-3$^{-/-}$ mice (*Schraw et al.*, 2003). Subsequent studies demonstrated that VAMP-8 is the primary v-SNARE in mouse platelets (*Ren et al.*, 2007). Secretion defects were not seen in VAMP-3$^{-/-}$, VAMP-2$^{+/-}$/VAMP-3$^{-/-}$ and VAMP-2$^{+/-}$ platelets and were only evident in VAMP-8$^{-/-}$ platelets, though not complete. The secretion defect is more pronounced in α-granule and lysosomal release when compared to dense granule release. Moreover, VAMP-8 independent release could be abolished by treating permeabilized VAMP-8$^{-/-}$ platelets with tetanus toxin, alluding to the fact that VAMP-2 and -3 constitute a secondary, albeit less efficient, secretion machinery.

Among t-SNAREs, syntaxin-2 and SNAP-23 have been shown to be involved in the release of all three granules using anti-SNARE antibodies in permeabilized platelets (*Chen et al.*, 2000a; *Chen et al.*, 1994; *Lemons et al.*, 2000). Syntaxin-4 was associated with α-granule (*Flaumenhaft et al.*, 1999) and lysosomal release (*Chen et al.*, 2000a). However, platelets from syntaxin-2 and -4, single or double knockout mice did not display any release defect. The platelets from Familial Hemophagocytic Lymphohistiocytosis type 4 (FHL4) patient, lacking syntaxin-11, had a severe secretion defect. This demonstrates that syntaxin-11 is the essential syntaxin in platelets.

Consistently, it was found to co-immunoprecipitate with VAMP-8 and SNAP-23 (*Ye et al.*, 2012). Taken together, it now appears that secretion from all three granules, dense, alpha, and lysosomal, is mediated by the same core secretory machinery elements, VAMP-8, SNAP-23, and syntaxin-11.

SNARE regulatory proteins dictate how, when and where SNARE complexes are formed to drive the fusion process. Our lab has identified three regulatory proteins Munc 13-4 (*Ren et al.*, 2010), Munc 18b (*Al Hawas et al.*, 2012) and tomosyn (*Ye et al., unpublished*) that play an important role in platelet secretion. *Unc13d* ^{Jinx} mice have a deficiency in an important priming factor for secretion, Munc 13-4 and display a severe dense granule secretion defect. α-Granule and lysosomal secretion was also severely compromised. Rab27, which is thought to be required for both dense granule biogenesis and exocytosis is also a Munc 13-4 binding protein (*Shirakawa et al.*, 2005). Munc 18b and tomosyn were initially identified due to their association with syntaxin-containing complexes. Munc 18 proteins chaperone the syntaxins and are found associated with the t-SNARE heterodimers and SNARE complexes (*Carr and Rizo*, 2010). The regulatory proteins reported to be associated with syntaxins/SNARE machinery are Munc 18b and tomosyn. Of the three isoforms of Munc 18 in platelets, Munc 18a/b/c, Munc 18b appears to be critical and platelets from FHL5 patients (lacking Munc 18b) have a severe platelet secretion defect (*Al Hawas et al.*, 2012). Platelet secretion deficiency was evident in all three granule types with Munc 18b deficiency. Tomosyn was thought to be a negative regulator that binds to t-SNARE heterodimers and control v-SNARE binding. Tomosyn was first identified in platelets in pull-down experiments using syntaxin/SNAP-23 complex as bait. Tomosyn deficient mouse platelets have a more pronounced α-granule and lysosomal secretion defect and a severe bleeding diathesis (*Ye et al., unpublished*). At this stage there are other elements of secretory machinery that are yet to be characterized. Platelets contain double C2 domain containing proteins (DOC2) and synaptotagmin-like proteins (SLP) whose functions are yet to be fully defined.

Platelet α-granule secretion-in health and disease

The more conventional role for platelets is in hemostasis. With more than 300 proteins known to constitute platelet secretome (*Maynard et al.*, 2007) (proteins thought to be released from α-granules), there is an increasing evidence that platelets can play a number of roles in the vasculature.

Hemostasis

α-Granules house a number of adhesive proteins like fibrinogen and vWF which mediate interplatelet and platelet-endothelial interactions. The adhesive receptors responsible for platelet adhesion are found in α-granules *viz.,* member of vWF receptor complex, GP Ibα-IX-V (*Berger et al.*, 1996), fibrinogen receptor, $\alpha_{IIb}\beta_3$ (*Niiya et al.*, 1987) and collagen receptor, GPVI (*Suzuki et al.*, 2003). They are constitutively expressed on the platelet surface. One-half to two-thirds of the total $\alpha_{IIb}\beta_3$ and one-third of the total GPVI population reside in the α-granule membrane (*Niiya et al.*, 1987; *Nurden et al.*, 2004; *Suzuki et al.*, 2003). This population contributes to an increase in their surface distribution upon stimulation. Coagulation factors like Factor V (*Hayward et al.*, 1995), XI (*Hu et al.*, 1998) and XIII (*Kiesselbach and Wagner*, 1972) are stored in platelet α-granules. Factor V is endocytosed from the plasma while the other two are synthesized in the megakaryocytes. Moreover, α-granules also store pro-thrombin (an inactive precursor of thrombin) and a number of proteins required for intrinsic clotting cascade. They have a number of protease inhibitors like plasminogen activation inhibitor-1 (PAI-1) and α_2-antiplasmin which inhibit plasmin mediated fibrinolysis (*Rendu and Brohard-Bohn*, 2001). All the enlisted entities stored in α-granules contribute to coagulation cascade demonstrating the importance of α-granules in the maintenance of hemostasis (*Nurden and Nurden*, 2007).

Inflammation

The receptors required for platelets to bind to other cell types such as endothelial cells, leukocytes, monocytes and lymphocytes, and the storage and release of inflammatory cytokines suggest a role for platelets in inflammation (*May et al.*, 2008).

Although the contribution of proteins like vWF and fibrinogen are important in establishing the interplatelet and platelet-endothelial cross-bridges, it is difficult to define the specific contribution of the platelet-derived pools. P-selectin participates in establishing interactions between platelets and endothelial cells / monocytes / lymphocytes / neutrophils (*Larsen et al.*, 1989). Irrespective of whether platelets are activated or not, platelets do adhere to intact activated endothelium, possibly through the binding of endothelial cell surface expressed P-selectin to constitutively expressed P-selectin glycoprotein ligand-1 (PSGL-1) or GP-Ibα on the platelet surface (*Frenette et al.*, 1995; *Massberg et al.*, 1998). The interactions are further strengthened upon platelet activation through their reciprocal interactions as P-selectin from the α-granules is exposed (*Gawaz et al.*, 2005). Variety of platelet-foreign cell interactions induce a series of pro-inflammatory consequences contributed by the release of several cytokines, chemokines, proteases and coagulation factors (*May et al.*, 2008).

There are several inflammatory factors stored and secreted from α-granules such as PF4, GRO-α, SDF-1α, β-TG, RANTES, IL-8, IL-2, MIP-1α etc (*Gleissner et al.*, 2008). PF4 is platelet-specific and abundant. It contributes to neutrophil adhesion and degranulation, differentiation of monocytes and macrophages to foam cells, all actions that exacerbate inflammation (*Kasper et al.*, 2007; *Kasper et al.*, 2004; *Scheuerer et al.*, 2000). Atherosclerosis, a chronic inflammatory disease exemplifies the role of platelets in inflammation. It is characterized by the infiltration of immune cells into sub-endothelial layers of arterial wall, and platelets are reported to play a significant role in both initiation and progression of the disease (*Croce and Libby*, 2007) by depositing chemotactic mediators on the endothelial surface (*von Hundelshausen and Weber*, 2007). Many cytokines from α-granules such as RANTES, MCP-1, MIP-1α etc. are detected in atherosclerotic plaques. Deficiency of P-selectin is associated with reduced fatty streaks and plaque lesion size in mouse models of atherosclerosis like LDL receptor [-/-] and apolipoprotein E [-/-] (*Collins et al.*, 2000; *Dong et al.*, 2000). Platelet, and not endothelial P-selectin is essential for neointimal layer formation upon vascular injury and facilitates lesion development (*Burger and Wagner*, 2003).

Angiogenesis

Though the involvement of platelets in angiogenesis has long been suspected (*Knighton et al.*, 1982), the mechanism of their role is only now being understood in more detail (*Kisucka et al.*, 2006). Both pro- and anti-angiogenic factors are present in platelets. Growth factors are angiogenic activators that promote vessel wall permeability, and recruit endothelial cells and fibroblasts. Relevant growth factors in α-granules of platelets include vascular endothelial growth factor (VEGF), basic fibroblast growth factor (bFGF), insulin-like growth factor (IGF), epidermal growth factor (EGF), and hepatocyte growth factor (HGF) (*Nurden et al.*, 2008; *Rendu and Brohard-Bohn*, 2001). The highly elevated VEGF concentrations after hemostatic plug formation (*Weltermann et al.*, 1999), is an example of how the platelet pool of growth factors can have an impact at the site of vascular injury. *In vivo*, VEGF is also accumulated in platelet thrombi (*Arisato et al.*, 2003). Platelet-derived VEGF, bFGF and PDGF have been shown to promote the sprouting of new vascular vessels in an *ex vivo* rat aortic ring model (*Brill et al.*, 2004). Platelets being a store house for a variety of growth factors have significant contribution in the process of wound healing. This has been shown *in vitro* through the migration of osteogenic cells (*Kark et al.*, 2006), proliferation of human tendon cells in culture (*Anitua et al.*, 2005) and healing of cutaneous wounds in diabetic rats (*Moulin et al.*, 1998).

α-Granules also store anti-angiogenic factors such as thrombospondin-1 (TSP-1), which has been shown to inhibit endothelial cell proliferation and promote apoptosis (*Jimenez et al.*, 2000). TSP-1 deficient mice exhibit pro-angigogenic activity, which was modulated by increased SDF-1α secretion from platelets (*Jimenez et al.*, 2000). PF4 is not only known for its inflammatory role but also acts as an anti-angiogenic cytokine that probably affects the binding of VEGF and FGF to their receptors (*Bikfalvi*, 2004; *Perollet et al.*, 1998). Platelet α-granules contain other anti-angiogenic factors like angiostatin, endostatin, tissue inhibitor of metalloproteinases-1 (TIMP-1), TIMP-4, etc. Fine balance between platelet derived pro- and anti-angiogenic factors therefore becomes important in determining the extent of angiogenesis at the site of platelet activation.

Antimicrobial action

Platelets, though known for a very long time to accentuate microbial infections because of their adhesion properties, they are now being categorized as agents for arresting microbial action. Platelets interact directly with bacteria (*Clawson CC*, 1975), virus (*Bik et al.*, 1982; *Zucker-Franklin et al.*, 1990), fungi (*Maisch and Calderone*, 1980) and protozoa (*McMorran et al.*, 2009). One of the more recent studies implying the antimicrobial action of platelets demonstrated that platelets can bind to plasmodia-infected erythrocytes and mediate their destruction (*McMorran et al.*, 2009). Several CXCL proteins in α-granules have both anti-inflammatory and microbicidal properties such as RANTES, connective tissue activation peptide 3 (CTAP3) and PF4 (*Cole et al.*, 2001; *Tang et al.*, 2002; *von Hundelshausen and Weber*, 2007).

Platelet heterogeneity

The short life span and the continued production of platelets from MKs generate inherent population heterogeneity. Platelet granule cargo molecules are generated in MKs or are endocytosed from circulation. This raises the possibility of MK environment determining the kind of granule cargo synthesized. This reasoning is bolstered by the rapidity of newly reported moieties in platelets (*Senis and García*, 2012). With the release of cargo molecules of opposing functions, platelets contribute significantly in delineating the microenvironment of the injury site. With heterogeneous contents of platelets dictating the redesign of the injured site, the pattern followed by the secretion process becomes essential to understand.

The concept that the contents with opposing physiological functions are packed in distinct granules in platelets and released selectively with distinct agonists, revolutionalized the concept of platelet secretion (*Italiano et al.*, 2008). Immuno-fluorescence and immuno-electron microscopy show distinct localizations for pro- and anti-angiogenic factors (*Italiano et al.*, 2008). Consistently, other studies have shown that stimulating platelets with different agonists (*i.e.* PAR1- and PAR4-agonists) causes differential release of certain cargo (*Chatterjee et al.*, 2011; *Italiano et al.*, 2008; *Ma et*

al., 2005). This led to the proposal that platelet secretion is contextually thematic: capable of releasing specific sets of cargo (*e.g.* pro- or anti-angiogenic factors) in response to specific agonists (*Folkman*, 2007; *Italiano et al.*, 2008). More recent studies have suggested that cargo is spatially segregated into sub-regions of the same membrane bound granules and that there is little co-localization of factors with like functions (*Kamykowski et al.*, 2011; *Sehgal and Storrie*, 2007). Though intriguing, it is difficult to ascertain how platelets release their myriad cargo in response to the agonists generated at the site of vascular damage. Addressing this question is significant since, if there is heterogeneity in cargo packing and/or secretion, regulating the release of specific α-granule sub-populations may allow specific manipulation of the microenvironment at an injury site without disturbing hemostasis. The platelets were raised from a conservative view that establishes non-selectivity in the release process to a more easily controllable system and an assertive solution in manipulating platelet secretion in the present times. My work addresses the question "Are platelets smart-bombs?" The ensemble of biochemical and mathematical analyses not only alluded to heterogeneity in platelet secretion but also an associated pattern dependent on agonist-potency.

Bioactive lipids

Platelets are not only reservoirs for small molecules and proteinaceous substances described above, but they also house a number of bioactive lipid molecules. Bioactive lipids like diacylglycerol (DAG) and inositol-1,4,5-trisphosphate (IP$_3$) (*Nishizuka*, 1992), eicosanoids (*Serhan and Savill*, 2005), multiple products of inositol phospholipid metabolism (*Hannun and Bell*, 1989), lyso-phosphatidic acid (LPA) and platelet activating factor (*Hannun and Obeid*, 2008) are of great physiological significance. In addition to the compounds listed above, sphingolipids occupy a special place in biology. These are major lipids in eukaryotic plasma membrane (*Kihara et al.*, 2007). Originally thought to be just structural components of cell membrane (*Simons and Ikonen*, 1997), sphingolipids are recognized to be biologically active and key for both inter and intra cellular signaling (*Leclercq and Pitson*, 2006). Many of the sphingolipid metabolites like

ceramide, sphingosine and sphingosine-1-phosphate (S1P) have been identified as bioactive lipids (*Yatomi et al.*, 1997).

In early 20th century it was noted that the barrier function of endothelium during organ reperfusion was controlled by platelets (*Danielli*, 1940). Later it was shown that platelets, in addition to their role during organ reperfusion, are also required for maintenance of normal vasculature (*Aursnes*, 1974; *Lo et al.*, 1988). The protective role of platelets was initially explained by an 'adhesion theory' in which, platelets mechanically filled the gaps in endothelium (*Danielli*, 1940; *Gimbrone et al.*, 1969). *In vitro* studies have shown the existence of several molecules in platelets that reduce vascular permeability like adenine nucleotides (*Paty et al.*, 1992), serotonin (*Shepro et al.*, 1984), S1P (*Schaphorst et al.*, 2003), LPA (*Alexander et al.*, 1998). Platelets serve as vascular guardians in developing blood vessels, lymphatics, and in the microvasculature at the sites of inflammation and tumor formation by reducing leukocyte infiltration (*Ho-Tin-Noé et al.*, 2011).

Bioactive lipids as platelet signaling molecules

TxA$_2$ is a highly potent intermediate in the conversion of arachidonic acid to thromboxanes (*Hamberg et al.*, 1974). It is an important inducer of platelet activation and is known to recruit platelets to the site of vascular injury. LPA is generated on the platelet surface (*Eichholtz T*, 1993) by autotaxin (Lysophospholipase D) (*Umezu-Goto et al.*, 2002). Generation and storage of S1P in platelets will be described in the following sections in detail. All these bioactive lipid mediators are shown to play a role in atherogenesis, tumor development and thrombogenesis.

Sphingolipid metabolism

Ceramide is the central metabolite in an intricate sphingolipid metabolic pathway. It can either be synthesized *de novo* or can be a break-down product of complex lipids like sphingomyelin. Condensation of serine and palmitoyl CoA by the action of serine palmitoyl CoA transferase (SPT) results in the formation of 3-keto dihydro sphingosine. Its subsequent reduction forms dihydrosphingosine (sphinganine)

which upon acylation by ceramide synthase results in the formation of ceramide with the intermediate dihydro ceramide (*Bartke and Hannun*, 2009; *Mandon et al.*, 1992). Ceramide is acted upon by ceramidase to form sphingosine (*Mao and Obeid*, 2008) which upon phosphorylation by sphingosine kinase forms S1P (*Hait et al.*, 2006; *Kohama et al.*, 1998). Being a central product of sphingolipid pathway, ceramide can also form sphingomyelin by the addition of phosphocholine head group from phosphatidyl choline (*Tafesse et al.*, 2006) or phosphorylated to ceramide-1-phosphate (C1P) or glycosylated to form glycosyl/galactosyl ceramide (*Ichikawa and Hirabayashi*, 1998). Each of these metabolites *via* a hydrolytic pathway catalyzed by specific enzymes can be turned into ceramide. As was mentioned above, sphingosine is phosphorylated to make S1P. This is achieved by the action of one of the two isoforms of sphingosine kinase – 1 or 2 (*Hait et al.*, 2006). Once formed S1P can be degraded back into sphingosine by the action of S1P phosphatase (*Johnson et al.*, 2003) or irreversibly to ethanol amine phosphate and hexadecenal by S1P lyase (*Bandhuvula and Saba*, 2007). A summary of sphingolipid metabolism is represented in **Figure 1.3**.

Sphingosine-1-Phosphate (S1P)

S1P has roles in processes such as cell migration, maturation, differentiation, vascular integrity and angiogenesis (*Hla*, 2004). This is facilitated by several S1P receptors previously referred to as EDG (Endothelial Differentiation Gene family) receptors. S1P receptors now form a new class and should not be confused with EDG receptors which bind to lyso-phosphatidic acid (*Chun et al.*, 2002). Expression of various isoforms of S1P receptors ($S1P_{1-5}$) on multiple cell types is responsible for the variety of extracellular roles of S1P (*Spiegel and Milstien*, 2003). $S1P_{1-3, 5}$ are absent, while $S1P_4$ mRNA has been detected in platelets (*Motohashi et al.*, 2000). The presence of $S1P_4$ in platelets might explain the induction of slight shape change of platelets incubated with exogenous S1P (*Yatomi et al.*, 1995). This response was inhibited by LPA treatment (*Yatomi et al.*, 1997). However, it is unclear whether $S1P_4$ protein is expressed and functional in platelets. One report did show diminished pro-platelet production by $S1P_4^{-/-}$ mice indicating the importance of it in MKs (*Golfier et al.*, 2010).

Apart from its extracellular roles, S1P is an important secondary messenger playing a role in the release of Ca^{2+} stores and is thus implicated in regulation of Ca^{2+} homeostasis (*Ghosh et al.*, 1990; *Ghosh et al.*, 1994). S1P has been shown to be associated more with high density lipoprotein (HDL) in blood and that it mediates anti-atherogenic actions like cell survival, migration and inhibition of the adhesion molecule expression through the S1P receptors present on the endothelial cells (*Kihara et al.*, 2007; *Okajima*, 2002). Along with this role, S1P is also involved in cell proliferation and survival (*Olivera and Spiegel*, 1993). The concept of a sphingolipid rheostat, which represents the dynamic balance between cellular S1P and sphingosine / ceramide, is widely accepted (*Spiegel and Milstien*, 2002). In this model, the fate of a cell is determined by the relative levels of sphingolipid metabolites (*e.g.* ceramide and sphingosine are pro-apoptopic, S1P and C1P are anti-apoptopic (*Chalfant and Spiegel*, 2005; *Cuvillier*, 2002)).

S1P is abundant in plasma and the reservoirs are thought to be platelets (*Yatomi et al.*, 2001), erythrocytes (*Pappu et al.*, 2007) and vascular endothelium (*Venkataraman et al.*, 2008). The source of S1P in the maintenance of vascular integrity is unknown. To address this question, a mutant mouse model with minimal availability of the enzyme required for S1P synthesis was made (*Camerer et al.*, 2009). As was mentioned above, synthesis of S1P from sphingosine requires SK1 and SK2 (*Hait et al.*, 2006). To overcome the embryonic lethality associated with complete loss of S1P synthesis (*Mizugishi et al.*, 2005), a mouse with one SK1 allele and one SK1 null allele in SK2 null background carrying a myxovirus resistance 1–Cre was generated. These mice will be referred to as plasma-S1P less mice from here on. Plasma-S1P less mice demonstrated the importance of S1P in the maintenance of vascular integrity (*Camerer et al.*, 2009). The aberration in vascular integrity of plasma-S1P less mice was restored by erythrocytes, which are responsible for bringing normal plasma-S1P levels back. Platelets and erythrocytes are the hematopoietic reservoirs of S1P. The release of S1P from RBCs is constitutive (*Hänel et al.*, 2007) while platelets have been reported to release S1P only upon their

stimulation (*Yatomi et al.*, 1995). This points to a role for platelets in determining the local concentrations of S1P and thus vascular integrity (**Figure 1.4**).

Transport of S1P

For signaling, availability of S1P is dependent upon its transport to the right location. ABC transporters have been shown to play a role in the release of S1P from various cell types.

ABCC1 exports S1P from mast cells (*Mitra et al.*, 2006). An ABCA-like exporter is thought to be involved in the release of S1P from platelets (*Kobayashi et al.*, 2006). ABCA1 mediates export in astrocytes (*Sato et al.*, 2007). The effects of various ABC transporter inhibitors led to these conclusions. However, it should be noted that deletion of any of these transporters had no effect on plasma S1P levels (*Kawahara et al.*, 2009; *Lee et al.*, 2007; *Osborne et al.*, 2008).

S1P transport in astrocytes

Astrocytes are the star-shaped neural cells present in both brain and spinal cord (abundant in brain). They help in the maintenance of the blood brain barrier and play an important role in the formation of scar after a traumatic brain injury. Rat astrocytes treated with retinoic acid and dibutyryl cAMP result in the formation of Apo E and HDL-like particles. This stimulated the release of accumulated S1P through ABCA1 transporter in the presence of exogenous sphingosine (*Sato et al.*, 2007). These events are demonstrated treating the cells with general ABC transporter inhibitor, small interfering RNAs specific to ABCA1 and through ABCA1$^{-/-}$ mice.

S1P transport in mast cells

S1P secretion from mast cells (both constitutive and Ag stimulated) was not associated with degranulation or exocytosis but has been reported to occur through ABCC1 transporters. ABCB1 and ABCC1 but not ABCC2 or ABCC3 are present on mast cells but only ABCC1 has been shown to be involved in S1P secretion (*Mitra et al.*, 2006).

Transport of S1P analog, FTY720-P (Fingolimod)

S1P in plasma is known to regulate circulating lymphocytes through $S1P_1$ (*Hla et al.*, 2008; *Rosen and Goetzl*, 2005). Similar to the conversion of sphingosine to S1P by the action of SK, its structural analog FTY720 (Fingolimod; 2-amino-2-[2-(4-octyl phenyl)ethyl]-1,3-propanediol) is converted to FTY720-P. FTY720-P binds to $S1P_1$ (*Brinkmann*, 2007; *Rosen and Goetzl*, 2005), expressed on lymphocytes/endothelial cells and acts as an immuno suppressive agent. Fingolimod has been approved in Russia and was approved by US FDA at the end of 2010 for the use in treatment of multiple sclerosis. The conversion of FTY720 to FTY720-P has been observed in platelets, but not in erythrocytes. The reason for this inability of erythrocytes is the absence of the kinase SK2 (*Anada et al.*, 2007). ABC transporters that have been suggested to transport S1P in different cell types, are incapable of transporting FTY720-P. However, it can be transported by spns2 (*Hisano et al.*, 2011). Moreover it is known that unlike S1P, FTY720-P is released from platelets irrespective of stimulation. The following is a short description of the identification of spns2 as a possible candidate for the transport of S1P.

The phenotype of the zebra fish model 'Miles apart' was cardiac bifidia (two hearts) in the embryonic development and the gene that was affected here is $S1P_2$. The ko^{157} mutant was isolated using N-Ethyl-N-nitrosourea (ENU) screening in an attempt to identify the regulators involved in the development of heart. The defect that was observed in this mutant was cardiac bifidia. The defect seen in the ko^{157} mutant coincided with the phenotype observed when the gene corresponding to spns2 is defective. Injection of mRNA of spns2 in the 'miles apart' model, compensated for the defect observed during the development of the heart. The same was also shown by introducing the human version of spns2 in the zebra fish model of 'miles apart'. This could not be replaced by spns1 (both zebra fish and human).

Spns2 transporter

Though the S1P levels of plasma are always very high (μM) and S1P is bound to HDL/albumin (*Aoki et al.*, 2005; *Argraves and Argraves*, 2007; *Christoffersen et al.*,

2011), there is high activity of S1P lyase in plasma. This is indicated by the degradation of C_{17}S1P with a half life of 15 min. Maintenance of S1P levels in plasma even with such rapid and continuous degradation signifies the contribution of S1P from platelets, erythrocytes and endothelial cells (*Lee et al.*, 2007; *Venkataraman et al.*, 2008; *Yatomi et al.*, 1997). This intensified the identification of residence of spns2. Spns2 deficient mice are lymphocytopenic. The development of all organs including the heart was normal in spns2 deficient mice suggesting its different physiological roles in zebra fish and mice. The sequence identity of spns2 in zebra fish with human/mouse is 72% and that between human and mouse is 95%. The plasma S1P levels when compared to wild type are reduced by 60% unaffecting the intracellular levels of S1P in brain/lung/spleen/thymus. The release of S1P from platelets and erythrocytes is not affected in spns2 deficient mice indicating that spns2 is not important for S1P transport in these cell types. Spns2 expression proved to be essential for the release of S1P from vascular endothelial cells (*Hisano et al.*, 2012). One of the mammalian physiological S1P transporter responsible for maintenance of plasma S1P levels is thus identified to be spns2.

S1P in platelets

S1P is known to perform its action ubiquitously. Its pleiotropic functions are attributed to its spatial and temporal availability. The plasma levels of S1P are maintained by platelets, endothelial cells and erythrocytes. S1P is maintained at low levels in most of the cell types through the action of S1P phosphatase or S1P lyase. S1P is produced momentarily when required. Uniquely, platelets store abundant quantities of S1P because they lack S1P lyase/S1P phosphatase. The rate of formation of S1P from sphingosine and the absence of enzymes degrading S1P in platelets do contribute to its high levels. The release of S1P from platelets is regulated but the mechanism is unknown.

The present knowledge about the release of S1P from platelets is dependent on the research that relies on the use of general ABC inhibitors. This was preceded by the work on astrocytes and mast cells. Its importance during development is highlighted by

the zebra fish 'miles apart' phenotype (*Osborne et al.*, 2008). The significance of S1P in the maintenance of vascular permeability barrier is exemplified by vascular leak in plasma-S1P less mice (*Camerer et al.*, 2009). S1P is able to exert its functions by binding to variety of receptors expressed on various cell types. Platelet secretory contents are known to modify vascular microenvironment upon injury. Identifying the mode of release of S1P from platelets will aid in understanding the extent of platelet S1P participation at the injury site.

Preamble to the thesis

With an established role in multiple disease states, the study of platelet secretion becomes extremely relevant. The identification of the modes of platelet exocytosis events will help to better identify the therapeutic targets for its regulation. Thematic release of platelet granule cargo has been suggested (*Italiano et al.*, 2008) which revolutionized the platelet field. One of the major focuses of the thesis is to address the question of platelet secretion heterogeneity. This was accomplished by looking at the release kinetics of thirty different cargo molecules upon stimulation of platelets with various agonists. Platelets form a circulatory reservoir of a bioactive lipid, S1P. The mode of release and its localization in platelets is unclear. The utilization of platelet secretion-deficient mice helped to identify two different pools of S1P in platelets. This thesis accentuates the importance of mode of platelet secretion, whether protein or lipid.

Type of defect	Name of the disorder	Description
Platelet Biogenesis	Bernard-Soulier syndrome (BSS)	Deficiency or the absence of GP Ib/IX/V; Macrothrombocytopenia.
	MYH9 related disorders	Macrothrombocytopenia, abnormal cytoskeletal rearrangements upon activation.
	Gray Platelet syndrome (GPS)	Anomalies in chromosome 3p; Defective storage of proteins in α-granules, macrothrombocytopenia.
Granule Genesis	Hermansky Pudlak syndrome (HPS)	Deficiency in dense granules; Occulocutaneous albinism; Decreased aggregation and secretion upon activation.
	Chediak-Higashi syndrome (CHS)	Deficiency in dense granules; Decreased aggregation and secretion upon activation.
	GPS	Empty α-granules
	Quebec syndrome	Abnormal content of α-granules
Receptor associated	($\alpha_2\beta_1$ collagen receptor, GPVI collagen receptor, P_2Y_{12} ADP receptor, TPα TxA$_2$ receptor) associated disorders	Mild bleeding disorders. Reduced response to their corresponding agonists.

Table 1.1. List of some platelet disorders

A list of platelet defects categorized as described in the left column. Name of the disorder is represented in the middle column while the right column includes description of platelets in the corresponding disorder.
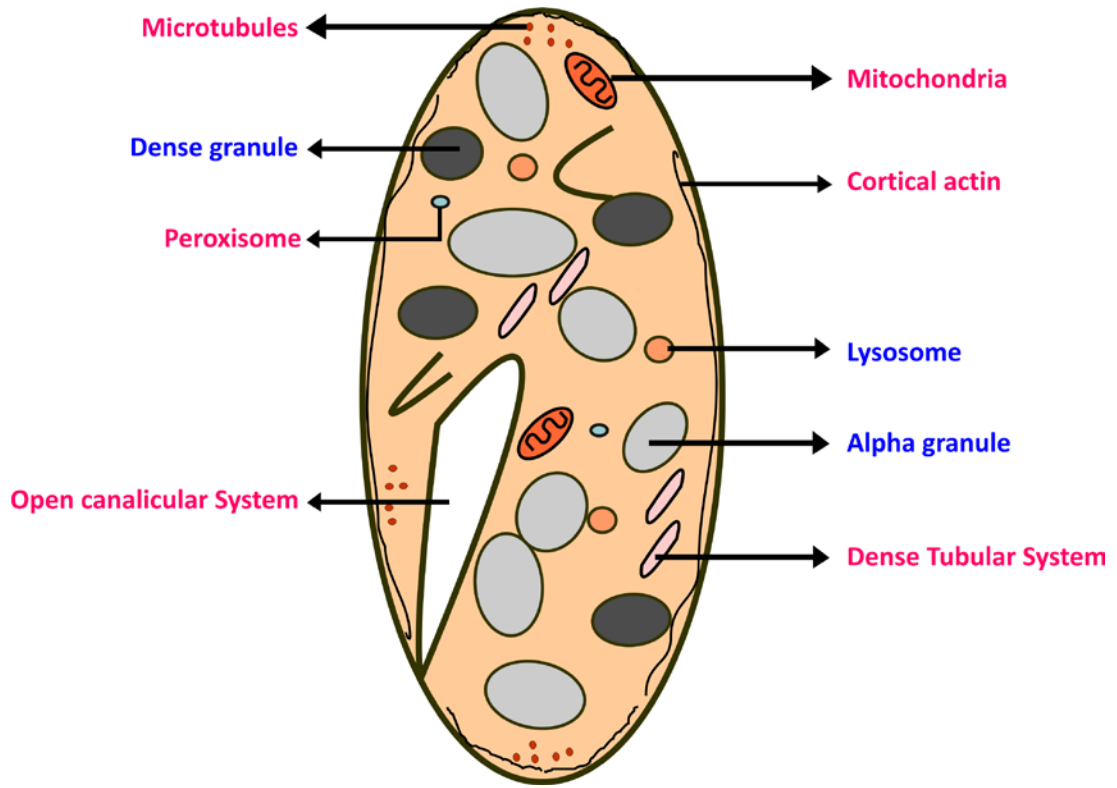
Figure 1.1. Platelet morphology

A cartoon of a platelet highlighting the morphological entities labeled in pink, while those in blue represent various granule populations of a platelet.

v-SNARE - VAMP-2, VAMP-3, VAMP-7, VAMP-8
t-SNARE - syntaxin-2, syntaxin-4, syntaxin-11, SNAP-23, SNAP-25
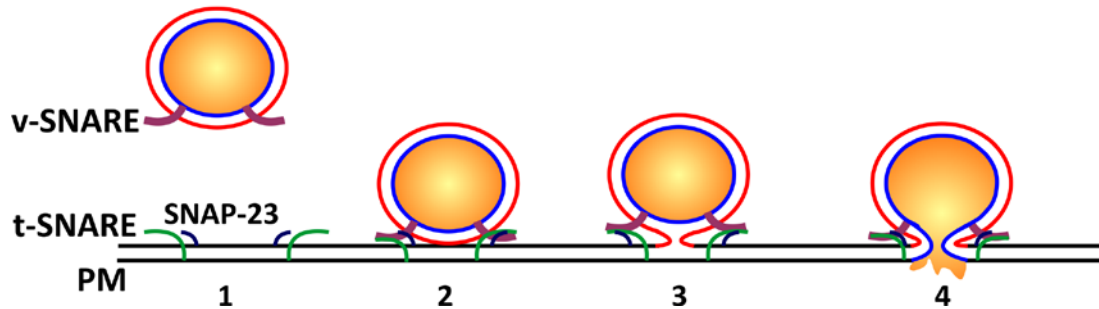
Figure 1.2. Platelet secretion machinery

Major v- and t-SNAREs present in platelets are listed and the functionally relevant SNAREs are highlighted in magenta, green and blue. Cognate v-SNARE (on vesicle) and t-SNARE (on plasma membrane [PM]) and SNAP-23 constitute potential platelet fusion machinery (1). Following docking of the vesicle (2), the membrane fusion proceeds further (3). Vesicle and the plasma membrane fusion leads to the release of vesicle contents to the exterior (4).
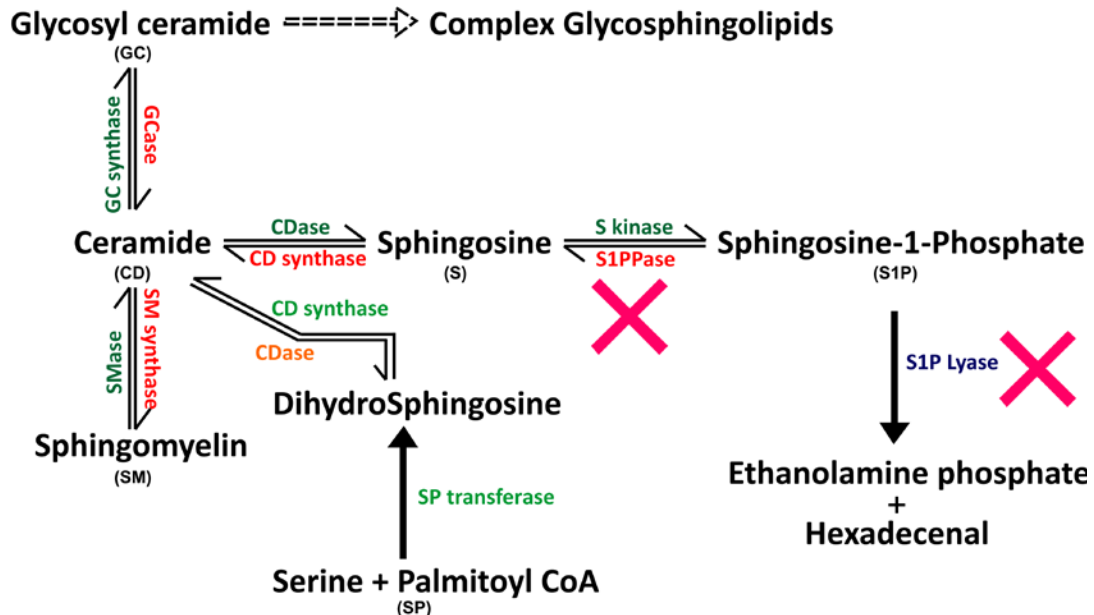
Figure 1.3. Sphingolipid metabolism

The central molecule of sphingolipid metabolism is ceramide (CD). Serine and palimitoyl CoA (SP) through the action of Serine Palmitoyl Transferase (SPT) form dihydrosphingosine. This can be converted to CD by the action of CD synthase. CD can be a breakdown product of sphingomyelin (SM) by the action of the enzyme Sphingomyelinase (SMase). CD can be converted back to SM by the action of SM synthase. CD can also be reversibly utilized for the formation of complex glycosphingolipids as represented. Sphingosine (S) is formed from ceramide by the action of CDase, which can be converted back to CD by CD synthase. Sphingosine further forms sphingosine-1-phosphate (S1P) by the action of sphingosine kinase (SK) or reversibly converted to Sphingosine by the action of S1P phosphatase (SPPase). S1P can also be irreversibly converted to ethanol amine phosphate and hexadecenal by the action of S1P lyase. The absence of S1PPase and S1P lyase enzymes in platelets is highlighted by the pink crosses.
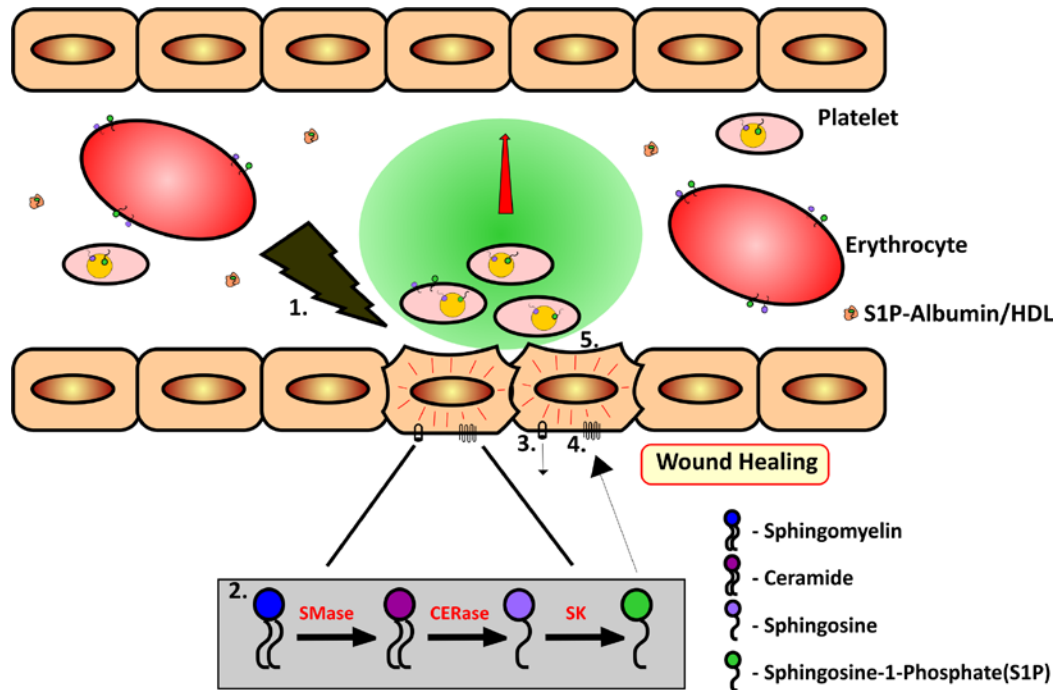
Figure 1.4. S1P in circulation

The cartoon represents microvascular injury and the sources of S1P. Endothelial cells are represented by the nucleated brown rectangular cells with smooth edges. Erythrocytes and platelets are red and pink ellipses respectively. The yellow circle in platelets represents a granule. S1P in circulation is bound to albumin or HDL and is represented by a green hydrophilic head group and a black hydrophobic tail encapsulated in an orange cup representative of albumin/HDL. Upon vascular injury (**1**), a series of reactions involving the conversion of SM to S1P as represented in the gray box (**2**) go on in endothelial cells. At the same time platelets are activated at the site of injury and the fading green circle is representation of diminishing gradient (red arrow) of released S1P from the platelets. The S1P from platelets/endothelial cells could be released *via* ABC transporters (**3**) and binds to S1P receptors present on endothelial cells (**4**). This further leads to intracellular signaling in endothelial cells (**5**) ultimately resulting in wound healing.

Chapter Two

Materials and Methods

Human platelet preparation

Fresh human platelets from male donors were isolated and adjusted to 1.2 x 10^9/mL. All the steps were performed at room temperature (RT). Blood was collected into acid citrate dextrose (ACD) vacutainer tubes by a phlebotomist at UK clinic. After pooling the collected blood into a falcon tube, samples were centrifuged at 250 × g for about 20 min to separate red blood cells (RBCs) from platelet rich plasma (PRP) [Banked human platelets are prepared from PRP obtained from the Kentucky Blood Center (KBC)]. All the centrifugation steps were carried out at intermediate acceleration and minimal deceleration. To label the dense granules, PRP was incubated with 0.4 µci/mL [^{3}H]-5-hydroxy tryptamine/[^{3}H]-serotonin (PerkinElmer) for 45 min. Prostaglandin I_2 (PGI$_2$) (50 ng/mL, Sigma) was employed at each step to maintain the platelets in a resting state during the centrifugation steps. The samples were then centrifuged at 140 × g for 13 min to eliminate residual RBCs. The PRP was carefully separated not disturbing the leukocyte layer present at the interface of RBCs and PRP. Separated PRP was then centrifuged at 1,000 × g for 12 min to pellet the platelets. The pellets were gently resuspended in Hepes Tyrode's (HT) buffer [10 mM HEPES, 5.56 mM Glucose, 137 mM NaCl, 12 mM NaHCO$_3$, 2.7 mM KCl, 0.36mM NaH$_2$PO$_4$.H$_2$O, 1mM MgCl$_2$.6H$_2$O] pH 6.5 containing PGI$_2$ and 1 mM EGTA. Another centrifugation step was included to remove any excess [^{3}H]-serotonin and the platelets were resuspended in a sufficient volume of HT buffer pH 7.4. The concentration of platelets was measured using a Z2 coulter particle counter (Beckman). Calcium (0.7 mM final) was added when resuspending the platelets for functional assays and 1% fatty acid – free bovine serum albumin (Sigma) was also added where indicated.

Mouse platelet preparation

Upon exposure of thoracic region, blood was collected by puncturing a ventricle of the heart with a 25G needle attached to I mL syringe filled with 150 µL 3.8% Sodium

citrate. The collected blood was diluted 1:1 with 1X PBS and platelets were prepared using methods similar to what is described above. The samples were centrifuged at 900 rpm for 10 min to separate the RBCs followed by centrifuging the separated PRP at 1,800 rpm for 10 min to pellet down the platelets. Prior to pelleting the platelets, they were labeled with [^{3}H]-serotonin, when using them for secretion assays. The subsequent two centrifugation steps were performed with slightly diminished speeds (1,700 rpm).

Platelet secretion assay conditions

Secretion from platelets, stimulated with the indicated agonists, was measured from 15 to 300 sec at RT. The agonists were thrombin (Chrono-Log, Havertown, PA), protease-activated-receptor agonists, {[SFLLRN for PAR1] (Bachem, King of Prussia, PA), [AYPGKF for PAR4] (Invitrogen Corporation, Carlsbad, CA)} and convulxin (Centerchem, Norwalk, CT). As already described in platelet preparation methods, platelets were labeled with [^{3}H]-serotonin. An initial titration experiment was performed to determine the minimal dose required to induce ~90% of maximal [^{3}H]-serotonin secretion in 2 min. This dose was used for the time-course experiments, which were employed to calculate exocytosis rates. The doses were: 0.3 U/mL for thrombin, 50 µM for PAR1-agonist, 500 µM for PAR4-agonist, and 0.3 µg/mL for convulxin generally. At the indicated times, platelets and releasates were separated by centrifugation at 13,000 x g for 2 min. The platelet pellets were solubilized with buffer (phosphate buffered saline, pH 7.4, 1% Triton X-100) on ice for 45 min. The releasate and the pellet samples were assayed for various granule markers as described below.

Detection of the dense granule marker [^{3}H]-serotonin

Radiolabeled serotonin in the releasate and the pellet was measured by liquid scintillation using Econo-Safe Scintillation cocktail (Research Products International Corp.) and a TRI-CARB 2100 TR liquid scintillation analyzer (Packard). A percent release value, at each time point, was calculated following the equation: (cpm in releasate)/cpm in (releasate + pellet).

Detection of the α-granule marker Platelet Factor 4 (PF4)

PF4 was quantified by ELISA using reagents obtained from R&D systems (R&D systems, Minneapolis, MN). The procedure followed for performing the assay and analyzing the data is summarized here. Human/mouse PF4 capture antibody (2 μg/mL) in 1X PBS was coated on 96 well microplate (Costar3369 Fisher Scientific) overnight at RT. Unbound antibody was removed by wash buffer PBS-T (1X PBS pH7.4, 0.05% Tween20,) and non-specific binding sites were blocked with PBS-T containing 1% BSA and 5% sucrose for 1 hr. Since PF4 is abundant, the samples were diluted in diluent buffer (1X TBS pH 7.4, 0.05% Tween20, 0.1% BSA) and 100 μL of it was added to the wells. The highest concentration of recombinant PF4 employed in the assay as a standard was 16 ng/mL for human and 2 ng/mL for mouse. This was serially diluted to construct a standard curve. Sample and capture antibody were incubated for 2 hrs at RT. The wells were washed with wash buffer and the bound PF4 was detected using a biotinylated antibody against PF4 (200 ng/mL and 100 ng/mL for human (Leinco Technologies Inc., St. Louis, MO) and mouse (R & D Systems) respectively). Following washing, the reaction was developed using HRP-Streptavidin (1:200) and TMB (3, 3', 5, 5' Tetra methyl benzidine) substrate (Thermo Scientific). Once the blue color was achieved, the signal was amplified upon addition of 2M H_2SO_4 and the OD was read at 450 nm using Elx 808 microplate reader (Biotek Instruments). The data were converted to a logarithmic scale and were normalized to the generated standard curve. A percent release of PF4 was calculated following the same equation as above.

Detection of the lysosomal marker β-hexosaminidase

β-Hexosaminidase was detected using a simple colorimetric assay. The substrate, *p*-nitrophenyl-N-acetyl-β-D-glucosaminide (PNP-GlucNAc) was resuspended (10 mM) in the citrate-phosphate buffer (0.2 M Na_2HPO_4 and 0.1M Citric acid, pH 4.5) and 100 μL was added into a 96 well microplate together with platelet releasate and pellet sample. To assure linearity of the assay, a random sample was selected to generate a standard curve. Equal volumes of the releasate and the pellet samples were added to represent one whole sample. This was serially diluted to generate a standard curve. The plate was

sealed and incubated at 37°C for 18 hrs. The reaction was then stopped by the addition of 1M NaOH to enhance the p-nitrophenyl color and the absorbance of each well was measured at 405 nm. A percent release of β-hexosaminidase was calculated as above.

Detection of released cargo using micro-ELISA arrays

Several techniques (*i.e.* mass spectrometry, multiplex bead assay) were considered for this study; however, it was felt that the micro-ELISA was the best method to quantify the individual components in the releasate. Custom micro-ELISA arrays were purchased from RayBiotech (Norcross, GA). The 28 antibodies, from the vendor's catalogue of compatible reagents, were distributed between two slides to avoid cross reactivity. Arrays were blocked for 30 min, and then incubated with 100 µL of standards or diluted platelet releasates at RT for 1 hr. The arrays were incubated with biotinylated, detection antibodies and then, with Alexa Fluor 555-conjugated streptavidin, each for 1 hr. The slides were rinsed and scanned with an Axon GenePix (Molecular Devices, Sunnyvale, CA) microarray scanner using λ_{ex} = 555 nm and λ_{em} = 565 nm (10 mm resolution). Each antigen was represented by four spots and the average fluorescence intensity was compared to that from a standard curve of like antigen (generated on the same array) to determine the concentrations of a cargo antigen in a given platelet releasate. One array was used to determine the dilution needed to detect all antigens in the linear range of the assay. In general, the arrays' sensitivities were pg/mL to ng/mL (**Table 3.2**). Array signals were reproducible, differing by < 15% in the nine arrays used for these studies.

Calculation of a rate constant (*K_{ex}*)

We cannot directly monitor granule fusion (*e.g.* by membrane capacitance); instead, we infer fusion rates from the rates of appearance of cargo outside the platelet. Analysis was performed using the following reasoning: if a cargo molecule has a fixed probability per unit time (rate), K_{ex}, of being released when its granule fuses with the plasma membrane, then the number of cargo molecules remaining at time *t* after stimulation is $N(t) = N_0 e^{-K_{ex}t}$, where N_0 is the initial number of molecules. Therefore,

cargo concentration outside the platelet is complementary to $N(t)$ and is

$P(t) = P_{max} \left(1 - e^{-K_{ex}t}\right)$, [1] where P_{max} is the concentration of released cargo at 5 min (the maximum time of stimulation) normalized to 100%. Raw data were fit to equation [1] using the curve fit function in IDL (ITT Visual Information Solutions, Boulder, CO) and confirmed with GraphPad Prism (version 4, GraphPad Software, La Jolla, CA). The curve fit returns the Mean Squared Error (*MSE*) defined as $MSE = \sum_{i=1}^{N} \left(P_i - P(t_i)\right)^2 / (N-2)$, where P_i is the measured percent release at time t_i and $P(t_i)$ is equation [1] evaluated at t_i. The denominator is the number of degrees of freedom where N is the number of time points from which 2 is subtracted because there are 2 parameters in equation [1]. We used K_{ex} values from only those fits where *MSE* < 150, taking into account the unavoidable inherent sampling error. Hence, 90 of 174 kinetic measurements were used for further analysis.

Note that the MSE is >> 1 only because we have transformed the maximum concentration to 100. More typical MSE values of <1 are simply obtained upon dividing by 100^2. The criterion *MSE* < 150 is somewhat arbitrary. We cannot determine if a fit is acceptable because replicate measurements cannot be done at each time point for all chemokines individually for all the arrays and we do know the inherent sampling error. Therefore we used 90 out of 174 kinetic measurements.

Fitting the probability density function

A histogram of all 90 values of K_{ex}, with bin widths of 0.0075 was made. The probability density function (*pdf)* was obtained from this histogram by dividing the number in each bin by the product of the total number of values (90) and the bin width. The total area under the *pdf* is 100. To estimate the number of cargo classes, the *pdf* was fit to either 2 or 3 Gaussian functions.

$$f\left(K_{ex}\right) = \sum_{i=1}^{n} A_i \exp\left(-\frac{\left(K_{ex} - \mu_i\right)^2}{2\sigma_i^2}\right), \text{ where } n = 2 \text{ or } 3 \qquad [2]$$

33

The parameters (A_i, μ_i, σ_i) were found using ProFit (version 6.0.6, Quansoft.com, Uetikon am See, Switzerland). We used the F-test to assess whether the 3-Gaussian function fit is statistically better than the 2-Gaussian function fit (Graph Pad Software Inc. San Diego, CA).

Modeling operator variance

The K_{ex} values vary over a range from 0.00193 s^{-1} to 0.24 s^{-1} (**Figure 3.13**). As our finest time resolution is 15 sec, timing errors have larger impact for fast release processes. This results in greater broadening of distribution of the estimated K_{ex} values even if there were no variation in the intrinsic value of K_{ex}. We exploited this broadening to estimate the number of cargo classes, the mean K_{ex} value for each class, and the operator variance σ_{op}^2. Factors contributing to the operator variance include timing errors, pipetting variations, *etc*. We used the following procedure to study the effect of operator variance on our analysis. (i) We chose 2 or 3 K_{ex} values to test whether the data is consistent with 2 or 3 cargo classes. The K_{ex} values were chosen to be the mean values of the individual Gaussian distributions (**Figure 3.12**) when the data were fit with 2 or 3 Gaussians. (ii) For each K_{ex}, we computed $P(t_i) = P_{\max} \left(1 - e^{-K_{ex}t_i}\right) \times (1 - r)$, where t_i is the time when our measurements were made $t_i \in \{0, 15, 30, 60, 300\}$ and r is a normally distributed random number with a mean of 0 and standard deviation σ_{op}. (iii) Based on these values of $P(t_i)$ we determined K_{ex} using the same procedure described here. (iv) Steps (ii) and (iii) were repeated $N_{samples}$ times. (v) The resulting $N_{samples}$ of K_{ex} were sorted by size and plotted as shown in **Figure 3.14**. The number of samples ($N_{samples}$) was chosen so that the number of different K_{ex} values (2 or 3) $\times N_{samples}$ equaled 90, the number of experimental data points used to construct the *pdf* shown in **Figure 3.12**. Steps (ii) through (v) provide just one particular sample of possible outcomes. We therefore repeated steps (ii) through (v) 50 times to see the range of possible K_{ex} estimates. **Figure 3.14** shows 90 $\times$ 50 K_{ex} values.

Lipid extraction

Lipids were extracted in acidified organic solvents as described in {Mathews, 2010 #55}. Platelets (50 μL) were added to a mixture of 2 mL CH_3OH and 1 mL $CHCl_3$ in 8 mL borosilicate glass tubes and 1 μM C_{17} S1P (Avanti polar lipids, Alabaster, AL) (50 μL) was added as an internal standard. The mixture was acidified with 0.45 mL 0.1 M HCl and the samples were vortexed for 5 min, and then placed at 4°C for 1 h. The extraction volume was increased by an additional 1 mL $CHCl_3$ and 1.3 mL 0.1M HCl. After vortexing for 5 min, the samples were centrifuged for 10 min at 4,000 rpm. The lower phase was then transferred to a 4 mL screw cap glass vial using a glass pasteur pipette carefully avoiding the protein interface. The samples were evaporated under N_2 stream and resuspended in 100 μL CH_3OH.

Detection of S1P by HPLC (ESI) MS/MS

The extracted lipids were analyzed by LC MS/MS. Analysis of S1P was carried out using a Shimadzu UFLC coupled with a 4000-Qtrap hybrid linear ion trap triple quadrapole mass spectrometer (AB SCIEX) in multiple reaction monitoring (MRM) mode. C_{17} S1P was used as an internal standard. S1P and C_{17} S1P were separated using Zorbax Eclipse XDB C8 column (5 μm, 4.6 × 150 mm, Agilent). The mobile phase consisted of 75/25 of CH_3OH / H_2O with HCOOH (0.5%) and 5 mM $HCOONH_4$ (0.1%) as solvent A and 99/1 of CH_3OH / H_2O with HCOOH (0.5%) and 5 mM $HCOONH_4$ (0.1%) as solvent B. For the analysis of S1P the separation was achieved using a gradient of 0% B for 1 min, 0% B to 100% B in the next one minute, maintained at 100% B for the next 10 min and equilibrated back to the initial conditions in 3 min. The flow rate was 0.5 mL/min with a column temperature of 30°C. The sample injection volume was 10 μL. The mass spectrometer was operated in the positive electron spray ionization mode with optimal ion source settings determined by synthetic standards of S1P and C_{17} S1P with a declustering potential of 61 V, entrance potential of 10 V, collision energy of 23 V, collision cell exit potential of 16 V, curtain gas of 20 psi, ion spray voltage of 5500 V, ion source gas1 / gas2 of 40 psi and temperature of 550°C. MRM transitions monitored were as follows: 366.141/250 for C17 S1P; and 380.124/264.1 for S1P.

Mouse models

C57BL/6, VAMP-8^{-/-} {Ren, 2007 #56} and *Unc13d* [Jinx] {Ren, 2010 #57} were generated as described. All experiments with animals were under the protocol 884M2005 approved by the University of Kentucky Institutional Animal Care and Use Committee.

Fluorescence microscopy

Washed platelets (5×10^8 / mL) were incubated with 1 µM mepacrine dihydrochloride (Sigma Aldrich, St. Louis, MO) or 1 µM lyso tracker red DND – 99 (Invitrogen, Eugene, Oregon) or 1 µM NBD – Sphingosine (Avanti Polar lipids, Alabaster, AL) for 30 min at 37°C. The platelets were pelleted at 1,600 rpm for 8 min and resuspended in fresh pH 7.4 HT buffer. Approximately 10 µL of the sample was placed onto a clean microscope slide and was laid over by a cover glass. The sample was allowed to settle for 30 min and viewed through 100X objective lens in oil immersion under Nikon Eclipse 600 (Melville, NY). Digital images were captured using Axiocam MRm and were processed using Axiovision software.

Thin layer chromatography

Samples, after liquid phase lipid – extraction, were separated by thin layer chromatography using human banked platelets (Merck KGaA, Darmstadt, Germany) with a mobile phase of: $CHCl_3$: CH_3OH : H_2O in the ratio 60 : 35 : 8. After development and drying, the separated fluorescently labeled NBD – Sphingosine-containing lipids were visualized using a Typhoon 9400 scanner (Amersham Biosciences, Piscataway, NJ) at excitation wavelength 457 nm and emission wavelength 532 nm. We thank Dr. Binks Wattenberg at University of Louisville for providing NBD – Sphingosine-1-phosphate standard for this analysis.

Sub – cellular fractionation

The procedure was modified from Broekman 1992 (*Broekman*, 1992). A unit of fresh PRP from KBC was centrifuged at 800 rpm for 15 min. Platelets were pelleted at 1,800 rpm for 15 min at RT and pellet was washed twice with 50 mL Tris - citrate buffer

(63 mM Tris, 95 mM NaCl, 5 mM KCl, 12 mM citric acid, pH 6.5/ HCl). The platelet pellet was finally resuspended in 12 mL Tris - citrate buffer and was then poured into the chamber of cell disruption bomb (Parr 4639, Parr Instrument Co., Moline, IL). The Parr bomb was pressurized with N_2 at 1,200 psi on ice for 15 min and the pressure was rapidly released to disrupt the cells. This cycle was repeated thrice and the platelet homogenates were cleared by centrifugation at 2,500 rpm for 10 min to remove cell debris and partially disrupted cells, prior to loading onto sucrose gradients. Roughly linear sucrose gradients were generated by layering 1.5 mL sucrose solutions (containing 5mM EDTA) of decreasing concentrations (from 60% to 30%, total 10.5 mL) into a 14 mL ultracentrifuge tube and the tubes were incubated overnight at 4°C. Homogenate (1.5 mL) was layered onto the top of the gradient and they were subjected to centrifugation at 40,000 rpm at 4°C using SW - 40 swinging - bucket rotor (Beckman, Fullerton, CA). After 90 min the tubes were recovered and snap - frozen in an ethanol/dry - ice bath and then placed at -80°C overnight. The frozen tubes were cut into 10 equal sizes (~1.2mL) using a clean steel saw. The fractions were then recovered and 200 µL of each fraction was diluted to 1mL with H_2O. After adding 100 µL of 2% Sodium deoxycholate and 200 µL of 72% tri chloro acetic acid (TCA), the samples were incubated on ice for 30 min followed by centrifugation at 13,000 × g for 10 min to recover the precipitated proteins. The pellets were washed with 1 mL of cold acetone, dried, and resuspended the pellet in 100 µL of 2X SDS sample buffer for analysis by SDS-PAGE and western blotting.

Western blotting

Samples recovered by TCA precipitation as described above were separated (15 µL) on 12.5% SDS-PAGE at 200 V for 45 min. The separated proteins were then transferred onto Immobilon-P polyvinylidene fluoride (PVDF) membrane (Millipore Corp., Bedford, MA) for 1 hr at 100 V in 1X transfer buffer (25 mM Tris, 192 mM Glycine, 20% Methanol pH 8.3). The PVDF membrane, with the transferred proteins, was initially blocked for 1 hr at RT with 5 % non-fat milk in TBS-T (25 mM Tris, 150 mM NaCl, 0.1% Tween-20 pH 7.4). This was followed by incubation with the primary antibody (diluted in blocking buffer) against indicated proteins ($\alpha_{IIb}\beta_3$, Rab-GDI, VAMP-8, malate

dehydrogenase, PF4) overnight at 4°C. Anti-$\alpha_{IIb}\beta_3$ rabbit polyclonal antibody was a generous gift from Dr. Bill Dean at University of Louisville. Anti-RabGDI polyclonal antibody was generated in our laboratory by Dr. Tara Rutledge using recombinant RabGDIα as antigen. Polyclonal rabbit-anti-human VAMP-8 was generated in our laboratory using recombinant cytoplasmic domain of human VAMP-8 (1-73 aa). Antibody against Malate DHase was a generous gift from Dr. Louis Hersh at University of Kentucky. After washing with TBS-T, the membrane was incubated with appropriate dilution of alkaline-phosphatase conjugated secondary antibody (Sigma) for 1 hr at RT. Following washing, the membrane was incubated for 5 min at RT with Vista-ECF substrate (Amersham Biosciences, Piscataway, NJ). The immunodecorated proteins were visualized using Typhoon 9400 scanner (Amersham Biosciences, Piscataway, NJ) at excitation wavelength 457 nm and emission wavelength 555 nm.

Chapter Three

Heterogeneity in Platelet Secretion

Introduction

Platelets are first responders to vascular damage. The damaged vasculature attracts and activates platelets to release cargo from granular stores: dense (δ), alpha (α), and lysosomal. Dense granules contain small molecules (*i.e.* ADP, and serotonin) (*Ge et al.*, 2009; *Holmsen and Weiss*, 1979; *McNicol and Israels*, 1999). α-Granules contain polypeptides (*Maynard et al.*, 2010) and lysosomes contain hydrolytic enzymes (*i.e.* β-hexosaminidase and cathepsins) (*Holmsen and Weiss*, 1979). Release of dense granule cargo is important to hemostasis, given the bleeding diatheses associated with genetic defects in dense granule biogenesis (*i.e.* Hermansky-Pudlak Syndrome, HPS) (*Gunay-Aygun et al.*, 2004). Released ADP enhances the responsiveness to other agonists generated at the site of vascular damage (*Graham et al.*, 2009). Release of α-granule cargo has a more heterogeneous impact. Patients that lack α-granules (*i.e.* Gray Platelet Syndrome, GPS) generally have more diverse bleeding phenotypes, ranging from severe to mild (*Gunay-Aygun et al.*, 2010; *Nurden and Nurden*, 2007). The role that lysosome release plays is unclear; the released hydrolytic enzymes could be important for thrombus remodeling. While it is clear that platelet secretion is important, it is not clear how the platelet release reaction modulates the microenvironment at vascular injury sites.

Present estimates suggest that activated platelets secrete hundreds of different molecules (*Maynard et al.*, 2007; *Senzel et al.*, 2009). While dense granules predominantly contain small molecules, α-granules contain a myriad cargo that comprise the bulk of the platelet "secretome". α-Granules contain hemostatic factors (*e.g.* Factor V, fibrinogen), angiogenic factors (*e.g.* angiogenin, VEGF), anti-angiogenic factors (*e.g.* angiostatin, PF4), growth factors (*e.g.* PDGF, SDF1α), proteases (*e.g.* MMP2, MMP9), necrosis factors (*e.g.* TNFα, TNFβ) and other cytokines(*Coppinger et al.*, 2004). Some are produced by megakaryocytes and are packaged into granules during their biosynthesis

(*Heijnen et al.*, 1998). Patients with GPS presumably have a defect in this process. Other α-granule cargo (*e.g.* fibrinogen and Factor V) are not made by megakaryocytes but are thought to be endocytosed by circulating platelets (*Louache et al.*, 1991). They are then transported to α-granules (*Harrison et al.*, 1989; *Heijnen et al.*, 1998).

The catalog of cargo suggests that platelet secretion is pivotal to establishing the microenvironment at an injury site. However, very little is understood about how platelet secretion occurs. Studies suggest that certain angiogenesis regulators are packaged into distinct populations of α-granules. Immuno-fluorescence and immuno-electron microscopy show distinct localizations for pro- and anti-angiogenic factors (*Italiano et al.*, 2008). Consistently, other studies have shown that stimulating platelets with different agonists (*i.e.* PAR1- and PAR4-agonists) causes differential release of certain cargo (*Chatterjee et al.*, 2011; *Folkman*, 2007; *Italiano et al.*, 2008; *Ma et al.*, 2005). This led to the proposal that platelet secretion is contextually thematic: capable of releasing specific sets of cargo (*e.g.* pro- or anti-angiogenic factors) in response to specific agonists (*Folkman*, 2007; *Italiano et al.*, 2008). More recent studies have suggested that cargo is spatially segregated into sub-regions of the same membrane bound granules and that there is little co-localization of factors with like functions (*Kamykowski et al.*, 2011; *Sehgal and Storrie*, 2007). Though intriguing, it is difficult to ascertain how platelets release their myriad cargo in response to the agonists generated at the site of vascular damage. Addressing this question is significant since, if there is heterogeneity in cargo packing and/or secretion, regulating the release of specific α-granule sub-populations may allow specific manipulation of the microenvironment at an injury site without disturbing hemostasis. Our study offers the first systematic examination of the platelet secretion process and its kinetics, and potential heterogeneity.

To define the extent of platelet secretion heterogeneity, we measured the release of serotonin, β-hexosaminidase, and 28 different α-granule cargo proteins. These proteins have a diverse range of biochemical properties, functions, and origins. Four

different agonists (PAR1- and 4-agonists, thrombin, and convulxin) were used to stimulate release and secretion time courses were measured with micro-ELISA arrays. The time course data was fit to a one phase exponential equation to calculate release rate constants for each cargo molecule detected. These rate constants were analyzed to identify patterns in the release kinetics. In general, the number of α-granule cargo proteins detected in platelet releasates correlated with agonist potency (thrombin > convulxin/PAR1 > PAR4). Though some cargo was more rapidly released than others, no coherent, functional pattern was observed. Detailed analysis of the release rate constants indicated that platelet release heterogeneity is kinetically-based and can be defined as three classes of events (fast, intermediate and slow).

Agonists used for stimulating platelets

Thrombin is a potent agonist that has been employed mostly throughout the study. As described in Chapter One, thrombin acts *via* PAR1 and PAR4 receptors on human platelets. The reaction is inhibited at the end of stimulation of platelets by using hirudin. Hirudin is an anti-coagulant derived from leeches (*Baskova et al.*, 1983; *Chang*, 1983). It directly binds to the serine protease, thrombin, and inhibits its cleavage of PARs. This ability to stop the reaction with an inhibitor is not possible when using other agonists chosen for this study. Upon centrifugation the releasate and the pellet fractions were rapidly separated in an attempt to stop the release reactions induced by convulxin, PAR1- and 4-agonists. The release of contents during this work up period is unavoidable and slightly lessens the resolution of the time course experiments.

Characteristics of granule secretion from platelets

Granule release upon thrombin stimulation

Platelet granule populations are distinguished into three classes based on their morphology, abundance, and contents. They include dense granules, α-granules and lysosomes. Platelet secretion was analyzed in a series of time-course experiments, initially using different concentrations of thrombin as agonist. Release of [^{3}H]-serotonin, as a metric of dense granule release; PF4, as a metric of α-granule release; and β-

hexosaminidase, as a metric of lysosome release was measured as previously reported {Chen, 2000 #107;Schraw, 2003 #95}. The thrombin doses used were 0.025 U/mL (**a**), 0.05 U/mL (**b**), 0.1 U/mL (**c**) and 0.4 U/mL (**d**). There was no detectable dense granule secretion upon treatment with 0.025 U/mL thrombin. A 30%, 40%, and 60% dense granule release was seen at 0.05 U/mL, 0.1 U/mL and 0.4 U/mL thrombin stimulation respectively. α-Granule exhibited 20%, 35%, 40% and 50% release, respectively. The same increasing pattern could be seen in lysosomal release. The idea that the extent or the rapidity of release is dependent upon the agonist dose can be visualized through **Figure 3.1**.

The data from the experiment described above was plotted to represent different granule (dense granule, α-granule and lysosome respectively) release patterns (**Figure 3.2**). Dense granule release was undetectable when platelets were stimulated with 0.025 U/mL thrombin while markers from the other two granules could be detected in the releasate. At high thrombin concentrations (0.4 U/mL of thrombin) dense granule release was maximal (~60%); α-granule release was 50%; and, lysosomal release was 30%. This release feature has been examined in 28 different proteins that are known to get secreted from platelets. The purpose of doing such analysis was to test if the concept of agonist potency determining the extent of secretion holds good for a broader group of secreted proteins.

Secretion assay conditions

An initial titration experiment was done for every trial performed to estimate the agonist concentration to be used. The choice was determined by the ability of the agonist to release between 80-90% of [^{3}H]-serotonin from platelets upon stimulation with the chosen agonist for 2 min (**Figure 3.3**). The same strategy was employed for all the agonists used in the study (thrombin (**a**), convulxin (**b**), PAR1 (**c**)) except for PAR4 where doing a titration every time was limited by the cost of the peptide. A maximum concentration of PAR4 (500 µM) was used for the study. By choosing the maximal concentration of each agonist for our analysis we assured that stimulation was optimal

and thus the release kinetics reflected platelet exocytosis process and not differential activation. Since different extents of platelet activation could account for secretion heterogeneity, we chose this strategy to lessen that variable and focus the analysis on release and not activation. Apyrase was included during platelet isolation to lessen the effects of released ADP. Platelets were not stirred. [^{3}H]-serotonin, PF4 and β-hexosaminidase release characteristics were used to standardize assay conditions.

Agonist dependency of cargo release

The release of serotonin, PF4, and β-hexosaminidase is considered as an evidence that secretion from dense granules, α-granules, and lysosomes has occurred, respectively. In agreement with previous studies (*Balduini et al.*, 2002; *Blair and Flaumenhaft*, 2009; *Ren et al.*, 2008), the relative release rates at the earlier time points were consistent - serotonin > PF4 > β-hexosaminidase, regardless of the agonist used. Agonist dose dependency on the release of granule cargo represented in **Figures 3.1** and **3.2** holds good not only for thrombin but also, convulxin, PAR1- and PAR4-agonists. Release of serotonin (**Figure 3.4**, ■), was most rapid and was generally the most extensive (highest percent release). Release of PF4 (**Figure 3.4**, ▲) was more extensive than that of β-hexosaminidase and did approach that of serotonin, especially when PAR-agonists were used. Release of the lysosomal cargo, β-hexosaminidase (**Figure 3.4**, ▼), was the least extensive. Interestingly, the extent of β-hexosaminidase release was most sensitive to agonist. Release induced by thrombin and convulxin was two-fold higher than that induced by either of the PAR-agonists. Serotonin and PF4 release were similarly affected by the agonist used, but not to the same degree.

Agonist potency affected the extent of cargo release. Strong agonists such as thrombin (**Figure 3.4A**) and convulxin (**Figure 3.4B**) induced rapid release that was extensive, reaching approximately 70% of total for serotonin, 50% for PF4, and 30% for β-hexosaminidase. With PAR1-agonist (**Figure 3.4C**), release kinetics were similar but the extents of release were less. PAR4-agonist stimulated release of the three markers was uniformly slower and less extensive (**Figure 3.4D**). Perhaps not surprisingly, these

results imply that the degree of platelet activation is directly reflected in the speed and/or magnitude of cargo release. Weaker agonists such as PAR4-agonist stimulated only partial release while stronger agonists such as thrombin stimulated rapid and nearly complete release of intra-platelet stores of cargo. This is most obvious in the release of lysosomal cargo.

Detection of the selected α-granule cargo

To probe the releasates for specific cargo proteins, custom micro-ELISA arrays were produced. This micro-ELISA configuration allows for simultaneous quantification of multiple proteins from the same releasate sample. The antigens to be detected were chosen based on their proposed functions (growth factor, angiogenic factor, cytokine, *etc.*, **Table 3.1**) and on the availability of suitable antibodies. The sensitivity of detection was in the pg/mL to ng/mL range. The entities probed for are listed in **Table 3.2** are detected through ELISA as described in Chapter Two.

Release of α-granule cargo

The percent release of multiple protein cargo released upon platelet stimulation is represented in **Figure 3.5**. The lowest time point of secretion from platelets that could be analyzed was 15 sec. It has to be kept in mind that the details of cargo release within these 15 sec cannot be addressed by this study due to manual limitation. The data shown in **Figure 3.5** is representative of several individual trials. In this pool of release data, it could be seen that the moieties that are released from platelets within a span of 5 min are released at different rates. The analysis done subsequently involved scrutiny of the rate constants of individual cargo released. Manual observation and mathematical tools served this purpose as will be seen from here on.

Differential release of α-granule cargo

We next sought to qualitatively determine if there were agonist-dependent differences in α-granule cargo release in response to different agonists. Micro-ELISA arrays and our standard assays were used to monitor the release of 30 different cargo molecules (28 are thought to come from α-granules). Platelets were stimulated with

optimized doses of agonists for 5 min and the releasates were probed (**Figure 3.6**).

Twenty nine cargo molecules were detected at least once in the releasates from

thrombin-stimulated platelets (3 trials) while only 17 were detected at least once when

PAR4-agonist was used (2 trials). Twenty seven cargo molecules were detected in

releasates from convulxin-stimulated platelets (2 trials) and PAR1-agonist induced the

release of 23 different cargo molecules (2 trials). Seven were released upon thrombin

stimulation that were not released by PAR1-agonist stimulation. Three were released in

response to thrombin but not in response to convulxin. No cargo molecule was released

only in response to thrombin or only in response to convulxin. When platelets from a

single donor were stimulated with the 4 agonists, thrombin (26 released) and PAR1-

agonist (23 released) induced the release of more proteins than did convulxin (16

released) or PAR4-agonist (17 released). The discordant response to convulxin by

platelets from this single donor is not clearly understood.

When the compositions of the releasates from PAR1- and PAR4-agonist

stimulated platelets were compared, there were clear differences. Eight cargo molecules

were specifically released only in response to PAR1-agonist while only 2 specifically

appeared in the releasates with PAR4-agonist (**Figure 3.6**). There were no obvious

functional patterns to these differences. As an example, release of the 3 angiogenic

regulators (angiostatin, oncostatin M, and angiogenin), were induced by both agonists.

These data show that PAR4-agonist, on average, does not induce release of as many

different molecules as does thrombin, convulxin or PAR1-agonist.

Calculation of release rate constants

The data above offer a qualitative analysis of platelet secretion at a specific time point,

post-stimulation. To more fully characterize platelet secretion and to identify potential

release patterns, we sought a metric that was less affected by the extent of cargo

release and more indicative of the secretion process. Thus, we analyzed the kinetics of

platelet exocytosis by measuring the rate constants describing the release of each cargo

molecule. Agonist-induced, release time-course measurements were made using micro-

ELISA arrays and the data were fit to the function $P_t = P_{max} (1-e^{-K_{ex}t})$ **(1)**. The logic supporting the use of this function is described in Chapter Two. The rates of release of each granule type when platelets were stimulated for 2 min with four different thrombin doses (0.025 - 0.4 U/mL) were calculated (**Figure 3.7**). Thrombin dose *Vs* rate (K_{ex}) graph was plotted. Serotonin release rate was higher than that of PF4, which is followed by β-hexosaminidase. This implies dense granule release > α-granule release > lysosomal release.

Extending this calculation of release rate constant to 28 different cargo molecules involved filtering of available release data. For most α-granule and lysosome cargo, sufficient data was available for good fits to the function with *MSE* < 150. Out of a pool of 174 total kinetic measurements, the data utilized for further analysis passed equation **1** with *MSE* < 150. This step was added to filter the available data. Only 90 out of 174 measurements met the criterion of *MSE* < 150. Representative release fits are shown in the **Figure 3.8**. By extending the criterion to MSE < 250, 106 of 174 granule release measurements could be used. Representatives of such analysis could be seen in **Figure 3.8**, panels **E** and **F**. Note that the *MSE* is >> 1 only because we have transformed the maximum concentration to 100. More typical *MSE* values of < 1 are simply obtained by dividing with 100^2. The criterion *MSE* < 150 is somewhat arbitrary. An inherent sampling error is inevitable as replicate measurements cannot be done at each time point for all cargo molecules on each array. Therefore we cannot statistically confirm whether a fit is acceptable.

Analysis of cargo release kinetics

The calculated K_{ex} values were used as descriptors to compare the release kinetics of different cargo molecules, regardless of the extent to which the cargo was released. Four types of analyses were applied to these values. The first was a simple rank ordering (largest K_{ex} to smallest; fastest to slowest) followed by an, albeit artificial, tertile sorting of the data (**Table 3.3**). We sought to determine if the release rates for a given molecule in response to a specific agonist were in the fastest or slowest third and if

there were patterns in the distribution. When measurements allowed, serotonin release was always in the fastest tertile, regardless of the agonist used. PF4 release was in the fastest tertile in response to 3 (thrombin, convulxin, and PAR1-agonist) of the 4 agonists tested. β-Hexosaminidase release was in the fastest tertile twice as were ANG, CD62P, and MIP1α release. SDF1α, TGFβ, EGF, MIP1δ, GROα, IL-1α, IL-1β, TNFβ and TIMP4 were at least found twice in the slowest tertile. PDGF release was in the middle tertile in response to 3 of the 4 agonists (convulxin, PAR1 and PAR4-agonists). Angiostatin and TARC release showed no consistent pattern and ranked in each of 3 tertiles in response to the 4 agonists used. There were no obvious patterns to how molecules were released. Illustrative of this, release of the angiogenic regulators, angiogenin, angiostatin, and oncostatin M were distributed in all 3 tertiles.

We next determined if the release rates correlated to any biochemical property of the cargo molecules. We plotted K_{ex} versus molecular weight (**Figure 3.9**), relative abundance (**Figure 3.10**), and isoelectric point (as a metric of relative charge; **Figure 3.11**). Linear regression analysis of these data showed no R^2 values that reached significance. This indicated that the release rates, as measured by K_{ex} values, did not directly correlate to any of these three biochemical properties. Of note, K_{ex} values did not show linear relationship with relative abundance, suggesting that platelet secretion is not simply a function of cargo concentration or abundance.

Probability density function analysis

A probability density function (*pdf*) is a scaled histogram function where the area under the curve is made to equal 100. This analysis included 90 K_{ex} values (MSE <150) shown by the bars in **Figure 3.12**. The heavy black curve is the 3-Gaussian function fit and the colored dashed curves are the individual Gaussian functions (**Figure 3.12** top panel). The means of the 3 Gaussians are 0.010, 0.067, and 0.148 s^{-1}. Similar distribution was seen when the larger dataset of K_{ex} values (MSE <250) was used (**Figure 3.12**, bottom panel). These results suggest that the release rates cluster into 3 classes with distinct means. Serotonin, when accurate measurements were made, was always in the

fastest class (**Figure 3.13**). TNFβ was in the slowest class in response to three of the four agonists. Release of TNFα, IL-1β, or EGF (when detectible) was always in the slowest class. TNFβ, angiostatin, PF4, and β-hexosaminidase release showed no consistent pattern and ranked in each of the three classes in response to the four agonists used. TNFβ release was in the fastest class once and the slowest class three times. As with the ranked-tertile analysis, no obvious functional patterns were detected. Release of the angiogenic regulators, angiostatin, VEGF, and oncostatin M were either in the middle or in slowest class while release of angiogenin occurred in all three classes. From this analysis, we conclude that there are three kinetically-distinct classes of cargo release.

Operator variance analysis

To confirm our conclusions, we examined how operator variance would affect the values of K_{ex} using the procedure described in Chapter Two. The questions posed were: (1) how many cargo classes are there and (2) what are the mean K_{ex} values for each class. **Figure 3.14** shows the distribution of the calculated K_{ex} values (*open symbols*) assuming 3 cargo classes with K_{ex} values equaling the mean values obtained from the 3-Gaussian distributions in **Figure 3.12**. The K_{ex} values used were 0.010, 0.067 and 0.148 s^{-1}. The *solid symbols* are from the 90 K_{ex} values obtained from our experiments. The *Index* is simply the ordinal number of the K_{ex} value. There is overlap of the experimental and simulated K_{ex} values in the low and high index ranges but not in the middle range. To obtain a better overlap, we adjusted the middle rate constant to 0.033 s^{-1}. **Panel B** shows that this adjustment produces a much better overlap. Assuming 2 cargo classes with K_{ex} = 0.010 s^{-1} and 0.148 s^{-1} results in the distribution shown in **panel C**. The "breaks" in the simulated and actual K_{ex} distributions occur at different places. Changes in K_{ex} did not improve the overlap. This result supports the F-test result (noted in Chapter Two) indicating that the 3-Gaussian fit is statistically superior to the 2-Gaussian fit.

The distributions in the **panels A, B,** and **C** were generated using σ_{op} = 0.2. To estimate the operator variance we changed σ_{op} between 0 and 0.3. **Panel D** shows the result when σ_{op} = 0.1 and K_{ex} = 0.010, 0.033 and 0.148 s^{-1}. The overlap is poorer

compared to **panel *B*** and, notably, the breaks in the distributions occur at different indices. σ_{op} = 0 produces 3 discontinuous horizontal distributions at K_{ex} = 0.010, 0.033 and 0.148 s^{-1}. When σ_{op} = 0.3, the data was so poor that we could not fit the data to equation (**1**). Therefore, the operator variance is between 0.1 and 0.3, and most likely 0.2.

Cargo molecules do not consistently associate with one class

To determine if a cargo molecule was consistently released *via* one kinetic class, we examined the K_{ex} values of 9 cargo molecules that were detected in 4 or more experiments. The K_{ex} values are given in **Table 3.4**. The last row is the ratio *r* of the largest to smallest K_{ex} value for that cargo molecule. If a cargo molecule is always present in one kinetic class then *r* would be ~1. However, *r* ranges from about 3 to 80. TNFα has the smallest *r* value of 3.3 with the smallest K_{ex} equaling 0.0210 and the largest 0.0691 s^{-1}. The larger K_{ex} is likely to be part of the fast kinetic class whose mean value is 0.148 s^{-1} while the smaller 3 K_{ex} values are likely to be part of the medium class whose mean is 0.033 s^{-1}. Angiogenin, PDGF, and serotonin appear in the fast and medium classes while angiostatin, SDF1α, TNFβ, and PF4 appear in all 3 classes.

Agonists do not activate only one cargo class

If an agonist were to activate only a single cargo class, then the K_{ex} values measured with that agonist would cluster about a single value. To test this hypothesis, we generated *pdf*s of K_{ex} values obtained in experiments where the platelets were stimulated with thrombin, PAR1-agonist, or convulxin. We did not use the PAR4-agonist data because the number of acceptable K_{ex} values (n=11) was too small for a sensible *pdf.* We had 43 K_{ex} values for thrombin, 19 for PAR1-agonist and 17 for convulxin. **Figure 3.15** shows the *pdf*s for the 3 agonists. The 3 Gaussian functions used to generate the best-fit distribution in **Figure 3.12** are superimposed on the *pdf*s. The individual *pdf*s follow approximately the 3 Gaussian functions suggesting that the 3 agonists activate all 3 cargo classes.

Discussion

The presented work is the first systematic analysis of human platelet secretion in which the release kinetics of multiple cargo molecules is examined. We simultaneously measured the time-dependent release of 30 distinct molecules from platelets stimulated separately with 4 different agonists. Agonist concentrations were chosen to maximize release and to minimize the ambiguities of partial platelet activation. Our qualitative analysis (**Figure 3.6** and **Table 3.3**) shows that the extent and rate of release are related to agonist potency: thrombin induced the most rapid release of the highest number of cargo molecules and the PAR4-agonist induced the slowest, least extensive release. There were no overt functional patterns in what was released when comparing the responses to the four agonists tested. Release speed (as represented by K_{ex}) did correlate with agonist potency (and agonist dose, data not shown) but not with molecular weight, charge, or abundance of the cargo (**Figures 3.9-3.11**). Our quantitative analyses of the distribution of K_{ex} values indicated that platelet secretion could be minimally described as the summation of 3, kinetically-distinct classes of release events (**Figure 3.12**). Distribution of cargo into these kinetic classes did not correlate with overt functional patterns. A recent report (*Kamykowski et al.*, 2011), suggests that α-granule cargo are stochastically packaged into subdomains within single granules, not segregated into specific granule subclasses. If packaging is random, then one might expect that platelet cargo release is a stochastic process controlled by other factors such as granule-plasma membrane fusion rates. Our data are consistent with that expectation.

Platelets have the potential to control the vascular microenvironment through the myriad molecules they secrete upon activation (*Brass*, 2010). The work of Italiano *et al* (*Italiano et al.*, 2008) and others (*Chatterjee et al.*, 2011; *Ma et al.*, 2005) suggested that pro- and anti-angiogenic factors could be differentially released in response to specific agonists. In general, these studies measured secretion at single time points (or agonist concentrations) making them difficult to compare with the kinetic measurements presented here. It is possible that the observed release heterogeneity

could be a function of partial platelet activation. Based on a detailed examination of our secretion time-courses and agonist titrations, one could devise specific conditions that could result in what appears to be thematically-differential release of platelet cargo. These conditions represent specific stages in the activation process and may not reflect the continuum of events occurring in a growing thrombus. Our choice of reaction conditions limited this variable and focused our analysis on the secretion process. At the site of vascular damage, the extent of platelet activation may be stratified and thus granule release may vary both spatially and temporally. Future studies of *in situ* platelet secretion are needed to fully understand platelet exocytosis; however, our data suggest that focus should be placed on the kinetics of the process.

Our analyses suggests that platelet release is best described as the summation of at least three classes of release processes differing in rate even though the distribution of cargo into each class is random. To conceptualize this we use a postal system analogy. The mailmen are the platelets delivering the granule cargo (the mail). There are three mail classes: Express, 1st Class and Bulk; each arriving at different rates. Serotonin, in dense granules, was the only true Express cargo; other α-granule cargo was distributed into all three classes. This implies that, aside from serotonin, the mail sorters are blinded to content and thus inclusion into each of the three mail classes is random. Random sorting of α-granule cargo is consistent with the lack of thematic co-localization of cargo reported by Storrie and colleagues (*Kamykowski et al.*, 2011; *Sehgal and Storrie*, 2007). The distinction between dense (*i.e.* serotonin) and α-granule cargo is also consistent with the fact that two distinct sorting machinery are required to make the two classes of granules (*Bonifacino*, 2004). How kinetic heterogeneity in α-granule cargo release is generated remains to be determined.

Simplistically, regulated exocytosis is the stimulation-dependent fusion of spherical, cargo-containing granules with the plasma membrane. A variation on this, compound fusion, occurs when granules fuse with each other prior or subsequent to fusion with the plasma membrane. The granules can be homogeneous (*e.g.* synaptic

vesicles in neurons) or heterogeneous (*e.g.* azurophil, peroxidase negative, *etc.* granules in neutrophils). In homogeneous systems, release occurs with two general kinetic components: burst and sustained. The rapid, burst phase represents vesicles that are docked with their secretory machinery primed for fusion (as perhaps seen for dense granules). The sustained phase represents release from vesicles that must be recruited to fusion sites. In heterogeneous systems, the different granule populations are thought to have distinct properties. At a first approximation, platelets are examples of the latter class. Dense granule release is more rapid than α-granule or lysosome release; a trend that held true for all agonists tested here (**Figure 3.4** and **3.13**). Since release from all three granules requires the same SNAREs (VAMP-8 (*Ren et al.*, 2007), SNAP-23 {Chen, 2000 #97;Chen, 2000 #107;Flaumenhaft, 1999 #101;Lemons, 2000 #106}, and syntaxin-11 (*Ye et al.*, 2012)) and at least two of the same SNARE regulators (Munc18b (*Al Hawas et al.*, 2012) and Munc13-4 (*Ren et al.*, 2010)) it is unclear how secretory machinery usage explains the observed differences. However, loss of VAMP-8 has a greater effect on PF4 release (*Ren et al.*, 2007). Deletion of Munc13-4 has a greater effect on serotonin release (*Ren et al.*, 2010). Loss of syntaxin-11 (*Ye et al.*, 2012) or Munc18b (*Al Hawas et al.*, 2012) affected serotonin and PF4 release more than β-hexosaminidase release. Thus differential use or regulation of the same secretory machinery could account for differences between the three granule populations. Alternatively, the underlying kinetic patterns might reflect the types of membrane fusion. Platelet granules (specifically α-granules) do undergo compound fusion during the exocytosis process (*Valentijn et al.*, 2010). The rates of these two types of membrane fusion (primary and compound) could partially account for the differential release kinetics, reported here. Another possibility may relate to the distribution of cargo proteins. Cargo is heterogeneously distributed inside a granule (*van Nispen tot Pannerden et al.*, 2010) and differential solubilization of these "cargo clusters", once granule and plasma membranes fuse, could underlie release heterogeneity. These explanations (as are our mathematical analyses) are based on the concept that platelet granules are spherical, like synaptic vesicles. Recent ultra structural analysis (*van Nispen tot Pannerden et al.*, 2010) indicates that α-granules may in fact be

tubular and thus their fusion could be polarized. Fusion at one end of a tube might cause differential release rates as the tube empties, depending on where in the tube the cargo resides. At this stage it is impossible to be more than speculative about the mechanism(s) until more "real-time" *in situ* measurements of platelet cargo release are obtained. Though these data provide insight into how platelets release their cargo, still a lot has to be learned.

Table 3.1. Cargo molecules probed in the secretion assays

		Symbol	Cargo Name
Growth Factors		bFGF	Basic Fibroblast Growth Factor
		EGF	Epidermal Growth Factor
		PDGF	Platelet Derived Growth Factor
		SDF1α	Stemcell Derived Factor - 1 α
		TPO	Thrombopoietin
Angiogenic Factors	Anti	ANS	Angiostatin
		OSM	Oncostatin M
	Pro	ANG	Angiogenin
		VEGF	Vascular Endothelial Growth Factor
Cytokines/Chemokines		CD40L	Cluster of Differentiation 40 Ligand
		CD62P	Cluster of Differentiation 62 Protein/ P - selectin
		GROα	Growth Related Oncogene - α
		IL-1α	Interleukin - 1 α
		IL-1β	Interleukin - 1 β
		IL-8	Interleukin - 8
		MCP2	Monocyte Chemoattractant Protein - 2
		MCP3	Monocyte Chemoattractant Protein - 3
		MIP1α	Macrophage Inflammatory Protein-1 α
		MIP1δ	Macrophage Inflammatory Protein-1 δ
		RANTES	Regulated upon Activation, normal T-cell expressed, and presumably secreted
		TARC	Thymus And Activation Regulated Chemokine
		TGFβ	Transforming Growth Factor - β
		MMP2	Matrix Metallo Proteinase - 2
		MMP9	Matrix Metallo Proteinase - 9
		TIMP4	Tissue Inhibitor of Metalloproteinase - 4
		TNFα	Tumor Necrosis Factor - α
		TNFβ	Tumor Necrosis Factor - β
Standard Markers of Secretion		PF4	Platelet Factor 4
		Serotonin	5 Hydroxy Tryptamine
		β hexo	β - Hexosaminidase

Listed are the cargo molecules probed on the micro-ELISA arrays. Their abbreviated names (**Symbol**) are indicated in the middle column. The cargo molecules are grouped according to their proposed functions (left-most column).

Table 3.2. Detection ranges of the probed cargo molecules

Linear Range of Antibody Array

Antigen (pg/ml)	Minimum	Maximum
bFGF	**123**	10,000
CD40L	1235	100000
EGF	2	200
GROα	617	50000
IL-1α	25	2000
IL-8	12	1000
MCP2	25	2000
MCP3	247	20000
MIP1α	123	10,000
MIP1δ	123	10,000
MMP2	1235	100000
MMP9	247	20000
PDGF	25	2000
SDF1α	1235	100000
TGFβ	1235	100000
TNFα	25	2000
TNFβ	617	50000
TPO	1235	100000
ANG	74	6000
ANS(ng/ml)	12	1000
IL-1β	25	2000
OSM	123	10,000
PF4	123	10,000
P-selectin	123	10,000
RANTES	123	10,000
TARC	123	10,000
TIMP4	617	50000
VEGF	123	10,000

The maximum and the minimum concentrations (pg/mL; except for ANG, which is listed as ng/mL) of the released cargo detectible by the micro-ELISA arrays are indicated. These values are based on the standard curves generated for each cargo antigen.

Table 3.3. Tertile ranking of K_{ex} values

Thrombin		Convulxin		PAR1		PAR4	
Serotonin	0.1501	MIP1α	0.2385	PF4	0.1414	MCP3	0.1914
ANG	0.1038	MMP9	0.1468	CD62P	0.1266	Serotonin	0.0599
MCP2	0.1024	CD62P	0.0898	β hexo	0.1112	ANG	0.0247
PDGF	0.0939	OSM	0.0761	TARC	0.1091	PDGF	0.0164
TNFβ	0.0887	β hexo	0.0739	SDF1α	0.1007	CD62P	0.0131
MMP2	0.0660	PF4	0.0371	PDGF	0.0738	PF4	0.0085
ANS	0.0635	IL-1α	0.0333	ANG	0.0673	β hexo	0.0061
MIP1α	0.0612	ANG	0.0307	GROα	0.0616	TNFβ	0.0044
PF4	0.0589	TARC	0.0262	MCP2	0.0425	IL-1α	0.0039
TPO	0.0550	PDGF	0.0260	IL-8	0.0327	SDF1α	0.0027
RANTES	0.0531	MIP1δ	0.0237	IL-1α	0.0225		
CD62P	0.0519	TNFα	0.0228	ANS	0.0206		
MCP3	0.0424	TNFβ	0.0207	TNFβ	0.0175		
OSM	0.0414	ANS	0.0194	TIMP4	0.0103		
TNFα	0.0388	TGFβ	0.0194	VEGF	0.0094		
β hexo	0.0357	TPO	0.0143	IL-1β	0.0090		
CD40L	0.0326	IL-1β	0.0126	OSM	0.0055		
SDF1α	0.0316	MMP2	0.0122				
bFGF	0.0272	RANTES	0.0114				
IL-8	0.0200	EGF	0.0046				
TGFβ	0.0195	GROα	0.0034				
EGF	0.0190						
MIP1δ	0.0169						
GROα	0.0158						
TARC	0.0154						
TIMP4	0.0054						

Human platelets (1.2×10^9 /mL) were prepared as described and stimulated with thrombin (0.3 U/mL; n = 3), convulxin (0.3 µg/mL; n = 2), PAR1-agonist (50 µM; n = 2), or PAR4-agonist (500 µM; n = 2) for 5 min. Releasates were probed using micro-ELISA arrays to obtain the rate constant K_{ex} for each cargo molecule. The average K_{ex} value was calculated for each cargo released upon stimulation of platelets with each agonist. The cargo was grouped into tertiles with no bias, based on K_{ex} values in descending order. The cargo in blue fall into fastest tertile, in green are the intermediate tertile, and the red category belong to the slowest tertile.

Table 3.4. Representation of cargo packaging by kinetics of release

Cargo	Angiogenin	Angiostatin	PDGF	SDF1α	TARC	TNFα	TNFβ	Serotonin	PF4
K_{ex} Values	0.0247 0.0266 0.0349 0.0466 0.0674 0.1321 0.1326	0.0024 0.0125 0.0288 0.0365 0.0635	0.0214 0.0306 0.0480 0.0728 0.0747 0.1398	0.0027 0.0292 0.0340 0.0370 0.1644	0.0103 0.0205 0.0262 0.1091	0.0210 0.0288 0.0263 0.0691	0.0019 0.0176 0.0207 0.0239 0.1535	0.0264 0.0672 0.0934 0.1657 0.2176	0.0083 0.0086 0.0390 0.0645 0.0732 0.1299 0.1529
r	**5.37**	**26.86**	**6.52**	**62.00**	**10.57**	**3.29**	**79.73**	**8.23**	**18.32**

Listed are the K_{ex} values of 9 different cargo molecules found in 4 or more releasate trials. The last row represents the ratio, *r*, of the largest to the smallest K_{ex} of the corresponding cargo.
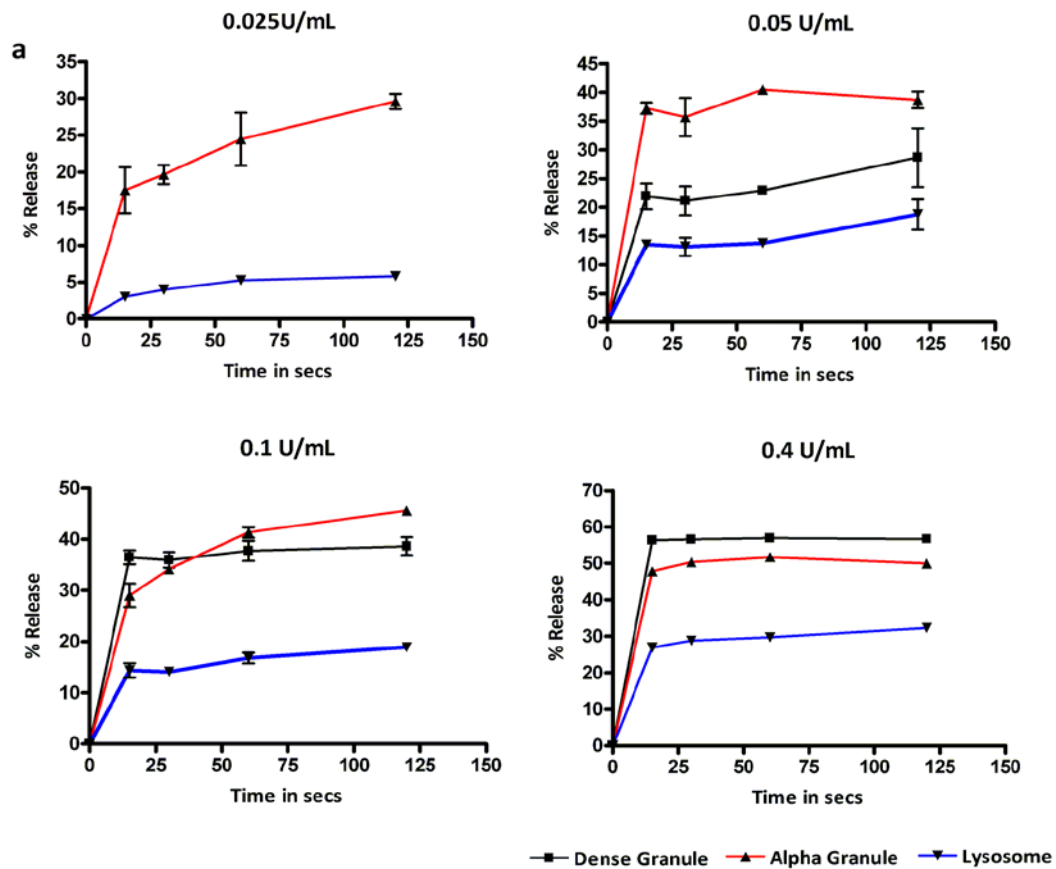
Figure 3.1. Thrombin dose dependence of granule release

Human platelets ($3×10^8$ /mL) were prepared as described and the samples were stimulated with 0.025 U/mL, 0.05 U/mL , 0.1 U/mL and 0.4 U/mL thrombin as represented in panels **a**, **b, c** and **d** respectively. The reaction was carried over 2 min with intermittent time points. Thrombin stimulation was stopped with 0.05 U/mL, 0.1 U/mL, 0.2 U/mL and 0.8 U/mL hirudin respectively, followed by centrifugation. Release from the three classes of granules was measured using the marker cargo molecules: [^{3}H]-serotonin for dense granules (black), PF4 for α-granules (red) and β-hexosaminidase for lysosomes (blue). Percent release was calculated using the equation [(Releasate)/ (Pellet + Releasate)] x 100. Measurements at each time point for each thrombin dose were done in triplicate, and the averages with standard deviations are indicated.
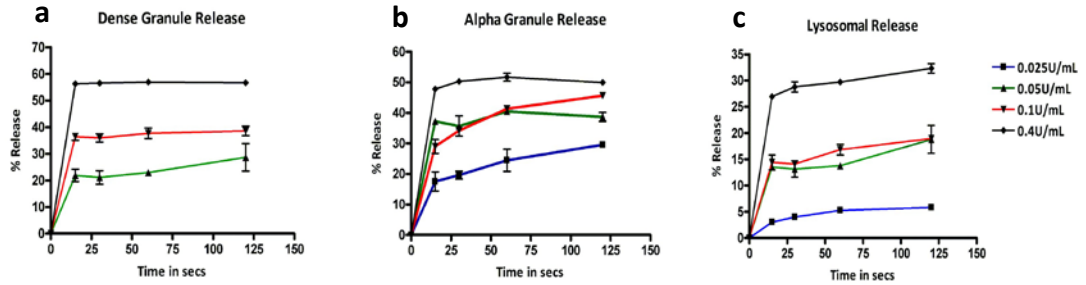
Figure 3.2. Granule exocytosis from platelets

Human platelets (3×10^8 /mL) were prepared as described and the samples were stimulated with 0.025 U/mL (blue,   ), 0.05 U/mL (green, ▲), 0.1 U/mL (red, ▼) and 0.4 U/mL (black, ◆) thrombin as represented in panels **a**, **b** and **c**. The reaction was carried over 2 min with intermittent time points. Thrombin stimulation was stopped with 0.05 U/mL, 0.1 U/mL, 0.2 U/mL and 0.8 U/mL hirudin respectively, followed by centrifugation. Release from the three classes of granules was measured using the marker cargo molecules: [^{3}H]-serotonin for dense granules (**a**), PF4 for α-granules (**b**) and β-hexosaminidase for lysosomes (**c**). Percent release was calculated using the equation [(Releasate)/ (Pellet + Releasate)] x 100. Each time point, at each thrombin dose was measured in triplicate and the averages with standard deviations are indicated.
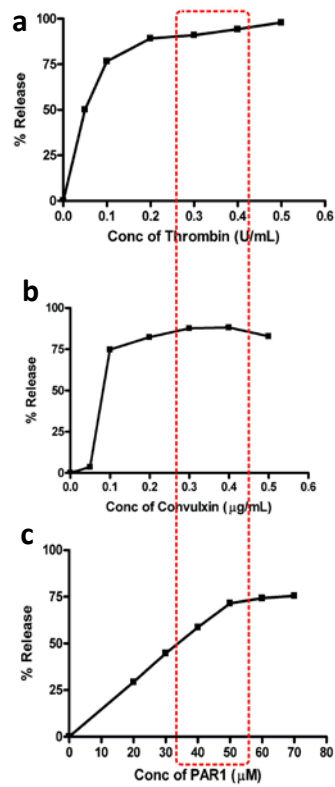
Figure 3.3. Agonist titration

Fresh human platelets were isolated (1.2×10^9 /mL) after incubating them with [^{3}H]-serotonin for 45 min. They were stimulated with increasing doses of thrombin (**a**), convulxin (**b**) or PAR1 (**c**). The reaction was stopped with hirudin at the end of 2 min in (**a**). For convulxin and PAR1 treated samples the reactions were stopped by centrifugation. Percent release was calculated using the equation [(Releasate)/ (Pellet + Releasate)] x 100 (see Chapter Two)*.*
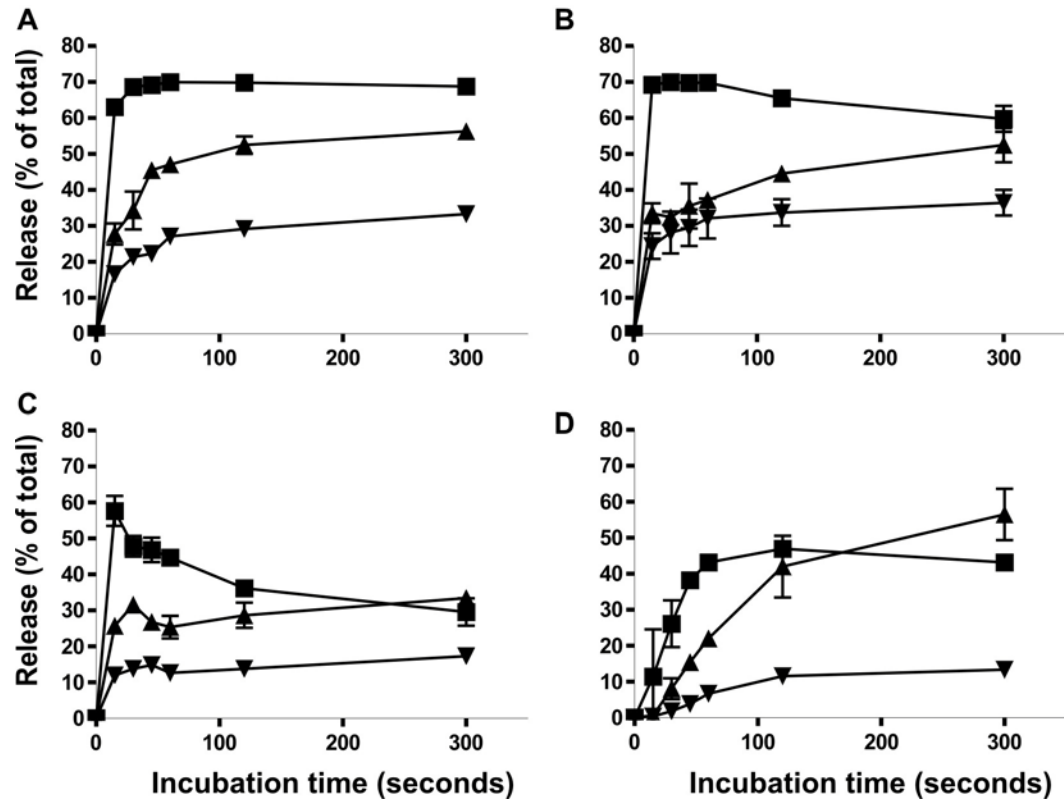
Figure 3.4. Time course of release from activated platelets

Human platelets (1.2×10^9 /mL) were prepared as described and were stimulated with thrombin (0.3 U/mL, **A**), convulxin (0.3 µg/mL, **B**), PAR1-agonist (50 µM, **C**), or PAR4-agonist (500 µM, **D**) for the indicated times. Thrombin stimulation was stopped with hirudin (0.6 U/mL) followed by centrifugation; the rest of the reactions were stopped by centrifugation and the releasates were recovered. Release from the three classes of granules was measured using the marker cargo molecules: [^{3}H]-serotonin for dense granules (■), PF4 for α-granules (▲) and β-hexosaminidase for lysosomes (▼). Percent release was calculated using the equation [(Releasate)/ (Pellet + Releasate)] x 100. Each time point was measured in triplicate and the averages and standard deviations are indicated.
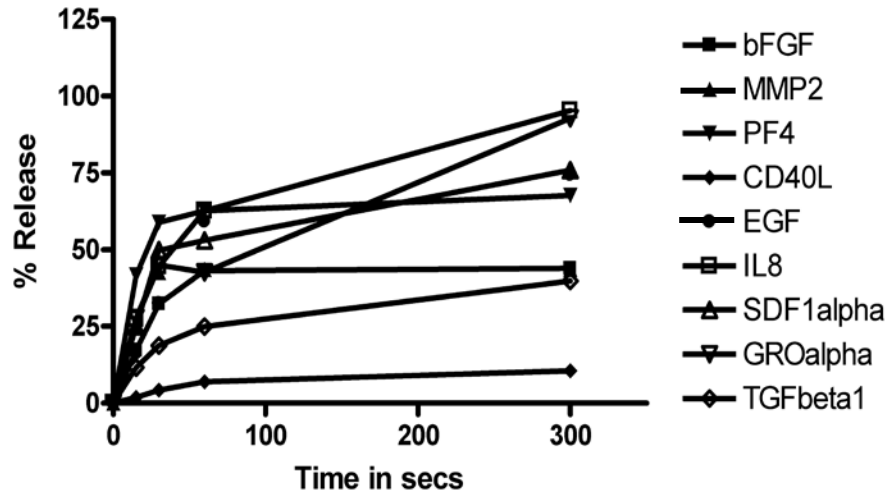
Figure 3.5. Release pattern followed by different cargo molecules

Human platelets (1.2×10^9 /mL) were prepared as described and were stimulated with thrombin (0.3 U/mL) and the reaction was stopped with hirudin (0.6 U/mL) followed by centrifugation. Releasates obtained at different time points were used to probe for the moieties indicated using micro-ELISAs. Percent release was calculated using the equation [(Releasate)/ (Pellet + Releasate)] x 100.

Cargo	Cumulative data				Single donor				PAR1/PAR4				Relative Abundance
	T	P-1	P-4	C	T	P-1	P-4	C	P-1	P-1	P-4	P-4	
GROα													388,082
PF4													132,756
RANTES													21,745
TGFβ													15,461
TNFβ													8,874
ANS													7,644
SDF1α													3,202
CD62P													1,715
PDGF													1,386
TARC													1,029
CD40L													876
MCP3													696
ANG													668
TNFα													589
bFGF													500
TIMP4													419
MIP1α													201
IL-8													134
MMP2													126
TPO													79
IL-1α													77
IL-1β													40
VEGF													39
MIP1δ													33
EGF													18
MMP9													17
OSM													17
MCP2													3
Serotonin													
β hexo													

Figure 3.6. Cargo release in response to different agonists

Human platelets (1.2×10^9 /mL) were prepared as described and were stimulated with thrombin (0.3 U/mL, **T**; n = 3), convulxin (0.3 µg/mL, **C**; n = 2), PAR1-agonist (50 µM, **P-1**; n = 2), or PAR4-agonist (500 µM, **P-4**; n = 2) for 5 min. Releasates were then probed using the micro-ELISA arrays and the presence (gray square) or absence (white square) of a given cargo molecule was recorded. **Cumulative data** indicates whether a cargo was released at least once in any of the secretion trials performed with the indicated agonist. **Single donor** indicates the cargo released by platelets from a single donor in response to different agonists. **PAR1/PAR4** indicates a direct comparison of the data for cargo release in response to stimulation of either the PAR1 or the PAR4 receptor. **Relative abundance** indicates the number of molecules of each cargo per resting platelet and was measured using the micro-ELISA arrays.
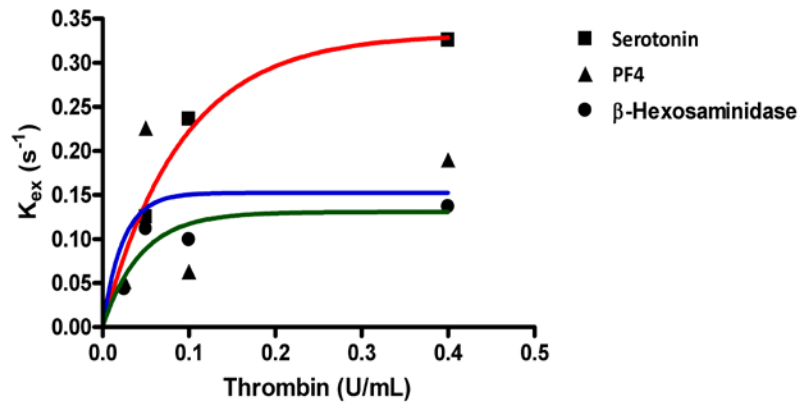
Figure 3.7. Rates of release of granule markers

Human platelets (3×10^8 /mL) were prepared as described. The rates of release of each granule type when platelets were stimulated for 2 min with four different thrombin doses (0.025 - 0.4 U/mL) were calculated [[^{3}H]-serotonin for dense granules (red), PF4 for α-granules (blue) and β-hexosaminidase for lysosomes (green)]. Thrombin dose *Vs* rate (K_{ex}) graph was plotted.
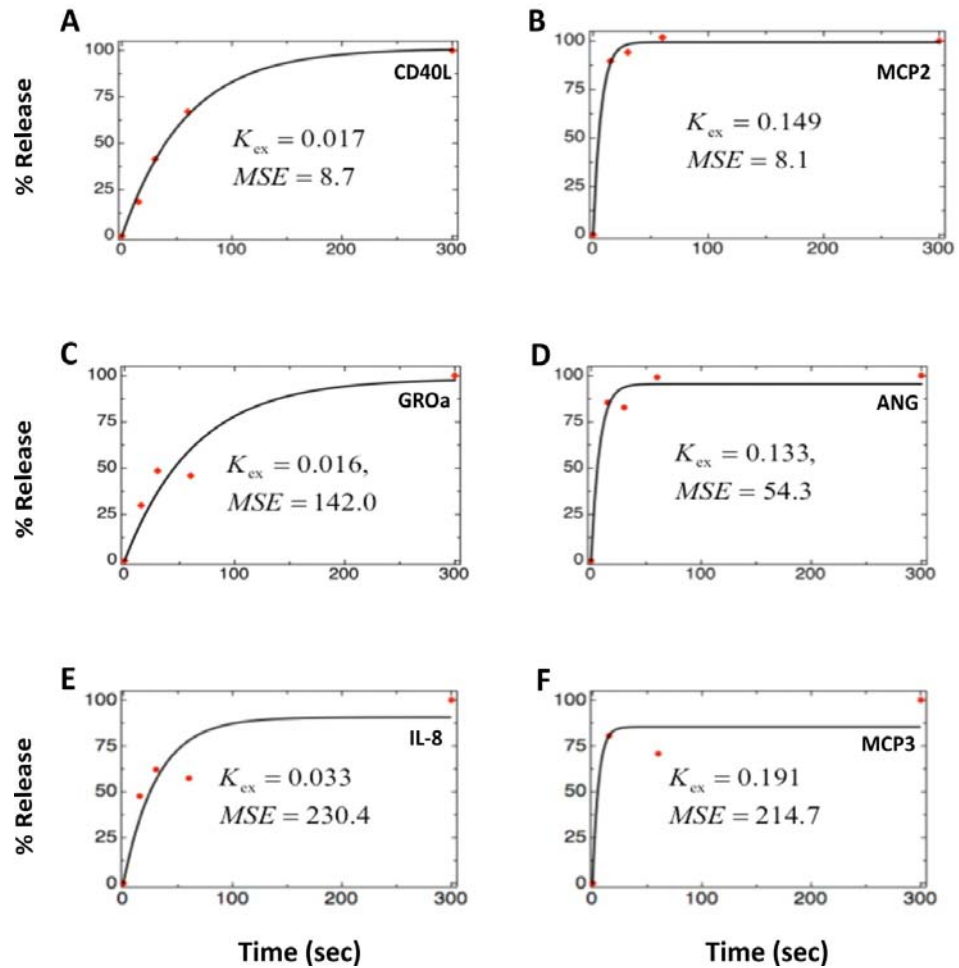
Figure 3.8. Fitting of the granule release data

The curves represent results of our measurements taken at t=0, 15, 30, 60, and 300 sec and fit to equation **1** with *MSE* < 150 (**A-D**) and *MSE* < 250 (**E** and **F**). Panels **A** and **B** show release curves with good fits (thrombin stimulated release of CD40L and MCP2, respectively). Panels **C** and **D** release curves with fits closer to *MSE* = 150 (thrombin stimulated release of GROα and angiogenin, respectively). Of 174 different granule release measurements, 90 had *MSE* < 150. Panels **E** and **F** show release curves with fits closer to *MSE* < 250 (PAR1-agonist stimulated release of IL-8 and PAR4-agonist stimulated release of MCP3, respectively). Of 174 different granule release measurements, 106 had *MSE* < 250.
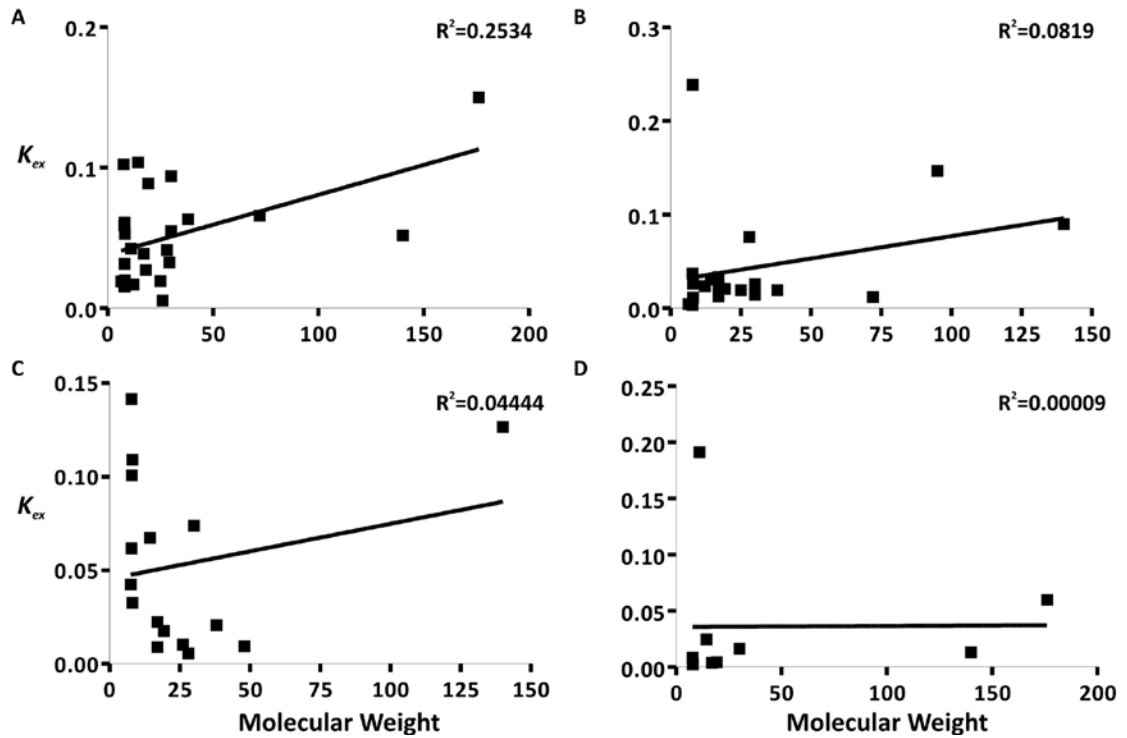
Figure 3.9. K_{ex} values do not correlate with the molecular weights

The average K_{ex} values for release of each cargo in response to stimulation with thrombin (0.3 U/mL, **A**), convulxin (50 µg/mL, **B**), PAR1-agonist (50 µM, **C**), or PAR4-agonist (500 µM, **D**) were plotted versus the molecular weights of the corresponding cargo molecule. Linear regression analysis was used to determine if any correlations exist between K_{ex} and molecular weight. No R^2 values reached significance.
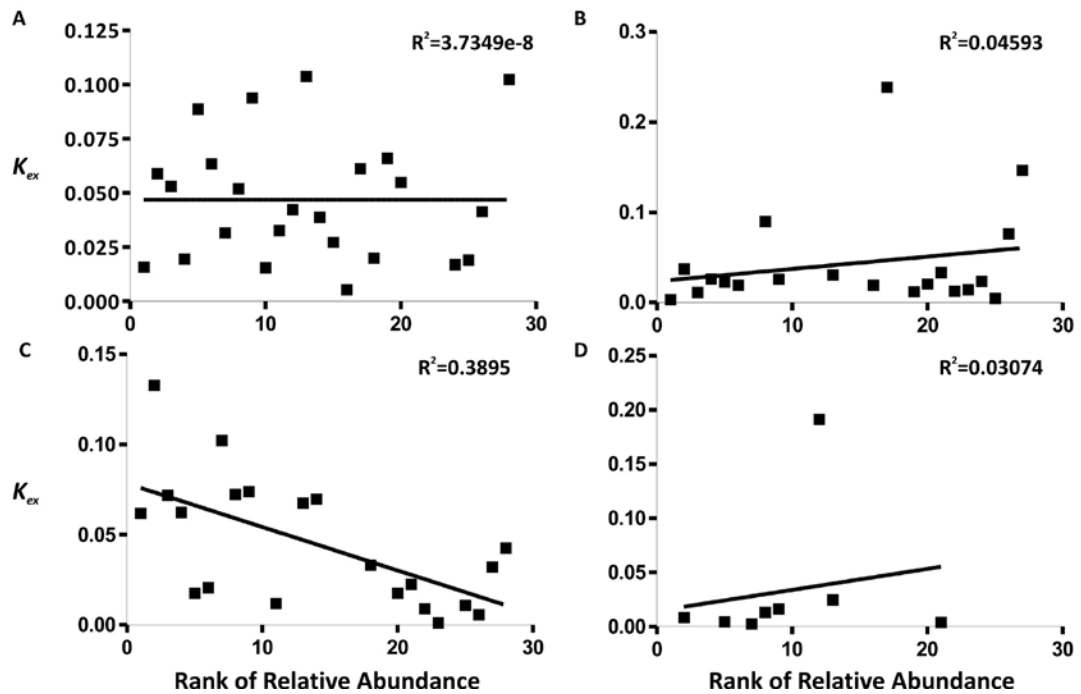
Figure 3.10. K_{ex} values do not correlate with the relative abundance

The average K_{ex} values for release of each cargo in response to stimulation with thrombin (0.3 U/mL, **A**), convulxin (50 μg/mL, **B**), PAR1-agonist (50 μM, **C**), or PAR4-agonist (500 μM, **D**) were plotted versus the ranked order of abundance of the corresponding cargo molecule. Linear regression analysis was used to determine if any correlations exist between K_{ex} and relative abundance. No R^2 values reached significance.
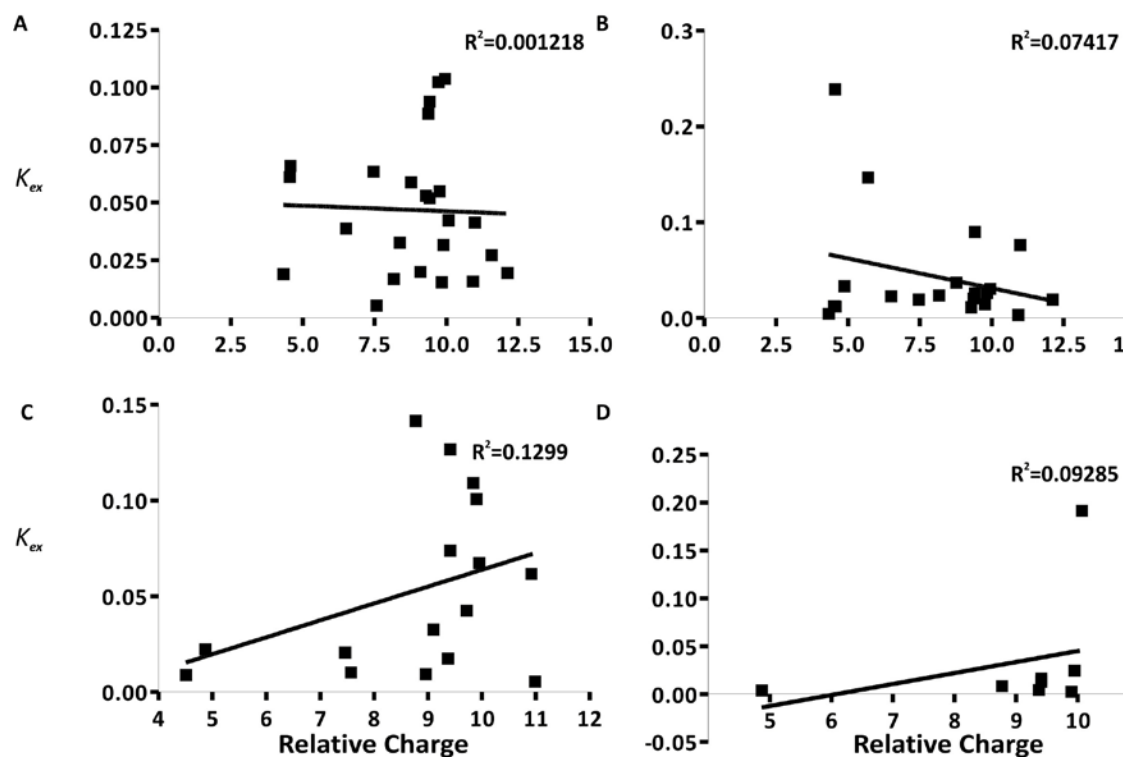
Figure 3.11. K_{ex} values do not correlate with the relative charge

The average K_{ex} values for release of each cargo in response to stimulation with thrombin (0.3 U/mL, **A**), convulxin (50 μg/mL, **B**), PAR1-agonist (50 μM, **C**), or PAR4-agonist (500 μM, **D**) were plotted versus the isoelectric points of the corresponding cargo molecules (represented as relative charge). Linear regression analysis was used to determine if any correlations exist between K_{ex} and the isoelectric point. No R^2 values reached significance.
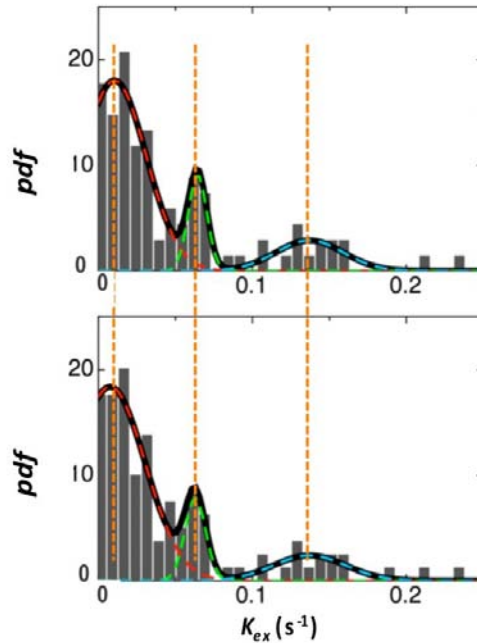
Figure 3.12. Comparative pdf of K_{ex} values from MSE, 150 and MSE < 250 datasets

Human platelets (1.2×10^9 /mL) were prepared as described and were stimulated with thrombin (0.3 U/mL; n = 3), convulxin (0.3 µg/mL; n = 2), PAR1-agonist (50 µM; n = 2), or PAR4-agonist (500 µM; n = 2) for increasing times. Releasates were probed using the micro-ELISA arrays and the rate constant, K_{ex} of release was calculated for each cargo molecule. The pool of K_{ex} values with *MSE* < 150 (**top panel;** 90/174) or *MSE* < 250 (**bottom panel;** 106/174) were used for constructing the *pdf* with a bin width of 0.0075. The best fit curve is seen in black corresponding to the existence of three different sub-classes. The dashed blue, green and red curves are the Gaussian functions that represent fast, intermediate and slow classes, respectively.

Thrombin		Convulxin		PAR1		PAR4	
Serotonin	0.1501	MIP1α	0.2385	PF4	0.1414	Serotonin	0.0599
ANG	0.1038	MMP9	0.1468	CD62P	0.1266	ANG	0.0247
MCP2	0.1024	CD62P	0.0898	β hexo	0.1112	PDGF	0.0164
PDGF	0.0939	OSM	0.0761	TARC	0.1091	PF4	0.0085
TNFβ	0.0887	β hexo	0.0739	SDF1α	0.1007	β hexo	0.0061
MMP2	0.0660	ANG	0.0307	PDGF	0.0738	IL-1α	0.0039
ANS	0.0635	TARC	0.0262	ANG	0.0673	SDF1α	0.0027
MIP1α	0.0612	PDGF	0.0260	GROα	0.0616	TNFβ	0.0019
PF4	0.0589	TNFα	0.0228	IL-1α	0.0225		
RANTES	0.0531	TNFβ	0.0207	ANS	0.0206		
P-selectin	0.0519	ANS	0.0194	TNFβ	0.0175		
TPO	0.0503	IL-1β	0.0126	TIMP4	0.0103		
MCP3	0.0424	MMP2	0.0122	VEGF	0.0094		
TNFα	0.0388	RANTES	0.0114	IL-1β	0.0090		
β hexo	0.0357			OSM	0.0055		
SDF1α	0.0316						
bFGF	0.0272						
IL-8	0.0200						
TGFβ	0.0195						
EGF	0.0190						
CD40L	0.0172						
MIP1δ	0.0169						
GROα	0.0158						
TARC	0.0154						
TIMP4	0.0054						

Figure 3.13. Distribution of K_{ex} values

The rate constants K_{ex} were calculated as described and the average was obtained for each from multiple trials involving various agonists for stimulating the platelets. The values are divided into three different classes represented by different colors based on their distribution in *pdf* in **Figure 3.12**. The cargo in blue, green and red correspond to the fast, intermediate and slow classes, respectively.
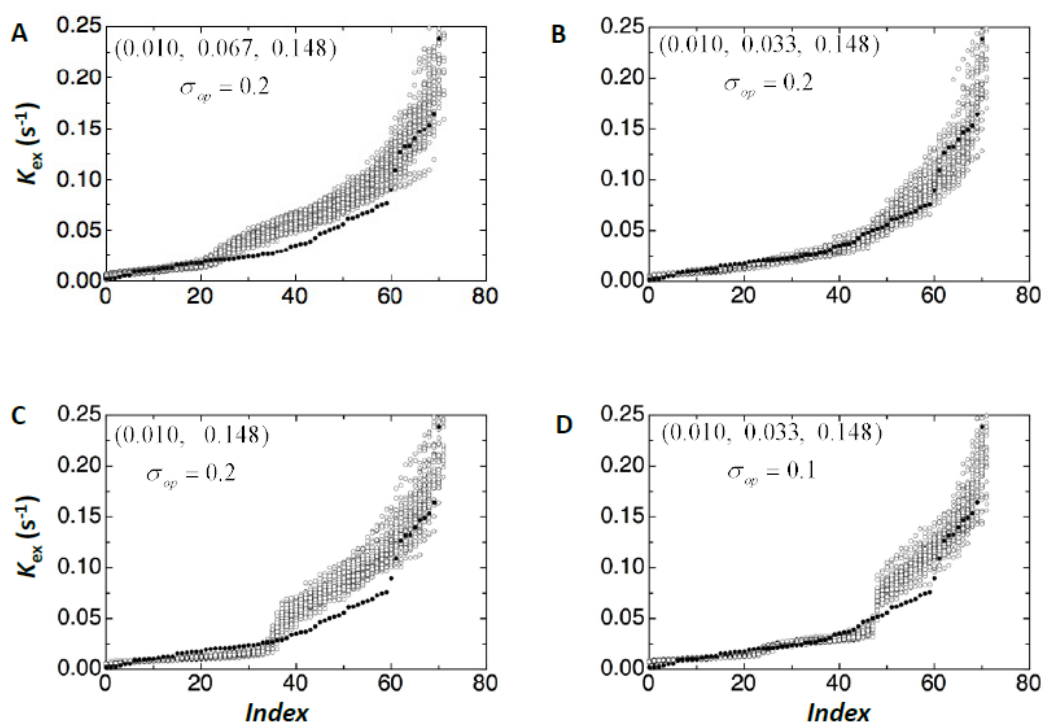
Figure 3.14. Cargo characteristics from modeling operator variance

The distribution of the simulated K_{ex} values (*open symbols*) assuming 3 (**A, B, D**) or 2 (**C**) cargo classes with K_{ex} values equaling the mean values obtained from the 3-Gaussian fit shown in **Figure 3.12** is shown. The *closed symbols* are the 90 K_{ex} values obtained from our experimental measurements. The *Index* is simply the ordinal number of the K_{ex} value. The rate constants and the operator variances used for the analysis are varied in different panels to get a better overlap with the obtained experimental K_{ex} values. The description of the variable in each panel is: 3 cargo classes, K_{ex} = 0.010, 0.067, 0.148, σ_{op} = 0.2 (**A**); 3 cargo classes, K_{ex} = 0.010, 0.033, 0.148, σ_{op} = 0.2 (**B**); 2 cargo classes, K_{ex} = 0.010, 0.148, σ_{op} = 0.2 (**C**); 3 cargo classes, K_{ex} = 0.010, 0.033, 0.148, σ_{op} = 0.1 (**D**).
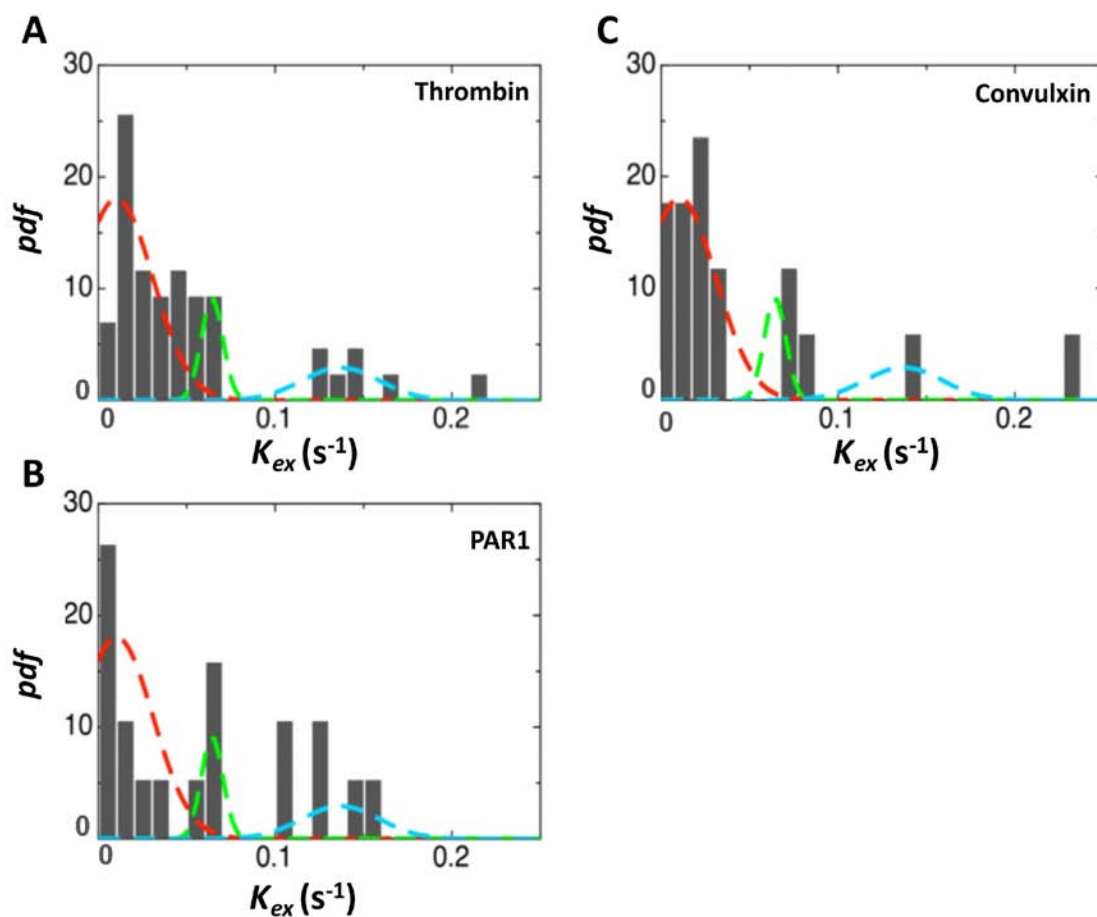
Figure 3.15. Frequency distribution of K_{ex} due to activation by different agonists

The rate constants K_{ex} were calculated as in Methods. The gray bars represent the frequency distribution of K_{ex} values obtained upon stimulation of platelets with various agonists as indicated. Superimposed dashed curves are the Gaussian functions shown in **Figure 3.12.** The number of K_{ex} values used in making the *pdf* incorporates 43 K_{ex} values for thrombin, 19 for PAR1-agonist and 17 for convulxin.

Chapter Four

Involvement of SNARE Machinery in Determining Heterogeneity in Platelet Secretion

Introduction

The work described in the previous chapter suggested that platelet secretion was more heterogeneous than originally thought. Our data demonstrated that platelet secretion was in general not thematic, but was dependent on agonist dose and potency. In the study of human platelets, our analysis was limited by the out-bred nature of our donor pool and by the fact that the full array of secretory machinery was present. As discussed in the Chapter One, platelets have at least two tiers of v-SNARE usage, the primary tier that uses VAMP-8, and the secondary tier that employs VAMP-2/3. If differential use of these v-SNAREs can affect release kinetics, then our analysis of human platelets may miss subtle differences in cargo release dynamics. For this reason we turned to a mouse platelet system in which there is a homogenous genetic background and in which we can manipulate the levels of the individual v-SNAREs. In this chapter, we describe the ground-work required for analysis of platelets from a number of VAMP-deficient mouse lines.

v-SNAREs, t-SNAREs, and a number of regulatory proteins determine the process of platelet secretion by facilitating granule fusion. As described earlier in the Chapter One, the minimal requirement for fusion to occur is the pairing of cognate v- and heterodimeric/trimeric t-SNAREs to form a transmembrane fusion complex (*Weber et al.*, 1998). The goal of the work described in this chapter is to see if the v-SNARE machinery in platelets contributes to any hidden pattern of platelet secretion. v-SNAREs are type II membrane proteins with a 60-70 amino acid conserved SNARE motif (*Jahn and Südhof*, 1999). Platelets contain VAMP-2 (synaptobrevin), VAMP-3 (cellubrevin), VAMP-7, and VAMP-8 (endobrevin) (*Bernstein and Whiteheart*, 1999; *Polgár et al.*, 2002; *Ren et al.*, 2007; *Schraw et al.*, 2003). The neurotoxin, tetanus toxin, is an endopeptidase, that specifically cleaves VAMP-1/2/3 (*Schiavo et al.*, 2000). This toxin was used in the early studies to determine the importance of v-SNAREs in platelets

(*Flaumenhaft et al.*, 1999). In a separate set of experiments an antibody directed against the N-terminus of VAMP-3 (*Feng et al.*, 2002) was used as an inhibitor. When either toxin or antibody was added to streptolysin *O* permeabilized platelets, both agents partially inhibited release (*Flaumenhaft et al.*, 1999). These results were contradicted by the lack of secretion defect in the platelets from VAMP-3$^{-/-}$ mice (*Schraw et al.*, 2003). Later studies showed a significant secretion defect in VAMP-8$^{-/-}$ platelets that could be further reduced by treatment of permeabilized VAMP-8$^{-/-}$ platelets with tetanus toxin (*Ren et al.*, 2007). The conclusion drawn from these results suggested that VAMP-8 was the primary v-SNARE since only its deletion caused a defect in release. VAMP-2/3 play a secondary role and could facilitate release in VAMP-8's absence, albeit less efficiently.

The fact that two v-SNARE-based systems could be functional in platelets led us to question whether the two systems could mediate the release of different arrays of granular cargo. For these studies, we sought to compare release from VAMP-8$^{-/-}$, VAMP-3$^{-/-}$, and RC Tox :: PF4 Cre mouse platelets. The RC Tox :: PF4 Cre mice express the tetanus toxin catalytic chain in response to the Platelet Factor 4 promoter-driven Cre recombinase. Release from these platelets will be analyzed using the micro ELISA scheme described in the Chapter Three. The work described here lays the foundation for future work with these mouse strains.

Choice of agonists for the study

The agonists used in this study are thrombin, convulxin and PAR4, as in the human study. PAR1-agonist was not included in the study as the mouse platelets have PAR3/4 receptors. The experiments done so far entailed an initial agonist titration to estimate the dose required for at least 80% secretion irrespective of the mouse-type used for the study. Though the concept is to activate all the mouse platelets completely, the secretion defect in VAMP-8$^{-/-}$ platelets was over-ridden by the increased agonist concentration suggesting that any physiologically relevant secretion heterogeneity pattern will be overwhelmed in this experimental paradigm. Future studies will require

the use of lower doses of thrombin. None-the-less, analysis of wild-type mouse platelets was informative.

Release of cargo from wild type mouse platelets

Mouse platelets were isolated as described in the Chapter Two. An initial agonist titration was performed for each agonist. The agonist dose that gave at least 80% of [^{3}H]-serotonin release was employed. The final concentrations of agonists used to stimulate the platelets were 0.2 U/mL for thrombin (**Figure 4.1, a**), 0.5 µg/mL convulxin (**Figure 4.1, b**) and 400 µM for PAR4-agonist (**Figure 4.1, c**). The cargo molecules probed for are listed in **Table 4.1**. The release profile over a time course of 5 min is indicated in **Figure 4.1**. As indicated in **Table 4.2**, potency of agonist determines the extent of release, as was seen in the human platelets. The number of molecules released upon stimulation with thrombin was 8, while it was 5 and 7 when convulxin or PAR4-agonist respectively.

Release of cargo from wild type and VAMP-8$^{-/-}$ platelets

Agonist titrations were performed before analyzing the releasates from the time course experiments. The agonist doses that induced at least 80% of [^{3}H]-serotonin release are indicated in the **Table 4.3**. It was 0.2 U/mL of thrombin for wild type while 0.4 U/mL for VAMP-8$^{-/-}$ platelets. It should be noted that the dense granule release deficiency from VAMP-8$^{-/-}$ platelets is overcome when stimulated with 0.5 U/mL thrombin (*Ren et al.*, 2007), therefore the higher levels of thrombin required for 80% release was expected. This was also true when PAR4-agonist was used (**Table 4.3**). The wild type platelets required 400 µM of PAR4-agonist while VAMP-8$^{-/-}$ platelets required 550 µM of PAR4-agonist for the same level of release. The rates of release of each standard granule marker are also indicated in the **Table 4.3**. The release rates were either less in VAMP-8$^{-/-}$ than in wild type platelets (dense and α-granule) or approximately equal (lysosome) when stimulated with thrombin. The release rates of all the three granules were almost the same between wild type and VAMP-8$^{-/-}$ platelets when stimulated with PAR4-agonist.

Discussion

The preliminary data obtained points towards the dependency of platelet secretion on agonist-potency. The goal of this project is to see if the v-SNARE machinery has any role in determining the phenotype of heterogeneity in the way platelets secrete. The trials done so far involved the utilization of an agonist-dose that imparted 80% dense granule release, irrespective of the agonist. As the goal was not to study differential platelet activation and its impact on secretion, this strategy was chosen. But, as any secretion deficiency due to the absence of v-SNARE (at least in VAMP-8 deficient platelets) is overcome by high agonist doses, future studies to answer this question would need to employ only minimal doses of agonist. Moreover, the choice of agonist used will be restricted to thrombin, as the release can be controlled more tightly by using hirudin to stop the release reactions. Cargo release will be further studied in VAMP-8$^{-/-}$, VAMP-3$^{-/-}$ and RC Tox :: PF4 Cre platelets as sufficient numbers of mice for these studies become available. The knowledge gained from these preliminary studies will help us guide this future analysis and to address whether v-SNARE usage contributes to platelet secretion heterogeneity.

Table 4.1. Mouse array cargo

	Symbol	Cargo Name
Growth Factors	EGF	Epidermal Growth Factor
	SDF-1α	Stromal Derived Growth Factor - 1α
	TPO	Thrombopoeitin
	bFGF	Basic Fibroblast Growth Factor
Pro-Angiogenic	VEGF	Vascular Endothelial Growth Factor
Anti-angiogenic	PF4	Platelet Factor 4
Cytokines/Chemokines	MMP2	Matrix Metalloproteinase -2
	P-Selectin	P-Selectin
	TGFβ	Transforming Growth Factor β
	IL-1α	Interleukin - 1α
	IL-1β	Interleukin - 1β
	MIP-1α	Macrophage Inflammatory Protein - 1α
	RANTES	Regulated upon Activation, normal T-cell expressed, and presumably secreted
	TARC	Thymus and Activation Regulated Chemokine
	TNFα	Tumor Necrosis Factor α

Listed are the cargo molecules probed for on the micro-ELISA arrays. Their abbreviated names (**Symbol**) are indicated in the middle column. The cargo molecules are grouped according to their proposed functions (left-most column).

Table 4.2. Rates of release from wild type mouse platelets

	Thrombin	Kex	Convulxin	Kex	PAR4	Kex
	bFGF	0.024	**IL-1α**	0.0043	**EGF**	0.0233
	IL-1α	0.0320	**IL-1β**	0.0203	**IL-1β**	0.0299
	IL-1β	0.0723	**TARC**	0.1081	**MIP-1α**	0.0343
	MIP-1α	0.0774	**TGFβ**	0.0164	**RANTES**	0.0239
	P-Selectin	0.0650	**TNFα**	0.0194	**TGFβ**	0.0251
	RANTES	0.1738			**TNFα**	0.0269
	TGFβ	0.0655			**TPO**	0.0253
	TNFα	0.0496				
# detected	**8**		**5**		**7**	

Mouse platelets (4×10^8 /mL) were prepared as described and stimulated with thrombin (0.2 U/mL), convulxin (0.5 µg/mL), or PAR4-agonist (400 µM) for 5 min. Releasates were probed using micro-ELISA arrays to obtain the rate constant K_{ex} for each cargo molecule as described in the Chapter Two. The total number of molecules detected in the releasate is represented in the last row.

Table 4.3. Comparison of rates of release between wild type and VAMP-8$^{-/-}$ platelets

	K_{ex} values			
	Thrombin		PAR4-agonist	
	Wild type (0.2 U/mL)	VAMP8 $^{-/-}$ (0.4 U/mL)	Wild type (400µM)	VAMP8 $^{-/-}$ (550µM)
Dense granule	0.4368	0.2263	0.1101	0.1362
α- Granule	0.1295	0.05625	0.0136	0.03296
Lysosome	0.09316	0.09116	0.01937	0.02171

Mouse platelets (4×10^8 /mL) were prepared as described and stimulated with thrombin and PAR4-agonist with the indicated concentrations over a span of 5 min. The rates of release (K_{ex}) were calculated for [^{3}H]-serotonin release for dense granule, PF4 release for α-granule and β-hexosaminidase release for lysosome as indicated.
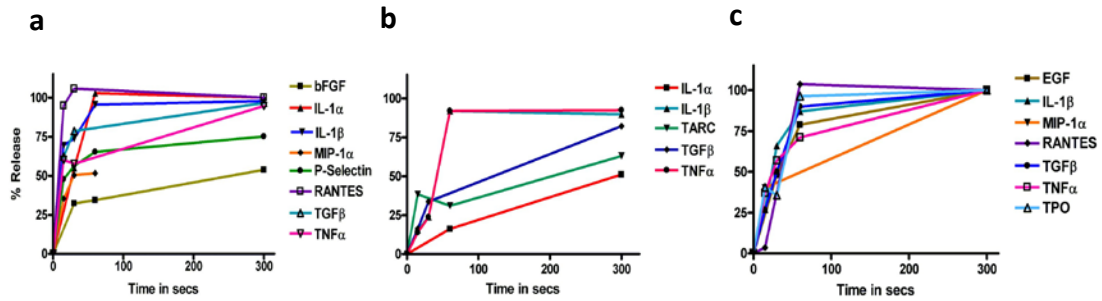
Figure 4.1. Release of cargo from the wild type mouse platelets

Wild type mouse platelets (4×10^8 /mL) were prepared as described and stimulated with thrombin (**a**; 0.2 U/mL), convulxin (**b**; 0.5 µg/mL), or PAR4-agonist (**c**; 400 µM) for 5 min. Releasates were probed using micro-ELISA arrays and the % release was calculated by the equation (Amount in the supernatant / Amount released at 5 min) × 100. For representing the data in the graphs, % release at 5 min point is set to 100% and the back ground (release at 0 time point) was negated. The released cargo represented by multicolored lines are listed adjacent to each panel.

80

Chapter Five

Sphingosine-1-Phosphate in Platelets

Introduction

The bioactive lyso sphingolipid, Sphingosine-1-Phosphate (S1P) plays an essential role in cellular metabolism (*Spiegel and Milstien*, 2003). S1P is essential for development, growth, immune function, inflammation and cell migration. S1P has gained further attention due its role in the formation of the vasculature. S1P is formed by the action of sphingosine kinase (SK) on sphingosine. There are two isoforms of SK – SK1 and SK2. Deletion of both the isoforms, in mice, is embryonic lethal (*Mizugishi et al.*, 2005). Of the two isoforms of S1P, a mouse expressing only one SK1 allele carrying a myxovirus resistance 1–Cre was generated. These mice demonstrated the importance of S1P in the maintenance of vascular integrity (*Camerer et al.*, 2009) as S1P levels in plasma are minimal. Erythrocytes restored normal plasma S1P levels in these mice and thus vascular integrity. Plasma levels of S1P are very high (*Hla*, 2004) and are thought to be maintained by endothelial cells, erythrocytes, platelets *etc*. None of the cell types appear to be the only source of plasma S1P.

Platelets and erythrocytes are the hematopoietic reservoirs of S1P. Absence of enzymes degrading S1P is responsible for the presence of ample amounts of S1P in them. The release of S1P from RBCs is constitutive (*Hänel et al.*, 2007). The interesting characteristic that makes platelets stand out is that S1P is released only upon stimulation (*Yatomi et al.*, 1995). The mechanism of release of platelet S1P is unclear. Constitutive and agonist stimulated release of S1P from mast cells (*Mitra et al.*, 2006), and S1P release in astrocytes (*Sato et al.*, 2007) occurs through ABC transporters and the same has been attributed to platelets. This is not supported by direct evidence. So the mechanism of S1P release from platelets remains enigmatic. Endothelial cells are recently reported to maintain normal plasma S1P levels (*Hisano et al.*, 2012). Though platelets may not be essential contributors to plasma S1P, their stores might become

significant in modifying the microenvironment upon vascular injury. Localized release of platelet S1P might help restore the vascular integrity.

The work described in this chapter attempts to address the mechanism of S1P release from platelets. The presence of a carrier molecule, like bovine serum albumin (BSA) was needed for detection of released S1P. This helped in the identification of a BSA-extractable pool that was distinct from a potentially granular pool of S1P, which was released upon platelet activation. This putative granular pool was not released from secretion-deficient VAMP-8$^{-/-}$ and *Unc13d* ^{Jinx} mice platelets suggesting that the standard exocytosis machinery was required for its release. Consistently, a NBD-derivatized Sphingosine (which was converted by platelets into NBD-S1P) was concentrated into a granular organelle as determined by fluorescence microscopy. This observation was further confirmed by sub-cellular fractionation studies. This is the first data to suggest that there are two pools of S1P in platelets – agranular and granular.

Detection of released S1P from platelets is dependent on the presence of a carrier-molecule in the media

We used mass spectrometry to measure released platelet S1P with an added C$_{17}$S1P as an internal standard for quantification. This approach enabled us to examine the total platelet S1P and was a superior method to previously used radiolabeling techniques which utilized [^{32}PO$_4$] that may misrepresent the importance of more metabolically active pools of the lipid. Platelets contain significant amounts of S1P, but, in our initial experiments there appeared to be very little that was releasable when platelets were stimulated with thrombin (0.3 U/mL) (**Figure 5.1a**) or convulxin (0.3 µg/mL) (**Figure 5.1b**). Similar results were seen with mouse platelets. The secretion of other granule components (PF4 and β-hexosaminidase) occurred normally. Given that S1P is a lipid and may not be freely soluble once released, we included 1% fatty acid-free bovine serum albumin (BSA) into the pH 7.4 HT buffer as a potential carrier or sink for S1P. No S1P was found present in the preparations of Fraction V, fatty acid-free BSA used throughout our studies (**Table 5.1** and data not shown). Using this new buffer

composition, release of S1P from either thrombin-stimulated (0.05 U/mL) human (**Figure 5.2a**) or mouse (**Figure 5.2b**) platelets could be readily detected. These data demonstrate that S1P can be released from activated platelets but to detect it in the supernatants of release reactions, a carrier, such as BSA, is required. All subsequent experiments contained added BSA unless specifically noted. It is thought that the hydrophobic binding sites on BSA serve as sink for the released S1P preventing it from becoming integrated into the platelet plasma membrane. This enabled the direct measure of released S1P in our assay system.

S1P levels in platelets and synthesis of S1P

One interesting feature of our data was the fact that the total levels of S1P in human (**Figure 5.3a**) and mouse (**Figure 5.3b**) platelets increased with increasing BSA concentrations. Even though the levels of human and mouse platelet S1P are different, a ten-fold increase in BSA in the media caused only a two fold increase in endogenous S1P. This suggested that new synthesis of S1P occurs in resting platelets when there is an external sink for S1P. S1P stored in human platelets was 2.8 ± 0.35 pmol/4×10^5 PLs and 0.139 ± 0.007/pmol/4×10^5 PLs in mouse platelets. Since the platelet S1P levels increased in the presence of a carrier molecule, we sought to determine if S1P was being synthesized through the action of a platelet sphingosine kinase. Human platelets were incubated with 6 µM C_{17} Sphingosine and the formation of C_{17} S1P was measured for one hour. All the exogenously added sphingosine was converted to S1P within this period. This indicates that sphingosine is converted into S1P rapidly and the enzyme responsible for the conversion, sphingosine kinase is very active in platelets. The data for C_{17} Sphingosine is not perfectly quantitative as D_7 S1P (deuterium labeled) was employed as an internal standard in its quantitation (**Figure 5.4**). Moreover, there was an associated increase in the S1P levels released upon stimulation with increasing concentrations of BSA (**Figure 5.5**).

Levels of S1P in stored human platelets and platelet poor plasma

With an available sink in plasma (albumin/HDL) and active SK in platelets, the extractable pool of S1P in platelets may be constantly turning over. To test this possibility and its relevance in stored platelet rich plasma (PRP), the levels of S1P in platelets and platelet poor plasma (PPP) were measured over time in a unit of platelets obtained from the Kentucky Blood Center. For each measurement, PRP was removed from the unit bag under sterile conditions and the bag was resealed. Over the time course measured, there was a decrease in the amount of S1P stored in platelets; but there was not a corresponding increase of S1P in the plasma (**Figure 5.6a**). This lack of change in the plasma S1P level is most likely due to the overwhelming levels of S1P in plasma (almost seven fold more) when compared to platelets. It is also possible that there was some degradation of S1P in plasma since there was an initial decrease in the plasma S1P levels that then leveled out (**Figure 5.6b**). The most overt loss of S1P was in platelets suggesting that it is either released or extracted over time and the platelet's ability to synthesize new S1P is exhausted over the same time course.

Stimulation-dependent release of S1P from platelets

As is true for any platelet secretion process, the presence of calcium in the media enhanced the release of S1P from platelets upon stimulation (**Figure 5.7a**). Release of S1P from stimulated platelets depended on the agonist-potency. Weak agonist like ADP released the least, while there was a dose-dependent increase in S1P release with agonists like thrombin and convulxin (**Figure 5.7b**). The dependency of the platelet release reaction on agonist potency has already been demonstrated for other granule cargo (Chapter Three). Mouse platelets followed the same trend in the release of S1P. This coincided with the release of a known α-granule cargo, PF4 (**Figure 5.8a**).

Time-dependent release of S1P from platelets

As the preliminary observations pointed towards a granular pool of S1P that could be mobilized upon stimulation, we examined the time-course of its release. Platelets were stimulated with thrombin for 15 sec – 5 min, and the released S1P levels

were compared with a known platelet granule cargo, PF4 (**Figure 5.8b**). S1P and PF4 followed the same trend in their release time course.

The route of S1P release from platelets

The ABC transporter inhibitor, glibenclamide's effects on S1P secretion

Glibenclamide, a sulfonylurea compound, was initially thought to inhibit ATP dependent K^+ channel (*Fosset et al.*, 1988). It was later shown to be a general ABC transporter inhibitor (*Hamon et al.*, 1997; *Haskó et al.*, 2002; *McNicholas et al.*, 1996; *Payen et al.*, 2001; *Schwanstecher et al.*, 1998). Previous studies with glibenclamide had suggested the involvement of an ABC transporter in S1P export from platelets. Specificity of this drug to inhibit S1P release from platelets was tested. Not only did glibenclamide inhibit the release of S1P from platelets (**Figure 5.9**), but it also inhibited dense granule release (**Figure 5.10a**), α-granule (**Figure 5.10b**) and lysosomal release (**Figure 5.10c**). These release events are true secretion processes and no involvement of an ABC transporter has ever been suggested. Therefore, these data would imply an off-target effect of glibenclamide that affects platelet activation. Such results cast doubt on the influence of glibenclamide on the release of S1P from platelets. Nevertheless the effect of glibenclamide on S1P release was tested in the absence/presence of BSA. The increased S1P release in the absence of BSA was surprising and unexplainable. As BSA is essential for the detection of released S1P, the inhibition data in its presence is more reliable. There was more than 20% reduction in the released S1P from platelets in the presence of 200 µM glibenclamide. However, the same level of drug caused a ~55% decrease in dense granule release (represented by detection of [^{3}H]-serotonin, a 30% reduction in PF4 release and a 19% reduction in β-hexosaminidase release. At this stage, it is unclear exactly what effect glibenclamide has on platelets, but it is clear that it does affect some aspect of platelet activation.

SNARE Machinery in S1P Secretion from Platelets

To test the involvement of the SNARE machinery in the release of S1P from platelets, we utilized platelet secretion deficient mouse strains. Platelets from VAMP-8$^{-/-}$

(V8$^{-/-}$) and Munc 13-4-deficient, *Unc13d* ^{Jinx} mice were tested for the release of S1P. Secretion of PF4 (**Figure 5.11a**) and S1P (**Figure 5.11b**) were analyzed. Secretion of S1P from VAMP-8$^{-/-}$ and *Unc13d* ^{Jinx} mice when compared to the wild type mice was reduced as was also seen for PF4 release (**Figure 5.11**). This provided convincing evidence for the involvement of exocytotic machinery in the release of S1P from stimulated platelets. Platelet secretion of S1P was reduced by 20% in VAMP-8$^{-/-}$ and 80% reduced in *Unc13d* ^{Jinx} mice when compared to wild type. The release of S1P was more severely affected in *Unc13d* ^{Jinx} mice platelets than VAMP8$^{-/-}$. *Unc13d* ^{Jinx} mice have a more robust defect in dense granule release when compared to alpha granule release. The defect in S1P release from the *Unc13d* ^{Jinx} platelets suggests that S1P may be released from the dense granule compartment.

Comparison of amounts of S1P in secretion-deficient mice

The platelet S1P levels are 0.58±0.04, 0.3±0.01 and 0.38±0.04 pmol/4×10^5 PLs for wild type, VAMP-8$^{-/-}$ and *Unc13d* ^{Jinx} mice respectively (**Figure 5.12a**). The plasma S1P levels in human and mouse platelets do not differ much (3.76±0.63 pmol). There is a slight increase in the amount of S1P found in VAMP-8$^{-/-}$ (4.61±0.48 pmol) and a decrease in *Unc13d* ^{Jinx} (2.97±0.53 pmol) mouse plasma as indicated in **Figure 5.12b.** These measurements are made per µL of platelet poor plasma left from the experiment performed to look at platelet secretion as described in the previous section. The S1P levels reported here are all in the presence of 1% fatty acid-free BSA. Though the observed differences are statistically significant (p value < 0.05) there was no obvious physiological significance.

Release of newly synthesized S1P

Given the apparent synthesis of S1P in platelets, we next wanted to see if the newly synthesized S1P is exocytosed. To test this, C57BL/6 and *Unc13d* ^{Jinx} mouse platelets were incubated with 2 µM C$_{17}$ Sphingosine for increasing time followed by stimulation with thrombin for 2 min. Though the levels of S1P detected (whether endogenous [C$_{18}$ S1P] or exogenous [C$_{17}$ S1P]) in resting platelets was high, the

percentage of S1P release was always less in *Unc13d* [Jinx] when compared to wild type consistent with our previous results (**Figure 5.13**). To see whether newly synthesized S1P was preferentially released (or not), fresh human platelets were treated with 6 μM C_{17} Sphingosine for 10 minutes and then stimulated for 5 minutes with two different doses of thrombin. Low dose thrombin (0.05 U/mL) induced a small amount of S1P release while higher thrombin (1 U/mL), induced more S1P release. This was true for both endogenous (C_{18}) and newly synthesized (C_{17}) S1P (**Figure 5.14**). This observation was made with several different batches of platelets and implies that the newly synthesized pools of S1P are integrated into both granular and agranular stores.

Granular and agranular localization of S1P in platelets

Fluorescence microscopy

To confirm the granule residence of S1P in platelets, we resorted to fluorescence microscopy. Platelets were incubated with fluorescently tagged sphingosine (NBD-Sphingosine). As sphingosine kinase is highly active in platelets, this label was expected to be almost completely converted into NBD-S1P. This was tested by incubating banked human platelets with 0.5 μM NBD-Sphingosine for 5-60 min to allow the synthesis of NBD-S1P. At the indicated time points, the lipids were extracted and then separated by thin layer chromatography. Within 10 min most of the NBD-Sphingosine was converted to NBD-S1P. NBD-Sphingosine is unstable in platelets and is indicated by the top-most bands (**Figure 5.15a**) which were thought to correspond to the cleaved NBD. Fresh human platelets (**Figure 5.15b**) were labeled with mepacrine (**A**) and lyso tracker red (**B**). Mepacrine is a green fluorescent dye used to label dense granules. Lyso tracker red is a red fluorescent dye that localizes to acidic compartments such as lysosomes. Thus, they serve as granule markers. This can be visualized in (**C**) where mepacrine and lyso tracker red co-localize. Platelets were also labeled with NBD-Sphingosine (**D**) and the punctuate appearance pointed towards granular localization. This was confirmed by co-localization with lyso tracker red as seen in (**F**). Similar observation could be seen in the mouse platelets (**Figure 5.15c**).

Sub-cellular fractionation

The granule localization of S1P was further analyzed by sucrose gradient sub-cellular fractionation of platelets as described in methods. The fractions were analyzed by western blotting for several compartment-specific marker proteins (**Figure 5.16a**): $\alpha_{IIb}\beta_3$ for plasma membrane; Rab-GDI, for cytosol; VAMP-8 for granule membranes; PF4 for alpha granule cargo; and malate dehydrogenase for mitochondria. Concomitantly, lipids were extracted from each fraction and were analyzed for S1P levels. There was a gradual increase in S1P levels from fractions 2-5. This coincided with the trend followed by the granule marker PF4. Fraction 1 in **panel B** included membrane composition along with the cytosol due to our limited ability to separate two fractions and is responsible for the observed abnormal high levels of S1P. Similar trend followed by VAMP-8 and S1P in 2-5 fractions, confirmed our previous interpretation of granular pool of S1P. Taken these data altogether, S1P was identified to constitute two pools - granular and agranular pools.

Platelet S1P in determining vascular permeability

Given the defect in S1P release seen in the *Unc13d* [Jinx] mice, we sought to determine if that defect affected vascular integrity by using the Evan's blue dye assay. In this assay, the Evan's blue dye is injected, i.v. into an animal and after a period of time, the animal is perfused and the lungs are removed. Blue dye in the lungs was quantified as a metric of vascular leakage. A ratio of the dye OD to the total lung weight measures the intactness of the vascular permeability barrier (**Table 2**) referred to as permeability ratio. The permeability ratio was 1.34±0.20 for wild type mice (n=3) while that measured for *Unc13d* [Jinx] mice was 1.43±1.02 (n=3). The vascular permeability barrier was defective in one of the three *Unc13d* [Jinx] mice, but not in the other two (**Table 2**). While we show no evidence that the released pool of platelet S1P contributes to vascular integrity, it may play a role in certain circumstances. Further experiments with other secretion deficient mouse lines may be needed to be analyzed in other assays of vascular permeability that involve environmental stressors.

Discussion

S1P was initially identified as a bioactive sphingolipid with an intracellular signaling role. The discovery of S1P receptors on different cell types explained the multifaceted roles of S1P - during development, formation of vasculature, in cell migration and differentiation, inflammation, cell growth, cell proliferation *etc*. (*Hannun and Obeid*, 2008). The spatial and temporal regulation of S1P determines cell fate. In most cell types, S1P is produced only upon requirement. Plasma S1P levels are reported to be maintained by platelets (*Yang et al.*, 1999b), erythrocytes (*Hänel et al.*, 2007) or endothelial cells (*Venkataraman et al.*, 2008) but, none of them have been confirmed to be the sole source. Erythrocytes and platelets constitute the circulatory reservoir of S1P. They accumulate S1P due to the absence of enzymes required for its degradation (S1P lyase/phosphatase). While erythrocytes constitutively release S1P, platelets release S1P upon stimulation (*Yatomi et al.*, 2000). The mechanism of release of S1P from platelets is unresolved. The work presented here demonstrates two pools of platelet S1P – agranular and granular. Based on the obtained results, release of the granular pool required the platelet secretory machinery.

S1P, in plasma, exists either bound to albumin or HDL particles (*Okajima*, 2002). Our data suggests that, there is a requirement for a carrier molecule, like BSA, to detect the release of S1P from platelets. Increased BSA availability in the media, increases S1P levels both in human and mouse platelets. We interpret that the S1P level in platelets is partially controlled by mass action. If there is a sink for S1P (i.e. BSA) then more is made until the pool of substrates is exhausted. Perhaps it is this mechanism that explains the platelets' contribution to plasma S1P levels under "resting" conditions.

Previous reports suggested the involvement of ABCA1 like transporters to be responsible for the release of S1P from stimulated platelets (*Kobayashi et al.*, 2006). Using a known ABC transporter inhibitor, glibenclamide, we showed that inhibition by this compound may not be specific for S1P release. It also inhibited dense granule, α-granule and lysosomal release from platelets which indicates that the regulated release

of S1P may not be solely transporter-mediated. Platelet secretion deficient mice demonstrated the existence of a granular pool of S1P. VAMP-8$^{-/-}$ mice lack the primary v-SNARE, VAMP-8 (*Ren et al.*, 2007) while *Unc13d* ^{Jinx} mice are deficient in Munc13-4, a regulatory molecule (*Ren et al.*, 2010). Both proteins are required for normal platelet secretion. S1P release from VAMP-8$^{-/-}$ and *Unc13d* ^{Jinx} mouse platelets was defective. As the dense granule release defect is more pronounced in *Unc13d* ^{Jinx} mice, we speculate that S1P may be stored in dense granules. The storage of S1P in dense granules can be tested using HPS mice which lack dense granules. Some models have diminished levels of dense granule cargo represented by limited population of dense granules, while some have ghost dense granules. These empty dense granules can still be stained by mepacrine, as there is no dysregulation in the uptake of contents. If S1P resides in dense granule membrane, then HPS mice with ghost dense granules could be labeled with NBD-S1P while those with no dense granules, might not incorporate NBD-S1P into granules.

The absence or dysregulation of the SNARE machinery does affect the release of platelet S1P. Whether this decreased S1P release affects the vascular permeability is still unanswered. An initial attempt to address this question was made in the present study. Secretion-deficient *Unc13d* ^{Jinx} mice had some leakage of the injected Evan's blue dye into the lungs indicating imperfect vascular permeability barrier when compared to the wild type mice. As the data was not statistically significant, the role of platelet S1P in the maintenance of vascular permeability has to be tested further. As the granular pool of S1P is more likely to influence the local microenvironment upon vascular injury, it may be more reasonable to assess the leakage of dye in the inflamed secretion-deficient mouse model or in a model where the lesion is localized. It seems unlikely that there will be global effect, especially given the fact that these mouse strains did not show any large changes in plasma S1P levels.

Sphingomyelin degradation to form S1P is thought to happen in platelets (*Tani et al.*, 2005). With abundant sphingomyelin present in the membranes, there appears to be

no need for platelets to have an external source of sphingosine or S1P. Though the release aspect of platelet S1P is addressed by our work, the sub-platelet distribution of S1P is still unclear. The fluorescent micrographs indicate the granular localization of S1P, but such analysis focuses only on where the lipid is concentrated. As S1P cannot be by itself, it either must be associated with some unknown protein in the platelets to exist in cytosol or it has to be membrane-associated. If in the granule lumen, it is likely to be in a complex with granular calcium salts.

The granular pool of S1P forms an easily accessible source to mediate localized effect in the microenvironment upon vascular injury. Involvement of a transporter for S1P export cannot be completely ruled out as the work presented here suggests only one possible mechanism for the release of S1P. If a transporter mediates S1P export, its availability on the surface might dictate S1P release. The granule membrane associated transporters add onto the already available surface transporters upon granule fusion. Thus, increase in transporter population might enable an increase in the probability of S1P export and its extraction by a carrier-molecule like BSA. Identification of this unknown receptor is still an open question.

Table 5.1. Quality-check on fatty acid-free BSA

Sample #	C_{17} S1P (exogenous)	C $_{18}$ S1P (endogenous)
Blank	0.00E+00	0.00E+00
1	1.39E+05	0.00E+00
2	1.95E+05	0.00E+00
3	1.70E+05	0.00E+00

Liquid phase lipid extraction was done on pH 7.4 HT buffer treated with 1% fatty acid-free BSA and C_{17} S1P. Any association of S1P with the BSA was detected by MS analysis. There was no detection of S1P in the blank sample that was not treated with any exogenous S1P (C_{17}) but with 1% fatty acid-free BSA. Samples #s 1, 2, 3 were treated with exogenous S1P (C_{17}). While that was detected, there was no detection of C_{18} S1P, which is the endogenous S1P moiety that was measured for all the subsequent experiments.

Table 5.2. Permeabilization of lungs with Evan's blue dye

Mouse type	OD	Lung weight (mg)	Permeability (OD/Lung weight)	SD
Wild type	178.09	132.87	1.34	0.20
Unc13d ^{Jinx}	221.32	156.73	1.43	1.02

Upon letting the indicated mouse strain to inhale isoflurane, 100µL of Evan's blue dye was injected into the jugular vein. The mice were allowed to stay calm for 15 min, and were sacrificed later. After perfusion, the lungs were separated, dried and weighed. Lungs were preserved in 1 mL of 1% paraformaldehyde. The intensity of the dye that got into lungs was measured with odyssey IR scanner and permeability was calculated as indicated in the table. The data is representative of the trials done on 3 mice each (SD-Standard deviation).
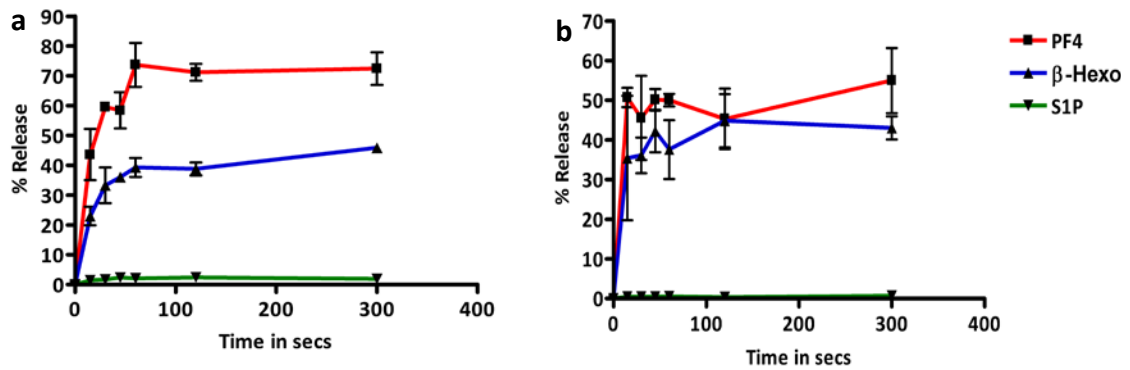
Figure 5.1. Release of S1P from platelets in the absence of carrier-molecule

Banked human platelets (2.5×10^8/mL) were resuspended in plain HT pH 7.4 buffer and stimulated over time with 0.05 U/mL thrombin (**a**) and 0.3 μg/mL of convulxin (**b**). The maximum time stimulated was 5 min. Granule cargo like PF4 was detected by ELISA and β-hexosaminidase by an enzyme assay as described in methods. S1P was detected by MS analysis upon extracting the lipids by liquid phase extraction detailed in methods. % Release was assessed for the respective moieties by calculating (Amount detected in the supernatant / Amount detected in supernatant + Pellet) × 100.
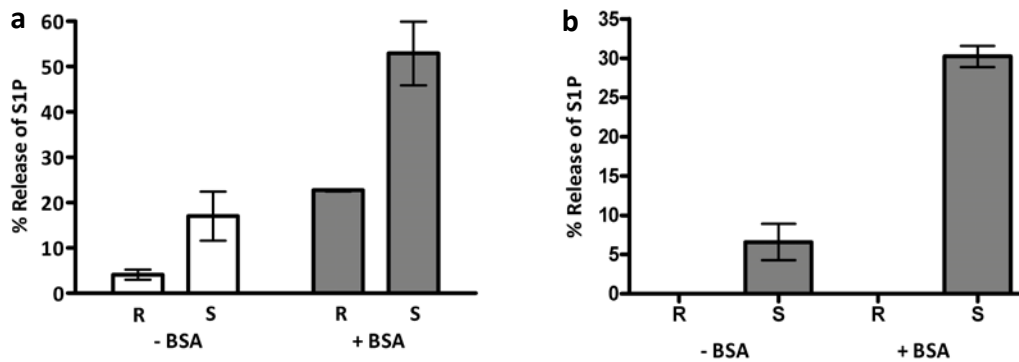
Figure 5.2. Detection of secreted S1P from platelets in the presence of BSA

Washed human (**a**) and mouse (**b**) platelets (2.5×10^8 /mL) were prepared as described. They were not stimulated (**R**=Resting) or stimulated with 0.05 U/mL thrombin for 45 seconds (**S**=Stimulated). Thrombin stimulation was stopped with 0.1 U/mL hirudin. The samples were centrifuged at 13,000 × g for 2 min followed by separation of releasate (supernatant) from platelets (pellet). This was done in the absence (**-**) or presence (**+**) of 1% fatty acid-free BSA. Lipids were then extracted as described in methods and detected by mass spectrometry (MS). The supernatant and the pellet fractions constituted the percentage release of S1P. The data are represented as the average ± SD, n = 3.
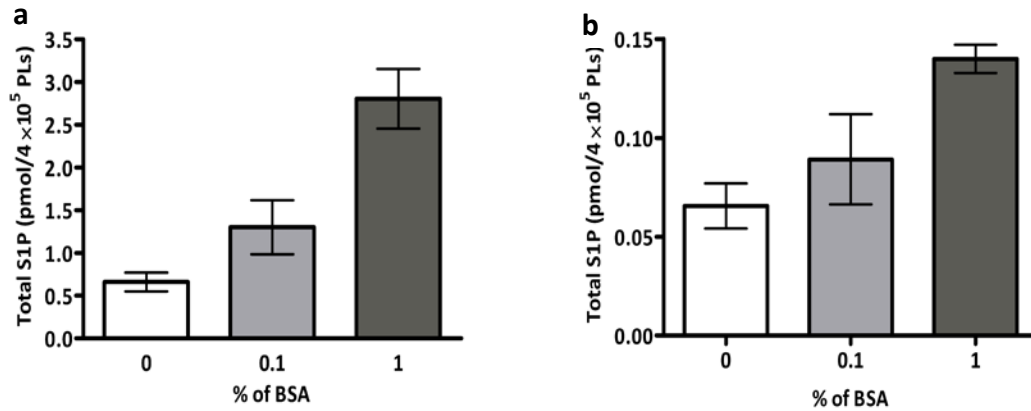
Figure 5.3. Endogenous human and mouse platelet S1P levels

Washed human (**a**) and mouse (**b**) platelets (2.5×10^8 /mL) were prepared as described. They were not stimulated or stimulated with 0.1 U/mL thrombin for 5 minutes and the reaction was stopped with 0.2 U/mL hirudin. This was done in the presence of increasing concentrations of fatty acid-free BSA as represented. Lipids were then extracted as described in methods and detected by MS. The total amount of S1P in 4×10^5 platelets has been calculated averaging the content in supernatant and pellet samples (no difference was observed between them). The data are represented as the average ± SD, n = 3.
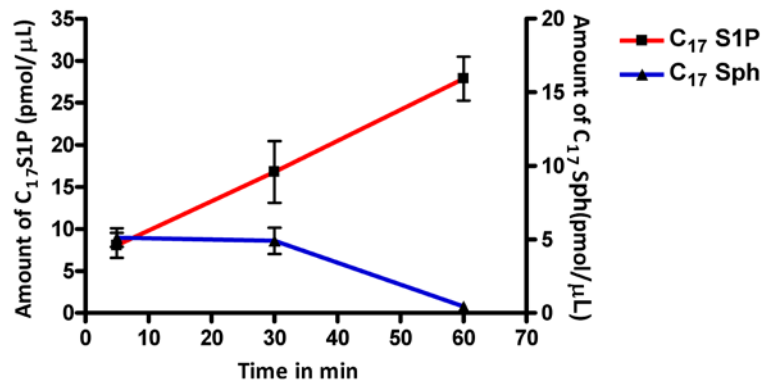
Figure 5.4. Synthesis of new S1P in platelets

Fresh human platelets (5×10^8/mL) were treated with 6 µM C_{17} Sphingosine over an hour as indicated. The lipids were extracted at the end points as indicated. The amounts of C_{17} Sphingosine and C_{17} S1P were detected through MS.   The data are represented as the average ± SD, n = 3.
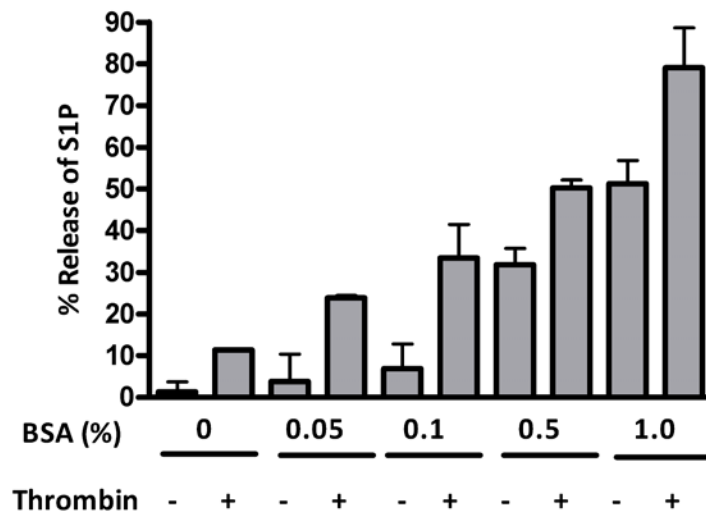
Figure 5.5. Influence of BSA on release of S1P from platelets

Banked human platelets (2.5×10^8/mL) were resuspended in pH 7.4 Hepes Tyrode's buffer without or with increasing concentrations of fatty acid-free BSA (0.05%, 0.1%, 0.5% and 1% respectively). Platelets were stimulated with 0.05U/mL of thrombin for 5 minutes. The reaction was stopped by 0.1U/mL of hirudin. Platelets were then pelleted at 13,000 × g and the supernatant was separated. Lipids were extracted and S1P was detected by MS. Percentage release of S1P was calculated. The data are representative of triplicate samples (average ± SD, n = 3).
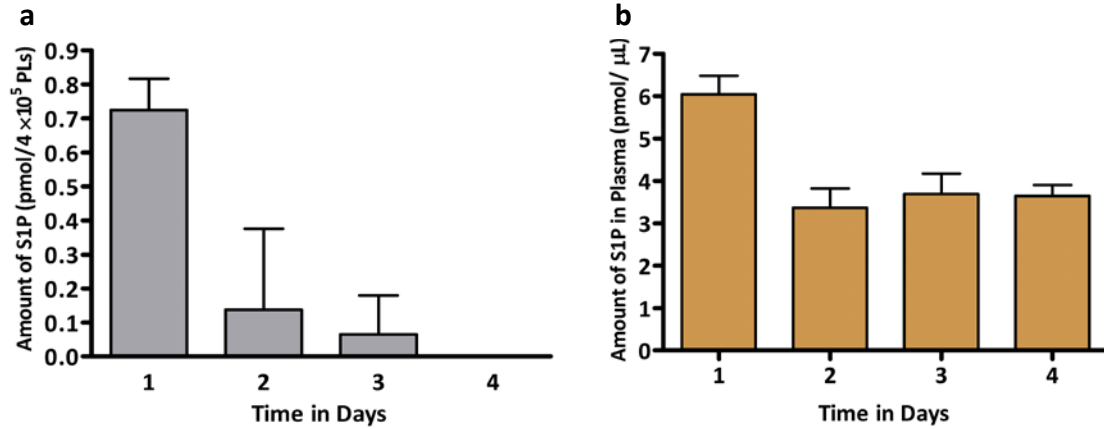
Figure 5.6. Influence of storage on S1P levels in platelets and PPP

Washed platelets were prepared for a period of four consecutive days from the same unit of PRP. Concomitantly PPP was saved from each preparation. Lipids were isolated each time in triplicates from platelets and PPP. S1P was detected by MS analysis. Amount of S1P was calculated as represented for platelets (**a**) and plasma (**b**). Each bar represents an average of triplicate samples (average ± SD, n = 3).
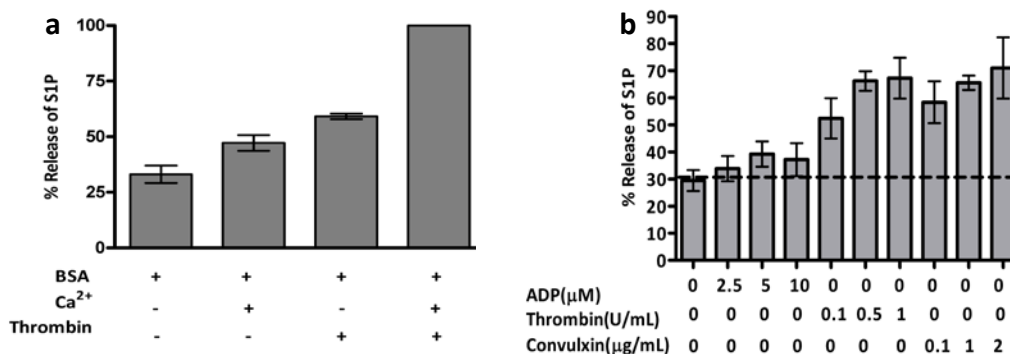
Figure 5.7. Release of S1P upon stimulation of platelets

Human platelets (2.5×10^8/mL) were prepared as described in 1% fatty acid-free BSA and with (+) or without (-) 1 mM Ca^{2+}. The platelets were then allowed to sit at RT for 30 min and 50 µL of them were stimulated with 0.05 U/mL thrombin for 5 min and stopped the reaction with 0.1 U/mL hirudin (**a**). Fresh human platelets (5×10^8/mL) were treated as before and stimulated with increasing concentrations of ADP, thrombin and convulxin as indicated for 5 min at RT (**b**). All the samples were done in triplicates. Lipids were extracted by liquid phase extraction and S1P was detected by MS analysis. % Release of S1P was calculated and the data are represented as the average ± SD, n = 3.
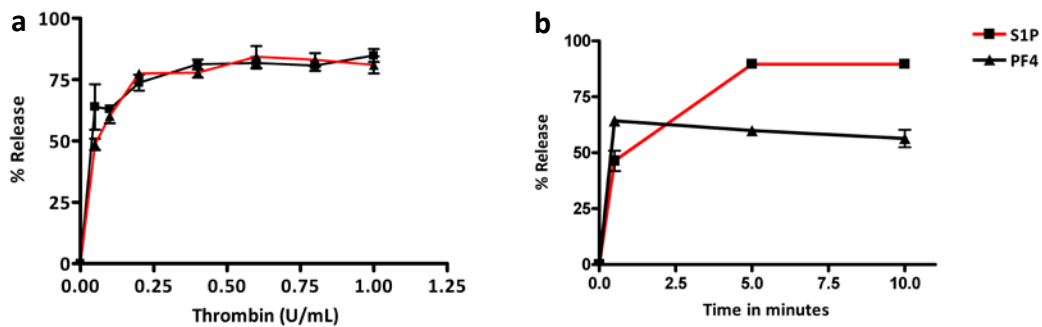
Figure 5.8. Platelet S1P release in a stimulation and time dependent manner

C57BL/6 mouse platelets (2.5×10^8 /mL) were isolated and resuspended in pH 7.4 HT buffer with 1% BSA. Platelets were stimulated with increasing concentrations of thrombin as indicated for 10 minutes at 37°C (**a**). Fresh human platelets (2.5×10^8/mL) in 1% fatty acid-free BSA were stimulated with 0.2 U/mL thrombin for indicated times and the stimulation was stopped with 0.4 U/mL hirudin at the end of each time point at RT (**b**). PF4 in both **a** and **b** was detected by ELISA. All the samples were done in triplicates. Lipids were extracted by liquid phase extraction and S1P was detected by MS analysis. % Release of S1P was calculated and the data are represented as the average ± SD, n = 3.
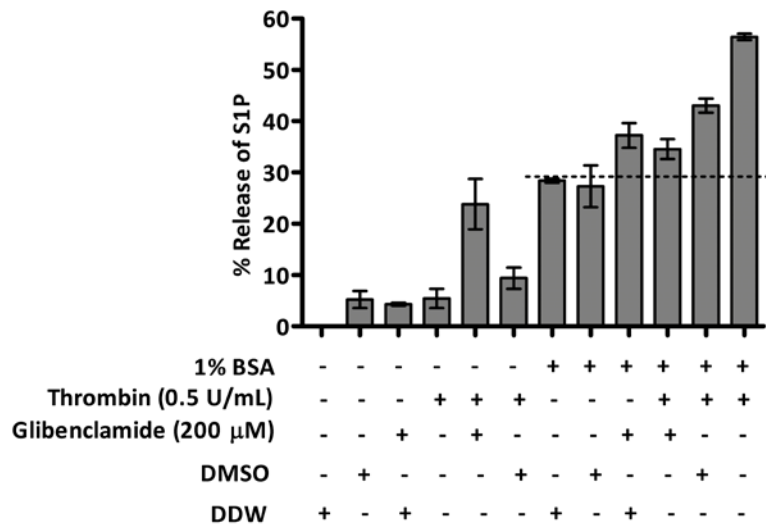
Figure 5.9. Effect of glibenclamide on S1P secretion from platelets

Fresh human platelets (5×10^8/mL) with or without 1% fatty acid-free BSA were incubated with or without 200 µM glibenclamide for 30 min and were then stimulated with 0.5 U/mL thrombin for 2 min as indicated. The reaction was stopped with 1 U/mL hirudin, platelets were separated by centrifuging the sample at 13,000 × g for 1 min and, % release ([Amount in the releasate / Amount in the releasate + Pellet] × 100) was calculated and plotted against time.
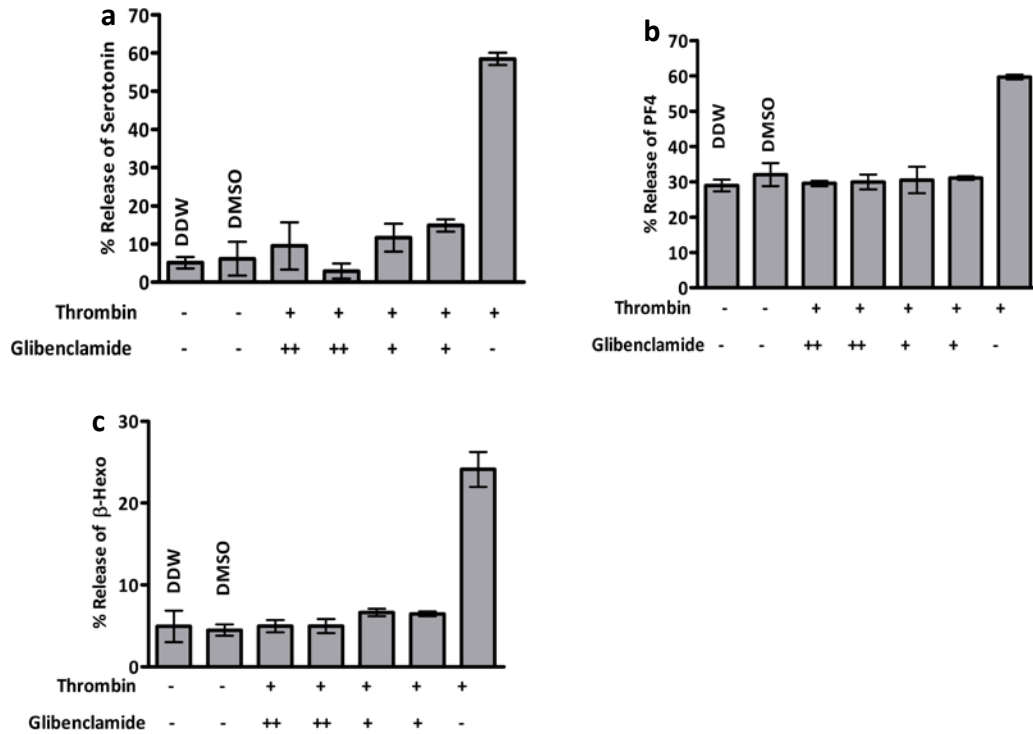
Figure 5.10. Effect of glibenclamide on secretion of known platelet granule cargo

Fresh human platelets were isolated after incubating the platelet rich plasma with [³H]-serotonin for 45 min. They were then treated with 200 µM (++) or 10 µM (+) glibenclamide for 30 min and stimulated with 0.2 U/mL thrombin for 2 min. % Release of serotonin was calculated interpreting [³H]-serotonin as a marker of dense granule secretion (**a**). % Release of PF4 was calculated through ELISA as a marker of α-granule secretion (**b**). % Release of β-hexosaminidase was calculated through an enzymatic assay as a marker of lysosomal secretion (**c**). All the samples were done in triplicates and are represented as the average ± SD, n = 3.
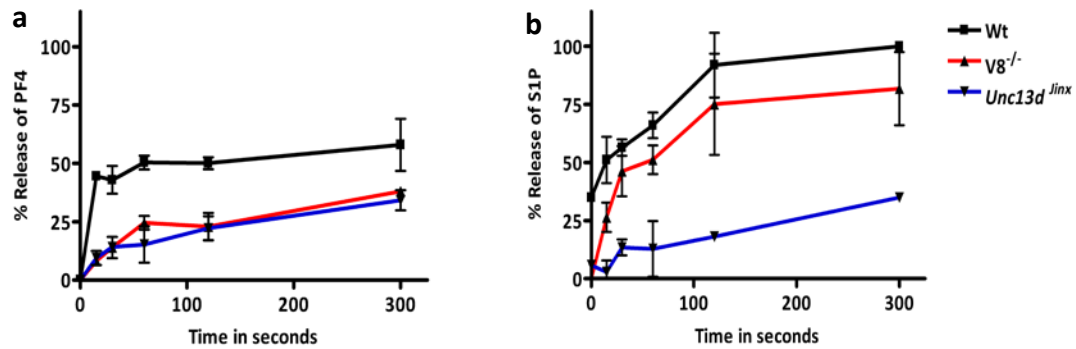
Figure 5.11. Involvement of SNARE machinery in secretion of S1P from platelets

Mouse platelets (2.5×10^8 /mL) were isolated each from C57BL/6, VAMP $8^{-/-}$ and *Unc13d* ^{Jinx} mice and were resuspended in 1% fatty acid-free BSA. They were stimulated with 0.05 U/mL thrombin for increasing amounts of time. The reaction was stopped with 0.1 U/mL hirudin and the platelets were separated from releasate by centrifuging at 13,000 × g for 2 min. All the samples were done in triplicates and the percentage release of PF4 at each point was determined by ELISA (**a**) and S1P was detected by MS (**b**). The data are plotted as % release ([Amount in the releasate / Amount in the releasate + Pellet] × 100) against time.
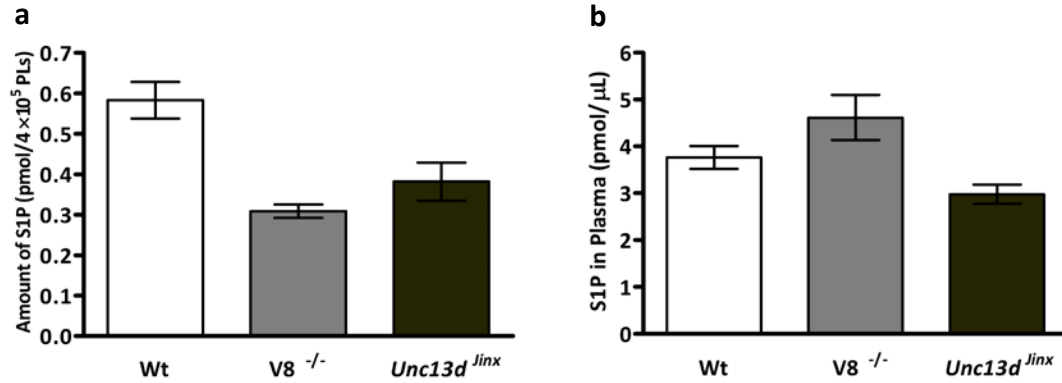
Figure 5.12. Levels of S1P in secretion-deficient mice

Washed mouse platelets (2.5×10^8 /mL) were prepared each from C57BL/6, VAMP8^{-/-} and *Unc13d* [Jinx] mice and were resuspended in pH 7.4 HT buffer containing 1% fatty acid – free BSA. They were stimulated with 0.05 U/mL thrombin for increasing amounts of time. The reaction was stopped with 0.1 U/mL hirudin at the end of the time point. The platelets were separated from releasate by centrifuging at $13,000 \times g$ for 2 min. S1P in the releasate and pellet was detected by MS after liquid phase lipid extraction. Total S1P as represented in the graph (**a**) was calculated combining the S1P levels in the releasate and pellet samples, and taking an average of all the samples included in the time course. All the samples at each time point were done in triplicates and represented in the graphs as average ± SD. The platelet poor plasma was separated from platelets by centrifuging at 1700 rpm for 10 min from the indicated mice type and S1P levels were calculated following the procedure as before (**b**). The data represented is an average of 7 samples from each mouse type.
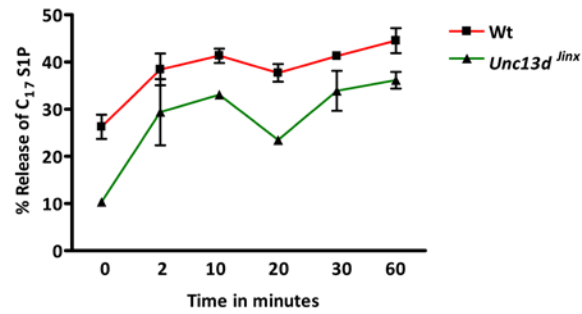
Figure 5.13. Release of newly synthesized S1P from secretion-deficient mice

C57BL/6 and *Unc13d* [Jinx] were incubated with 2 µM C_{17} Sphingosine for different amounts of time until 60 min as indicated in the graph for platelets to synthesize C_{17} S1P. Following incubation they were stimulated with 0.05 U/mL thrombin for 2 min and stopping the reaction by adding 0.1 U/mL hirudin. Platelets were then pelleted by centrifuging at 13,000 × g for 1 min. S1P levels were detected and % release was calculated as before.
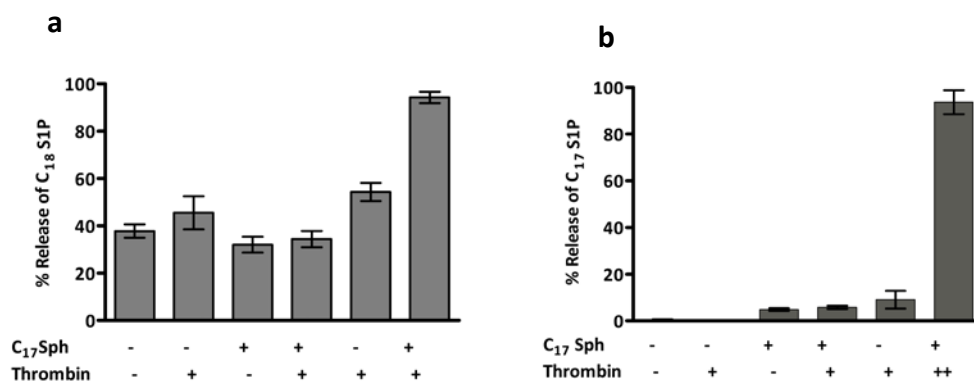
Figure 5.14. Agonist dose-dependent release of newly synthesized S1P

Fresh human platelets (5×10^8 / mL) were prepared and resuspended in pH 7.4 HT buffer with 1% fatty acid-free BSA. They were incubated with 6 µM C_{17} Sphingosine for 10 min and were later stimulated with either 0.05 U/mL (**+**) or 1U/mL (**++**) thrombin for 5 min. The reaction was stopped with 0.1 U/mL and 2 U/mL hirudin respectively. Platelets were pelleted by centrifuging the samples at 13,000 × g for 1 min. Lipids were extracted by liquid phase extraction and, endogenous (C_{18}) and exogenous (C_{17}) S1P was calculated as described before and the % release was obtained. The data are representative of 3 samples each (average ± SD).

a

NBD

NBD-Sphingosine

NBD-S1P

5   10   30   60 min

c   Wild type

Mepacrine   NBD-Sphingosine

Mepacrine   NBD-Sphingosine

Unc 13d [Jinx]

b

A   Mepacrine   B   Lyso tracker red   C   Merge

D   NBD-Sphingosine   E   Lyso tracker red   F   Merge
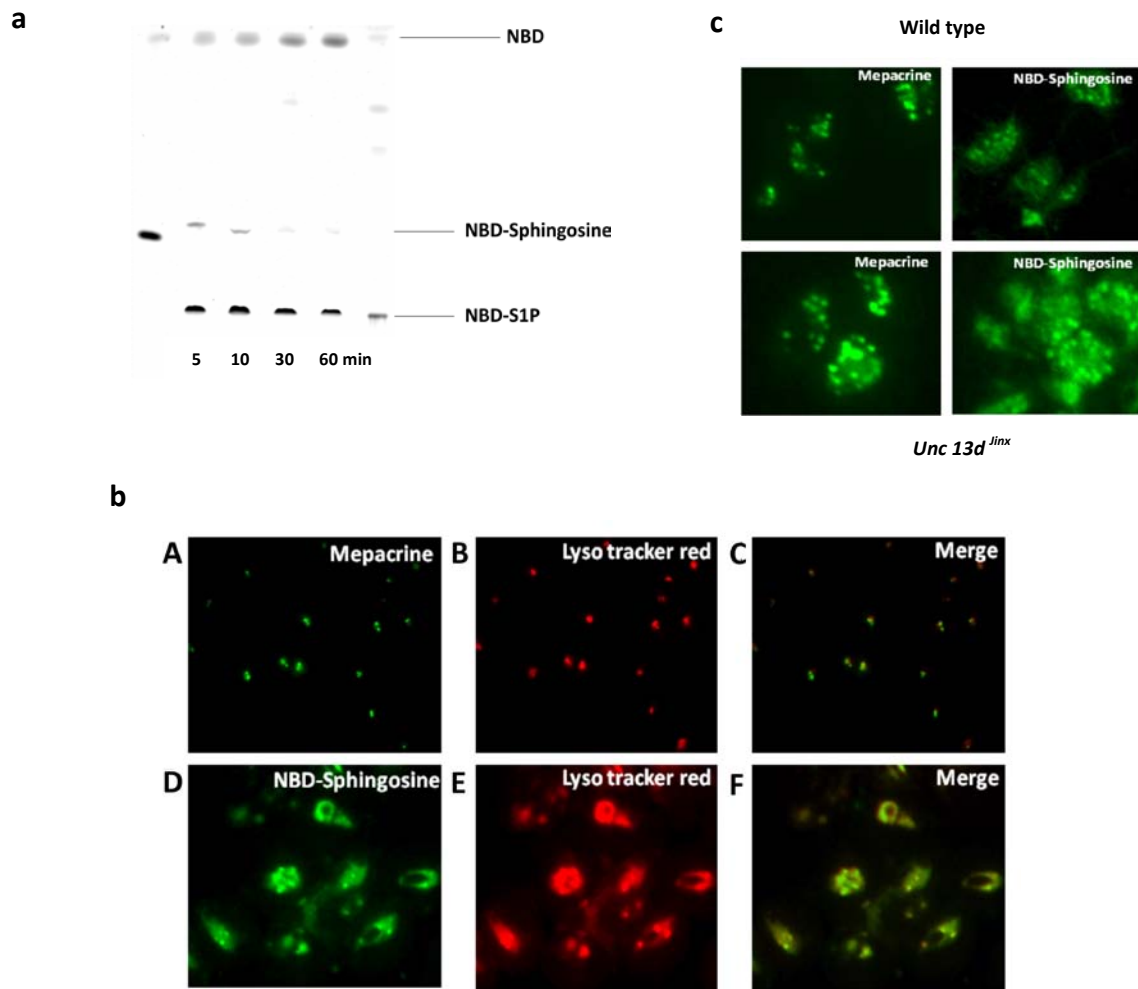
Figure 5.15. Localization of S1P in platelets

Banked human platelets (4.5×10^9/mL) in the presence of 1mM Ca^{2+} and 1% fatty acid-free BSA were incubated with 0.5 µM NBD-Sphingosine for 5, 10, 30 and 60 min as indicated. Lipids were extracted by liquid phase extraction and loaded on a TLC plate as described in methods (**a**). The first and the last lanes had NBD-Sphingosine and NBD-S1P as controls respectively. Banked human platelets (5×10^8 /mL) were prepared as described before and resuspended in pH 7.4 HT containing 1% fatty acid-free BSA (**b**). They were incubated either with 1 µM mepacrine (**A**) and 1 µM lyso tracker red (**B**) OR 1µM NBD-Sphingosine (**D**) and 1µM lyso tracker red (**E**) for 30 min at 37°C. This was followed by centrifuging the samples at 1600 rpm for 5 min and resuspension in fresh HT buffer without BSA. About 10µL of the sample was put on a microscope slide and a cover

slip was laid over. The slides were allowed to incubate for 30 min for the platelets to settle down and viewed through 100X objective lens in oil immersion under Nikon Eclipse 600. The same was performed for the wild type and $Unc13d^{Jinx}$ mouse platelets (**c**).
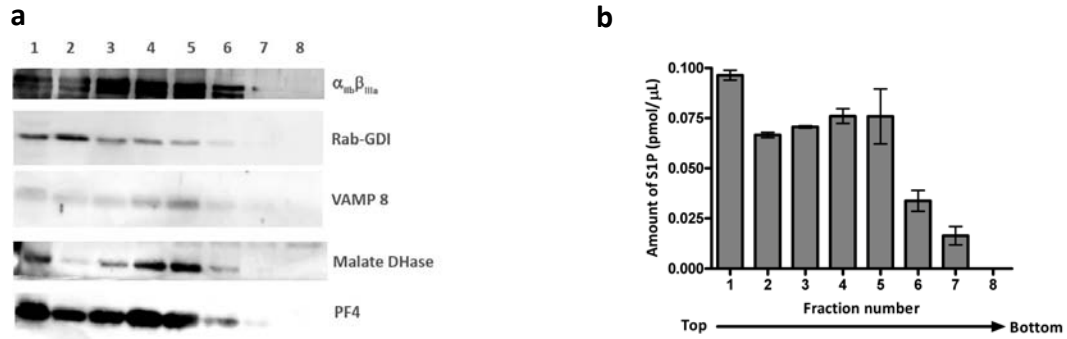
Figure 5.16. Sub-cellular fractionation of platelets

Human platelet homogenate was prepared as described in methods. Sucrose gradient from 60% to 30% was prepared. Two milliliters of platelet homogenate obtained upon nitrogen cavitation was overlaid. The fractions were separated by ultracentrifuging at 40,000 rpm at 4°C for 90 min, which were snap-frozen and stored overnight at -80°C. The obtained fractions were concentrated by TCA precipitation and loaded on 12.5% SDS-PAGE gel and analyzed for the indicated proteins by western blotting (**a**). The corresponding fraction numbers are indicated above. S1P was detected by MS analysis after liquid phase lipid extraction from the corresponding fractions (**b**).

Chapter Six

Discussion

Part I - Existing view on platelet secretion

Platelets are presently recognized as the reservoirs of numerous proteinaceous substances which appear to be mainly stored in α-granules. Since many of these cargo molecules can affect different physiological processes, *e.g.* proliferation, angiogenesis, inflammation, atherosclerosis *etc.*, their roles may not be restricted to thrombosis. The expanding boundaries of their participation underline the importance of understanding the process of how they are released from platelets. The release pattern followed by activated platelets is determined by the way they are packed. The cargo molecules can be packaged into the α-granules either during platelet generation from megakaryocytes (*e.g.* PF-4) or endocytosed during circulation (*e.g.* VEGF).

The importance of α-granule content release from activated platelets is best demonstrated in GPS patients. Their platelets are characterized by numerous, giant, ghost vacuoles representing empty α-granules. The proteins synthesized in megakaryocytes, instead of being loaded into α-granules leak into the bone marrow resulting in myelofibrosis (*Nurden and Nurden*, 2007). Though not life-threatening, alarmingly variable symptoms are associated with this syndrome. The variability in the extent of bruising seen in GPS patients confirms the importance of normal storage of contents in α-granules. The defect has been recently identified to be localized to chromosome 3p (*Fabbro et al.*, 2011; *Gunay-Aygun et al.*, 2010) and caused by a defect in the NBEAL2 protein (*Urban et al.*, 2012).

The distribution of platelet cargo in α-granules into distinct locations (*Italiano et al.*, 2008) and their secretion being dictated by the mode of platelet activation (*Ma et al.*, 2005) has raised a number of questions about platelet secretion. Are platelets "smart bombs", able to release thematically consistent cargo in response to specific agonists or are they passive carriers that stochastically release their cargo in direct correlation with their degree of stimulation? The work of Italiano *et al.* suggests that

angiogenesis regulators can be packaged into distinct populations of α-granules. Immuno-fluorescence and immuno-electron micrographs point towards distinct localizations for pro- and anti-angiogenic factors (*Italiano et al.*, 2008). Supporting these studies, several groups (*Chatterjee et al.*, 2011; *Ma et al.*, 2005) have shown that stimulating platelets with different agonists (*i.e.* PAR1- and PAR4-agonists) causes differential release of some cargo. Pro-angiogenic factors have been proposed to be released only upon stimulation with PAR1-agonist while anti-angiogenic factors are released upon stimulation of platelets with PAR4-agonist. An alluring concept of platelet secretion being contextually thematic was thus proposed. The flaws in these studies are the focus on a narrow set of cargo molecules, limited set of agonist concentrations and single time points used. Our data shows that partial activation contributes to the perception of release heterogeneity (see Chapter Three). More recent work by Storrie and colleagues has shown that cargo may be spatially segregated into sub-regions of the same membrane-bound granule with minimal co-localization of factors with like functions (*Kamykowski et al.*, 2011; *Sehgal and Storrie*, 2007). This would imply stochastic packaging of cargo and perhaps some degree of homo-oligomerization similar to what has been reported in chromaffin cells (*Salazar et al.*, 2009). These views of platelet secretion are conflicting and hence the need for the studies presented in this dissertation. If there is heterogeneity in cargo packing and/or secretion as suggested, regulating the release of specific α-granule sub-populations may allow specific manipulation of the microenvironment at an injury site without disturbing hemostasis. The work described here was an attempt to understand platelet secretion heterogeneity and to overcome the drawbacks of the previous work. We used agonist concentrations that yield maximal release responses and we examined the kinetics of release of a significant number of platelet cargo molecules.

Summary of the presented work

The secretion trends seen in the representative markers ([^{3}H]-serotonin for dense granules, PF4 for α-granules and β-hexosaminidase for lysosomes) provided an early clue for the initial characterization of platelet secretion process. Also, the importance of agonist-potency was obvious from the studies using thrombin titrations. The study was broadened utilizing micro-ELISA chips to analyze 28 different cargo molecules. These included pro- and anti-angiogenic factors, growth factors, inflammatory factors and miscellaneous cytokines/chemokines. Release of these cargo molecules was simultaneously measured upon stimulation of human platelets over a time-course of 5 min with different agonists (thrombin, PAR1/4-agonists, and convulxin). To avoid the consequences of differential levels of activation, an initial agonist titration was done. An agonist concentration yielding ~ 90% dense granule release was selected for further analysis. Thrombin is a very potent agonist, which cleaves PAR1/4 exposing the tethered ligand. To dissect the role of PAR1 and PAR4 activation individually, platelets were stimulated directly with the respective peptides (SFLLRN for PAR1 and AYPGKF for PAR4). To compare platelet secretion, stimulated through a different signaling pathway, convulxin was employed as an agonist. It stimulates the platelets through GPVI pathway, requiring tyrosine kinase activation. Hence, the choice of agonists used for the study was designed to address the questions of extent of stimulation (thrombin *vs.* PAR1/4) and mode of stimulation (thrombin *vs.* convulxin). Manual and mathematical analyses were used to develop descriptors of the secretion process that could be used for comparisons and analysis.

Agonist-potency determined the extent of platelet secretion. More cargo molecules were detected in the releasate when the platelets were stimulated by a potent agonist like thrombin; not as many were detected when platelets were stimulated with less potent agonists, like PAR4. Evaluating the kinetic data by calculating the rates of secretion (and their probability density function (*pdf*) enabled us to better understand platelet secretion. The distribution of cargo molecules into three different kinetic classes identified in the *pdf* analysis was confirmed by the operator

variance analysis. This approach takes into account inherent pipetting errors, cargo-packaging, granule geometry, location of granule, mode of granule fusion - all factors which contribute to the final observations. So many variables generate complexity in data that cannot be entirely controlled. Operator variance analysis was included to partially address this issue. Taken together, these analyses indicate that platelet cargo release is distributed into three kinetic classes. The manual categorization of the values combined with the statistical analyses (*pdf* and operator variance analyses) directed towards the kinetic distribution of the platelet cargo into three classes – the fast, intermediate and slow. There was no thematic pattern associated with the release of cargo molecules. This was exemplified by the random distribution of angiogenic factors *e.g*. angiogenin, VEGF, angiostatin, and oncostatin M upon stimulation of platelets with agonists differing in their potency. This was true for all the cargo molecules selected for the study irrespective of their physiological activity. Several factors leading to heterogeneity in platelet exocytosis are represented in **Figure 6.1**.

Our study minimized the heterogeneity in platelet secretion generated by partial activation by using optimal doses of various agonists to ascertain same degree of activation. Heterogeneity in platelet secretion detected in our experiments did not follow any functionally relevant thematic pattern. Both qualitative and quantitative analyses pointed towards the distribution of cargo molecules into three different kinetic classes. This heterogeneity stems from diverse factors contributing to the complexity seen in our kinetic analysis. An attempt to describe the need for heterogeneity in secretion and some of the factors and multiple possibilities are described below.

Importance of existence of kinetic heterogeneity in secretion

Physiologically, the process of granule fusion is indispensable in synapses, chromaffin cells, pancreatic β-cells, mast cells, *etc.* Some of these fusion events occur in milliseconds, other in a few hundred seconds. The rate of fusion is thus controlled to maintain normal physiology. Any deviation from the normal rates of fusion results in an anomaly that could affect a number of processes. As described in Kasai *et al.* (*Kasai et*

114

al., 2012), different cell types employ different rates of fusion, based on their requirement. For example, the exocytotic rates in neurons fall in the range of few milliseconds for expedite neurotransmission. The release of insulin from the pancreatic β-cells is more sustained, and can take up to 600s to control the blood glucose levels. The release events associated with several cell types have been categorized based on the rates of fusion – ultrafast, fast and slow exocytosis events. Neurons stand out as the exocytotic events of the synaptic vesicles can fall into all three categories. Based on our work, platelets may be similar since platelet release rates can be categorized into three kinetic classes. This sub-division, based on release rates, might be relevant for platelets to carry on their functions, from the initiation phase in thrombus formation to the final perpetuation phase. The sustained release exhibited by platelets becomes important in regulating the microenvironment upon vascular injury.

The various possible contributors to the observed release kinetics are discussed in the following sections: granule cargo packaging, geometry and location, and depicted in the **Figure 6.2**.

Granule cargo packaging

The cargo could be packed distinctly in different α-granules (**a**). Even though α-granules outnumber dense granules and lysosomes, the hundreds of known cargo proteins cannot be housed in <50 granules, a typical platelet contains. Therefore, this strategy of individually designated granule cargo packaging is not plausible. The cargo molecules are thought to exist as clusters and might be in the form of calcium-bound aggregates. In this way, each granule could house cargo molecules of varying natures (**b**). Moreover, there might be no restriction on the number of granule cargo molecules to be housed by each granule. Such granule packaging may be satisfied by thematic localization of cargo, cargo molecules with similar function (*Italiano et al.*, 2008) (**c**) or cargo with unrelated/contrasting functions to a distinct granule (*Kamykowski et al.*, 2011) (**d**).

Granule geometry

Platelet α-granules are spherical in electron micrographs (**e**). For modeling the kinetic data, we hypothesized granules to be spherical. Moreover, as the curvature of vesicles determines the ease of fusion pore formation, a vesicle being spherical is more accepted. More recent electron tomographic analysis suggests that granules are elongated and tubular (*van Nispen tot Pannerden et al.*, 2010) (**f**). The formation of fusion pore is thought to be more efficient if the vesicle membrane has more curvature. If the distribution of the cargo is homogeneous and the granule is spherical, then irrespective of the granule fusion site, the rate of secretion should be uniform. If the granule geometry is tubular (our data supports this hypothesis) and the distribution of the cargo is more heterogeneous and clustered (analogous to the multi-colored candy in a pixy-stick), the fusion site on the granule will determine the sequence of release of cargo molecules and thus, their rates of release. Both Weibel Palade bodies (WPBs) of endothelial cells and α-granules are reservoirs of vWF. WPBs are known to be tubular (*Huang et al.*, 2008). Through cryoelectron tomography and immuno EM, it has been shown that α-granules are divided into at least, two sub-types, based on their morphology – spherical and tubular (*van Nispen tot Pannerden et al.*, 2010). While the membrane proteins like $\alpha_{IIb}\beta_3$ and GLUT4 have been observed to be localized to tubular sub-population, vWF and β-TG localized to the spherical granules. Fibrinogen was distributed equally between spherical and tubular granules. As it was mentioned before, WPBs, the stores of vWF are tubular; it is improbable that the content dictates the geometry. But, a high spatial segregation is observed in these studies (*van Nispen tot Pannerden et al.*, 2010). Presence of both spherical and tubular α-granules adds to the complexity of the release pattern.

Granule location

In addition to factors described above, an added feature that might contribute to heterogeneity is the location of a granule. The way platelets are thought to exocytose their contents is through the centralization of granules followed by fusion with OCS. As introduced in Chapter One, OCS is the extra membranous system that is in continuity

with the plasma membrane of the platelet. OCS serves as a route for secretion of granule contents upon platelet activation (*Escolar et al.*, 1989). If the granule is closer to OCS or to the plasma membrane, the probability of exocytosing their content faster is greater when compared to the granules away from the fusion site. Moreover, as represented in **Figure 6.2**, the granules fusing with the plasma membrane can either be spherical (**g**) or tubular (**h**). The shape of the granule might determine the sequential/indiscriminate delivery of the granule contents to the exterior. The vicinity of these granules to OCS/plasma membrane will determine the probability of granular fusion.

One tier of the observed heterogeneity in granule secretion can be associated with all the above described features. The second tier contributing to secretion heterogeneity involves the mode of granule fusion. The multiple possibilities that might determine the release rates are represented schematically in **Figure 6.3** and are discussed below.

The expedited fusion events are represented by the docked vesicles fusing with the plasma membrane upon stimulation (**a**). They constitute the cargo molecules falling in the fast kinetic class. Dense granules are already known to fall into this class, but there is every possibility that an α-granule can also be a member of this class, though less frequently. The release rates of several α-granule cargo molecules fall into the same class as serotonin (a dense granule cargo) in our study. On the other extreme, most of the granule cargo falls into the slow class. These events can be successful upon gradual fusion of the undocked vesicles engaging in successful formation of SNARE complex and finally fusing to release the contents (**b**). The third class of cargo release observed in the *pdf* includes the intermediate class. The fusion events responsible for intermediate cargo class in our kinetic analysis are represented in **c** and **d**. They represent bi-/multi-granule fusion events respectively. Apart from the already docked vesicle fusing with the membrane upon stimulation, this might be associated with the initial inter-granular fusion followed by fusion with the vesicle already fused with the plasma membrane (**c**)

117

and this ultimately can be represented by the final stage in (**d**) or can form a continuous thread of vesicles releasing their contents through the vesicle that is fused to the plasma membrane (**d**). This multigranular exocytosis is associated with the release of cargo in bulk. As a result, the sequential release of cargo is more organized and restricted. This would not prioritize cargo release based on their physiological function.

The mode by which the cargo molecules are released is most certainly a combination of possibilities represented in **Figures 6.2** and **6.3**. Our initial analysis of the granule fusion was built on the premise of spherical granules. Taking into account the possible tubular geometry of a granule, the release events could be more organized based on the original packaging. Moreover, a large number of cargo molecules are represented in the slow class irrespective of the agonist used for stimulating the platelets. Therefore, it is plausible that the release events represented by this class are a combination of events depicted in **Figure 6.3 b, c, d**.

SNARE machinery constitutes the final contributor to the platelet secretion heterogeneity. The following section in the discussion entails the contribution of SNARE machinery.

Distribution of SNARE machinery

The role of SNARE machinery in driving granule fusion is depicted in the **Figure 6.4.** The minimal requirement for granule fusion to occur involves the participation of cognate t- and v-SNAREs. Though true, the rate at which the fusion process proceeds *in vitro* does not coincide with the rates of fusion *in vivo* demonstrating the importance of a number of SNARE-regulators that control when and where the fusion complexes form, and lead to a successful exocytotic event. The regulatory molecule, Munc 13-4 indicated in **2** of **Figure 6.4** drives granule fusion to completion. In the resting state, vesicles can either be distal to their target membrane, undocked (**1**) or be proximal to the target membrane, where the cognate v- and t-SNAREs have found each other, docked (**2**). The regulatory molecule like Munc13-4 has been observed to anchor the cognate v- and t-SNAREs in place aiding in the granule fusion process (Chicka *et al*, unpublished). If the

granule is undocked, the release of cargo will be much slower since the time for the movement of granule to the appropriate fusion site and for the cognate v- and t-SNAREs to approach and recognize each other. On the other hand, if the granule is docked (**2**), the cognate v- and t-SNAREs are already in place and are awaiting a trigger to proceed with the granule fusion and release the cargo. These cargo molecules are associated with faster release rates. A regulatory molecule, Munc 13-4 as already mentioned has been observed to be involved in holding the docked vesicles intact (Chicka *et al* unpublished). Stages **4**, **5**, and **6** represent possible explanations for the observed three different kinetic classes of secretion in platelets. The underlying aspect in these stages is the degree to which the SNARE machinery is employed. Loose, intermediate and the tight stages of granule fusion explain the ranking of v- and t-SNAREs pairing in the increasing order, signifying the ease of the fusion process to go to completion. In neurons, calcium has been shown to act as a catalyst hastening fusion. The listed exocytotic stages are categorized based on the proximity of v- and t-SNAREs to ascertain a successful granule fusion event. The release rates of cargo molecules are dictated by the stage of fusion that the granules are in. To be explicit, the cargo molecules stored in a stage **5** granule are released faster when compared to those in stage **3**. For the fusion process to proceed from stages **3** to **5**, the availability and continual participation of the SNARE machinery is essential. This might involve recycling of SNAREs for maximal availability. Not only is the position of granule relative to the target membrane important in determining the fusion rate but also, the availability and prompt participation of cognate SNAREs is important. The anchoring of t-SNAREs to the membrane by acyl groups (*Chen et al.*, 1999) points towards the possibility of t-SNAREs to recycle enabling their increased availability to increase the granule fusion events. As it is now understood that the release rates of the granule cargo are a function of granule fusion process, controlling SNARE machinery determining the fusion rates has enhanced significance. To our present knowledge, VAMP-8 is the primary platelet v-SNARE, while VAMP-2/3 are considered to be the secondary v-SNAREs. Syntaxin-11 has recently been identified as an important platelet t-SNARE. Selectivity of SNARE population to various

granules is still an open question. To test the involvement of SNARE machinery in determining platelet kinetic secretion heterogeneity, comparison of secretion kinetics of VAMP-8 $^{-/-}$ and RC Tox :: PF4 Cre will be helpful. Moreover, subpopulations of α-granules in the spreading platelets have been identified (*Peters et al.*, 2012) to be associated with distinct VAMPs. α-Granules employing VAMP-3 and VAMP-8 are more localized towards the center of a spreading platelet while the granules employing VAMP-7 are concentrated more towards the periphery. The differential utilization of SNARE machinery thus might contribute to distinct kinetic classes in platelet secretion.

The observed platelet secretion heterogeneity is a combination of: granule cargo packaging, granule geometry, granule location, modes of granule fusion and distribution of SNARE machinery. **Figure 6.1** is a schematic representation of all the described features that could contribute to secretion heterogeneity. What was not explicitly considered was the possibility that the granules are tubular. This is represented under the 'cargo release' of **Figure 6.1**. Envisioning the extremity of the tubular granule fusing with the membrane and resulting in sequential release of the cargo based on the order in which they are packed is perhaps obvious. A 'pixy-stick' is a perfect analogy to describe the process. The candy that is close to the opening comes out first while the farther ones come out later sequentially. If the fusion does not involve the extremity of the tubular granule, the release of the contents might follow a different release strategy. The distribution of SNARE machinery therefore becomes very important factor in determining the release rates.

A caveat to the work is that a cargo molecule stored in multiple granules cannot be differentiated by the rate of release. The conclusion from the present study represents only an average of several granules with similar cargo releasing their contents following different patterns. The resultant signal is an average, representative of heterogeneous release patterns as depicted in **Figure 6.5**. Whether or not the individual platelet secretion of contents is sorted out, the resultant of the release of cargo molecules in the microenvironment of vasculature/injury site is going to be the

dominant character. Secretion in WPBs has been known to be time dependent and selective (*Babich et al.*, 2008). WPBs are heterogeneous, meaning have distinct granules differing in their contents, and differential, meaning their release can be controlled selectively by stimulation with distinct agonists (*Cleator et al.*, 2006). We see that platelet granules are heterogeneous in nature, but their release cannot be controlled selectively. The difference in the assay methods employed as well as the endogenous heterogeneity, as discussed, might contribute to the observed variability. Employment of distinct SNAREs might attribute platelets to release their contents differentially. Preliminary studies show that elimination of, secondary SNAREs (VAMP-2 and -3) or VAMP-8, -2 and -3 selectively in mouse platelets had a diminished platelet secretion (Joshi *et al*, unpublished). This demonstrates employment of distinct SNAREs dictating variable fusion rates. Taken together, these analyses might indicate that VAMP-7 is associated with granules localized to periphery in spreading platelets (faster K_{ex}) and the remaining identified SNAREs, VAMP-8, -2, -3, are associated with the centrally localized granules (intermediate and slow K_{ex}). Moreover this selective distribution of SNAREs might not only determine fusion rates but also, if the cargo molecules released can be effective in performing their physiological function based on the fusion site, more of which will be discussed in the following section. The work presented here involves the study of platelet secretion process, but does not address the influence of shear force in circulation. None of the studies done so far involved the platelet secretion dynamics under flow conditions. Employment of microfluidic devices (*King and Diamond*, 2012) in the study of platelet secretion has a viable role in unveiling the granule characteristics in platelets.

Importance of platelet secretion kinetic heterogeneity

Our data suggests that the platelets release their contents in three distinct kinetic classes – fast, intermediate and slow. Serotonin was always associated with the fast release kinetic class. Measurements could not be made in all the trials as the release of serotonin was too fast for our analysis scheme. The remaining chemokines irrespective of their function were distributed into all three kinetic pools; hence there

was no detectable thematic pattern. Recent studies (*Stalker et al.*, 2013) utilizing confocal intravital microscopy have indicated hierarchical organization of the thrombus at the site of vascular injury. The growing thrombus can be divided into a core region and shell region (**Figure 6.6**). Upon vascular injury, platelets roll down the endothelial lesion site, adhere, degranulate and recruit further more platelets. The core region constitutes the most proximal region to the injury site. The core is characterized by lower porosity with more fibrin and thrombin generation, and P-selectin exposure indicative of α-granule release. The shell region is more distal to the site of injury and is more porous and unstable. It is composed of platelets that are partially activated by ADP and TxA_2. Being small in size, molecules like ADP and TxA_2 can extrude the core region to activate platelets in the shell region. As the platelets in the shell region are tethered and are partially activated, they are still capable of going back into circulation blocking capillaries. Moreover, clopidogrel and cangrelor, which inhibit P_2Y_{12} receptors (receptors for ADP), reduced the size of shell region but not the core (*Stalker et al.*, 2013). This suggests that, manipulating the size of the shell region might prevent the vascular occlusion that might lead to conditions like stroke and heart attack. Taken all the observations together, kinetically segregated platelet secretion provides a layer to regulation of microenvironment.

Our kinetic secretion data fits perfectly with this *in vivo* data (*Stalker et al.*, 2013). The cargo with fast and intermediate release kinetics might contribute to the formation of the core region. It might result in faster wound healing if the constituents associated with these release kinetics are growth factors and/or pro-angiogenic factors. The contents that are slowly released might diffuse away with minimal localized effect. The secondary agonists like ADP generated by platelets constituting the core region result in activation of recruited platelets constituting the shell region. As thrombin production is limited proximal to the injury site (core), platelets are likely to be activated by weak agonists like ADP potentially decreasing the ability of platelets to completely degranulate (shell). Therefore, the degranulation of platelets in distinct phases might provide platelets the ability to stick to the lesion site, become active, recruit more

platelets and the large number of molecules constituting the slow kinetic class might be responsible for the modification/healing of the lesion site. The inflammatory molecules discharged might limit the entry of infectious agents, the necrotic factors destroy the damaged cells, growth and angiogenic factors help in the renewal of the damaged site. Release of all molecules in bolus, might result in inefficient delivery of the required factors at the right time. Those not essential for further platelet activation or recruitment might drift away over time or those with short half-life lose their potency or increased probability of encountering their inhibitors as they diffuse away. This provides suitable explanation for the importance of existence of kinetic heterogeneity in platelet secretion.

The results of the work presented here show that the granule cargo is heterogeneous and there is no thematic pattern associated with the way they are released. The significant feature that was detectable through our studies is differential kinetic distribution of the cargo. Release of cargo over time as indicated by our studies is beneficial in modifying the lesion site. The efficiency of the released cargo might as well depend on the microenvironment it first sees after its release and thus spatial orientation becomes an essential factor in deciding the fate of the released cargo. The effect of cargo molecule accumulation would lead to pronounced localized effect if the exit site of the cargo molecule of interest is towards the lesion site. If the exit site is away, diagonal or opposite of the lesion site, the efficiency of the cargo molecule to act is restricted and/or diminished. Release of contents in hierarchy following a thematic pattern onto a lesion site cannot be addressed here as our secretion experiments are conducted in suspension. Release of angiogenic and growth factors towards a lesion surface might hasten modification of the damaged environment. Provision of a platform for platelet secretion might accentuate the movement of the granules within a platelet towards the surface (lesion site). This might result in increased probability of granule fusion towards the lesion site thus increasing the chance of the released cargo to exhibit its physiological function. The presence of a platform determining the directionality of release events is yet to be tested. If there is a thematic pattern associated with platelets

in releasing their contents upon activation, it coupled with detected kinetic heterogeneity would add onto controlled platelet secretion. Though it is too early to say, the above mentioned possibilities might entitle platelets to be called 'smart bombs'.

Part II - Distribution and movement of lipids

The asymmetric distribution of lipids across membrane bilayer is an important determinant of cell metabolism. This is exemplified by the exposure of phosphatidylserine (PS) on outer leaflet of plasma membrane in a dead cell. This asymmetry is not only limited to the plasma membrane, but extends to cellular organelles (*Pomorski et al.*, 2004). The eukaryotic cell membranes are rich in sphingolipids, cholesterol, and PS, whereas ER is depleted of these lipids. This is made possible in a cell by a constant inward and outward diffusion of lipids. The spontaneous movement of neutral lipids, like cholesterol; charged lipids like free fatty acids, phosphatidic acid, phosphatidyl glycerol in their protonated form is fast (*Hamilton*, 2003). Lipids with polar head groups like PC, PS, PE, and glycolipids with large carbohydrate moeities are considerably slower (*Buton et al.*, 1996; *McConnell and Kornberg*, 1971). To overcome this difficulty and maintain this dynamic equilibrium, there are a number of supporting proteins (*Bretscher*, 1973). They can be energy independent (e.g. scramblase) or dependent (e.g. translocases). Scramblases are activated by calcium, usually associated with cell activation (as seen in platelets) (*Pomorski et al.*, 2001). The energy involvement in the maintenance of asymmetrical distribution of lipids was first identified in erythrocyte membranes where PS from the outer leaflet was incorporated into the cytosolic leaflet by unidirectional aminophospholipid translocase (*Middelkoop et al.*, 1989). This stands as an example for inward translocation of lipids. The outward translocation of lipids was illustrated through the studies involving multi drug resistance (MDR) proteins (*Dekkers et al.*, 1998). These are ATP binding cassette (ABC) family of proteins that extrude a variety of amphipathic drugs from cells. Specific ABC transporters for transport of distinct lipids have been identified. Selective maintenance of asymmetric distribution of lipids in cells is therefore a highly controlled process.

Bioactive lipids

The importance of bioactive lipids in various cell types is widely appreciated. This is due to their involvement in regulating various cellular processes like cell growth, survival, development, cell division, fusion of vesicles and intracellular signaling (*Spiegel and Milstien*, 2003). Distinct lipids like phosphatidyl choline (PC) and free cholesterol (FC) are dominant in different blood cell types. Platelets stand out because they have a high amount of cholesterol esters when compared to other blood cells (*Leidl et al.*, 2008). More than two decades ago, the concept of 'bioactive' lipids emerged. Changes in the levels of these lipids have biological implications highlighting the fact that lipids are not merely passive cellular components and membrane constituents but do affect cellular pathways and behavior. The involvement of lipids in the activation of PKC by diacylglycerol (DAG) was demonstrated (*Nishizuka*, 1992). Eicosanoids, phosphatidyl inositol 3,4,5 triphosphate (PIP3), phosphatidic acid (PA), lyso-phosphatidic acid (LPA) , platelet activating factor (PAF), sphingolipids, thromboxane A_2 *etc.* form a list of bioactive lipids that are relevant to platelets. Transport of these bioactive lipids is essential to many functional responses.

The studies in Chapter Five focused on a bioactive lyso sphingolipid, Sphingosine-1-Phosphate (S1P). The sphingolipid metabolism is complicated and is demonstrated by the number of enzymes involved (*e.g.* 26 for ceramide) and the number of distinct moieties of same compound grouped based on their desaturation, acyl chains and hydroxylations (*e.g.* 50 distinct species for ceramide) (*Hannun and Obeid*, 2008). The site of their generation and action often do not coincide. For example, S1P is generated on the inner leaflet of the plasma membrane and can act by binding to its receptors expressed on the cell surface. For this to happen, complex living systems developed transporters and flippases. S1P transport is now known to be mediated by members of ABC transporter superfamily (CFTR (*Boujaoude et al.*, 2001), ABCC1 (*Mitra et al.*, 2006)), SPNS2 (*Hisano et al.*, 2012). Flip-flop mechanism has been extensively studied in ceramide transport. A ceramide transfer protein was identified which transports ceramide from ER (site of synthesis) to the Golgi, where it is further metabolized into

sphingomyelin (*Hanada et al.*, 2003). Restricting the flip-flopping of these lipids does impact their biological function (*Marchesini and Hannun*, 2004; *Pomorski et al.*, 2004).

Transporters in platelets

Several transporters have been identified in platelets. Solute carriers (SLCs) and ABC proteins have been identified to transport drugs, endogenous metabolites and signaling molecules. The C – branch ABC proteins (*Jedlitschky et al.*, 2004) (*e.g.* MRP4) and A – branch ABC proteins (*Albrecht and Viturro*, 2007) play essential roles in the maintenance of lipid homeostasis in platelets. Initially, ABCC4 [multidrug resistance protein (MRP4)] was shown to be involved in pumping adenine nucleotides into dense granules (*Jedlitschky et al.*, 2004). MRP4 expression in platelets is on the dense granule membrane as well as on the plasma membrane (*Jedlitschky et al.*, 2004). Prostaglandins (PGs) and thromboxane A_2, initially thought to be passively transported, are now identified to be actively transported by MRP4 in platelets (*Tornhamre et al.*, 1998). MRP4 is also identified to release cAMP and cGMP (*Deeley et al.*, 2006; *Jedlitschky et al.*, 2004; *Russel et al.*, 2008) which are the known intracellular second messengers to maintain platelets in resting stage. Various transporters are therefore known to contribute to platelet regulation.

Export of platelet S1P is important, as a bolus of S1P will be supplied on platelet activation to modify the microenvironment. S1P is abundant in plasma, erythrocytes and platelets. Platelet S1P pools become significant as they aid in localized effect upon activation. The released platelet S1P is trapped at the growing thrombus in the vascular injury site and not washed away by the shear flow of circulation. MK571, an inhibitor for MRP1, also interfering with MRP4, blocked secretion of S1P from platelets (*Ulrych et al.*, 2011). S1P is also reported to be released via ABCA1-like transporter in platelets (*Kobayashi et al.*, 2006). Moreover, ABCA7 is identified in platelets and is expected to play a role in the transport of S1P (*Sasaki et al.*, 2003). None of the reports provided a strong evidence for the transporter involved in platelet S1P transport.

The work that is presented in Chapter Five addresses the route of S1P release from platelets. The data suggested that there are two pools of S1P in platelets – agranular and granular.

Summary of the presented work

Contrary to the instant turnover of S1P by the action of sphingosine kinase on sphingosine seen in other cells, platelets store abundant amounts of S1P. This is possible due to the absence of S1P lyase, the enzyme that results in its degradation. Mass spectrometric detection of S1P secreted upon activation of platelets could only be detected in the presence of a carrier-molecule like BSA, perhaps serving as a sink for the bioactive lipid. Interestingly, with increasing BSA in the media, there was an increase in total levels of S1P, in both resting and stimulated platelets. Synthesis of S1P from sphingosine in platelets has been shown to be almost instantaneous due to the activity of sphingosine kinase. The increased S1P in the presence of BSA might be consistent with a mass-action effect in which BSA-extraction shifts the flux between S1P and precursor pools and thus drives the synthesis of more S1P. This observation implies that there is a readily-extractable pool of S1P in platelets that can partition into BSA's hydrophobic binding sites.

Release of S1P can also be measured in response to platelet activation. The stimulation and time-dependent release of S1P from platelets was inhibited by glibenclamide (ABC transporter inhibitor) as shown previously (*Kobayashi et al.*, 2006). However, glibenclamide also inhibited release of other platelet granule cargo suggesting a non-specific affect of the inhibitor. The involvement of ABC transporters in the release of S1P from platelets is therefore equivocal. Our studies are the first suggestion that SNARE machinery is involved in the release of S1P from platelets. S1P release from secretion-deficient mice, VAMP-8$^{-/-}$ and *Unc13d* ^{Jinx} mice was significantly affected. VAMP-8$^{-/-}$ mice are deficient in a primary v-SNARE important for platelet secretion. *Unc13d* ^{Jinx} mice are deficient in a regulatory molecule, Munc 13-4, important for platelet secretion. Also, stimulation-dependent release of newly synthesized S1P was observed

in platelets. The granular and agranular (BSA extractable) stores of S1P in platelets have been confirmed through fluorescence microscopy and sub-cellular fractionation. The importance of released platelet S1P in the maintenance of vascular permeability barrier has been tested through Evan's blue dye assay, with limited success as the data was not statistically significant. Leakage of the injected dye into lungs was taken as a measure of the strength of vascular permeability barrier. The contribution of platelet S1P in the maintenance of vascular permeability barrier under inflamed conditions is much more relevant. It can be tested in platelet secretion-deficient mouse model, *Unc13d* [Jinx], upon induction of inflammation by perhaps injecting an inflammatory agent like lipopolysaccharide (LPS). This might be of significance as platelet granular pool of S1P is more likely to play a physiological role upon vascular injury.

Mechanistic insights on the release of S1P from platelets

Subcellular localization of any bioactive sphingolipid is expected to affect the efficiency of its signaling function. Based on their ionic charge and the associated hydrophobicity, the bioactive lipid can/cannot voluntarily flip-flop across the membranes (*Hannun and Obeid*, 2008). On the other hand, bioactive lipids like S1P, LPA, *etc.* due to their amphipathic nature can move between the membranes. Restriction of distribution of these bioactive lipids can limit their functionality (*Pomorski et al.*, 2004).

The existence of agranular and granular pools of S1P in platelets has been implied by the present study. The plasma membrane associated pools constitute agranular pools of S1P while the granular membrane associated and the granular cytosol distributed S1P constitute granular S1P pools in the platelets. The membrane localization (whether granular membrane or plasma membrane) of S1P is understandable due to the amphipathic nature of S1P. S1P in plasma is always seen associated with HDL or albumin, and therefore its independent existence is unlikely. Either S1P has to be associated with unknown carrier protein or should exist in an insoluble form in association with other phosphate salts. The granular pool of S1P in platelets has been exposed utilizing the platelet secretion-deficient mouse strains. As S1P secretion deficiency was more evident

in *Unc13d* ^{*Jinx*} mice which have an absolute dense granule secretion deficiency, S1P is thought to be stored in dense granules of platelets. If true, the defective release of S1P might also be seen in patients with dense granule SPD (HPS). Some HPS mice have no dense granules at all while some have membrane ghosts that actually could serve as reservoirs for S1P if it was pumped into the granule.

Biological insights on the release of S1P from platelets

The activity of sphingosine kinase as well as S1P lyase/phosphatase and its distribution has a significant impact on metabolic status of the cell as they control the levels of S1P. S1P is known to be important for the maintenance of calcium homeostasis (*Ghosh et al.*, 1990; *Ghosh et al.*, 1994). S1P by itself, independent of phospho lipase-C can mobilize calcium stores (*Mattie et al.*, 1994). It is known that calcium is sufficient for activating platelets and allowing the SNAREs to mediate membrane fusion. S1P is stored abundantly in platelets due to the absence of enzymes degrading it. The intracellular calcium pools are encapsulated in dense tubular system in platelets and in the mitochondria. To maintain the resting status of platelets, availability of S1P has to be restricted. Hence it is essential to limit the movement of S1P in a resting platelet. The idea of it being restricted to granules or associated with some unknown entity is therefore viable.

S1P has been implicated in the regulation of cell migration essential for embryonic development, organogenesis, wound healing and the immune response (*Spiegel and Milstien*, 2003). S1P also plays an important role in angiogenesis(*Lee et al.*, 1999), vasculature formation, vascular permeability (*Garcia et al.*, 2001) and vascular maturation (*Liu et al.*, 2000). These are possible through binding of S1P to S1P receptors (S1P$_{1-5}$) in various cell types. Spatial and temporal regulation of S1P therefore becomes important. The ability of S1P in the maintenance of the microenvironment might correspond to the diminishing concentration gradient of S1P from its central site of production. The intracellular concentration of S1P is transiently high, unlike plasma, erythrocytes and platelets that maintain huge levels of S1P. Out of all the abundant

sources of S1P, plasma maintains the highest S1P levels. As already mentioned, S1P in plasma exists bound to either HDL or albumin. Several sources of plasma S1P have been reported which include, endothelial cells (*Venkataraman et al.*, 2008), erythrocytes (*Hänel et al.*, 2007) and platelets (*Yang et al.*, 1999a). Although different sources of plasma S1P have their own significance, erythrocytes (*Hänel et al.*, 2007) have been found sufficient to maintain plasma S1P levels.

The data described here suggests two pools of S1P in platelets – agranular and granular. If the release of S1P from any cell type is dependent on law of mass action, the sink will be plasma due to the availability of ready carrier-proteins like HDL/albumin. Erythrocytes are the circulatory reservoirs that release S1P into plasma constitutively while platelets are known to release S1P only upon stimulation. Moreover no cell type has been shown to be the sole supplier of S1P to plasma. This indicates that the S1P stored in platelets is not to maintain plasma S1P levels. S1P stored in platelets might become important at the site of injury. Platelets are activated naturally at the site of injury and thus release S1P, whether granular or agranular. The released S1P from platelets is susceptible to influence the micro-environment at the site of injury. The therapeutic strategies aimed to diminish, but not completely abrogate platelet secretion also would limit the availability of S1P at pathological damage site (*e.g.* plaque rupture). This would in turn decrease the deployment of other immune cells and thus diminish inflammation. Platelet S1P having any role in the maintenance of vascular permeability is still questionable.

The conduit for the release of platelet S1P is still a gray area. The ABC inhibitors used in the literature appear to be non-specific in platelets, and do not support ABC transporters as candidates for releasing platelet S1P. SPNS2 has recently been found not to be the S1P transporter on platelets but is for endothelial cells (*Hisano et al.*, 2012). The identification of S1P transporter on platelets is still unknown. The data presented here suggests an increase in the availability of transporters required for S1P export on platelet surface upon exocytosis. Platelets cannot synthesize S1P *de novo*. Sphingosine is

thought to form through sphingomyelin degradation, and by the action of sphingosine kinase on sphingosine, S1P is formed in platelets (*Tani et al.*, 2005). With abundant sphingomyelin present in the membranes, there appears to be no need for platelets to have an external source of sphingosine or S1P. This might be one of the possibilities for a continuous supply of S1P at the site of platelet activation, long after the exocytosis event.

The work described here implies that there are two pools of S1P in platelets. One that is BSA extractable in resting platelets, and one that requires the SNARE machinery to get released upon activation (granular). The granular pool might be used to give a bolus of S1P at the site of vascular damage so as to improve vascular integrity at the site. Though plasma levels of S1P are high, the granular pool of S1P provides a localized effect at the site of vascular injury. The S1P released from platelets is trapped in the growing thrombus, and because it is not under the influence of shear flow, it is retained at the site of release and is thus available to mediate localized effects.
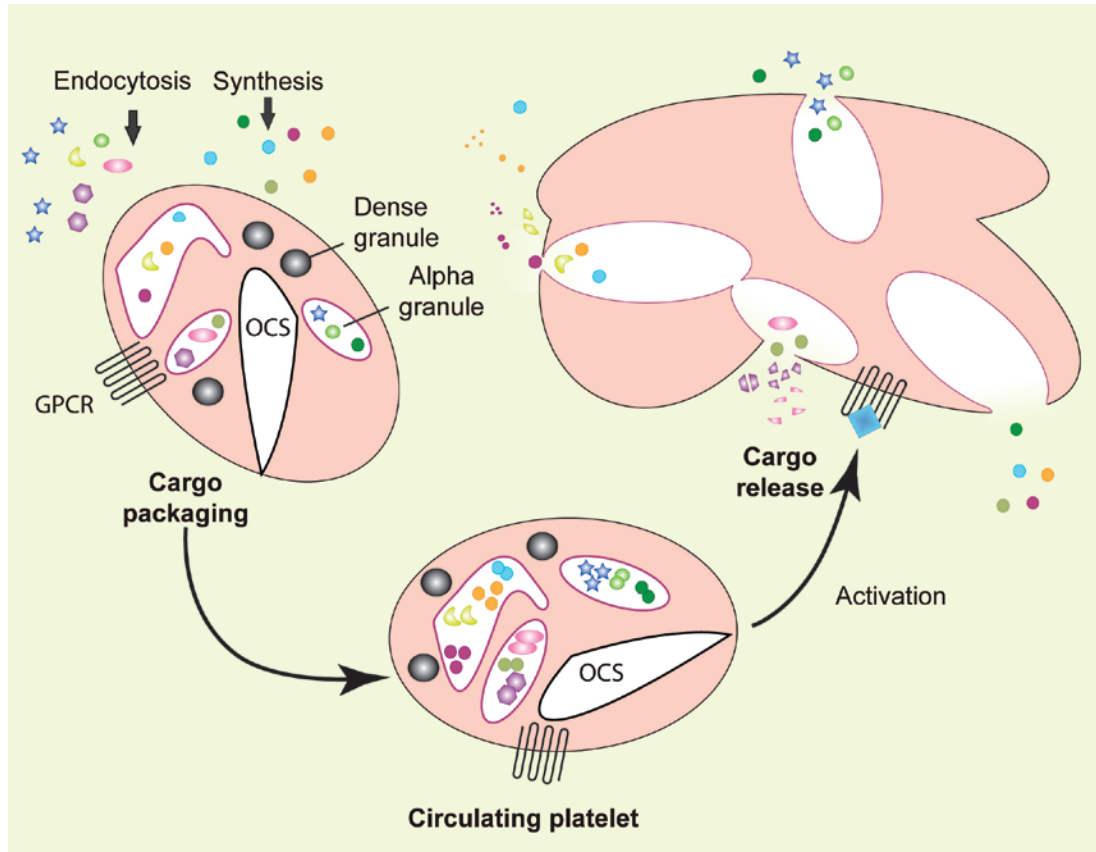
Figure 6.1. Schematic of release of contents from platelet

Endocytosed and megakaryocyte originated cargo are represented as multi-shaped and circular structures respectively and are ultimately stored in α-granule. GPCR (G-protein coupled receptor) represents one of the ways platelets are activated upon binding to an agonist. Upon activation the inter-granule fusion and fusion of the granule with plasma membrane leading to the release of contents is depicted as a sequential release dictated by the granule fusion site and the granule geometry.

Granule Cargo Packaging

a   b

c   d

Granule Geometry

e   f

Granule Location

g   h
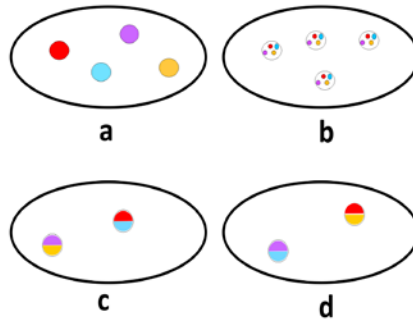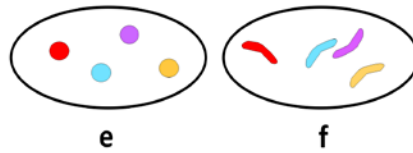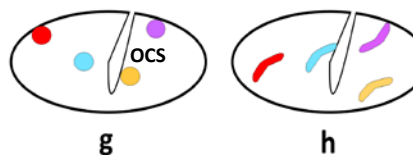
Figure 6.2. Design of platelet granule determining the fusion rate

The cargo molecules can be packaged homogeneously as represented by multicolored spherical granules (**a**) or each granule can be packed heterogeneously with similar contents in multiple granules (**b**). This packaging can be in accordance with cargo molecules of like functions (**c**) or with opposing functions (**d**). The granules can be spherical (**e**) or tubular (**f**). Spherical (**g**) or tubular (**h**) vesicles can differ in vicinity to the fusion site (OCS/plasma membrane).
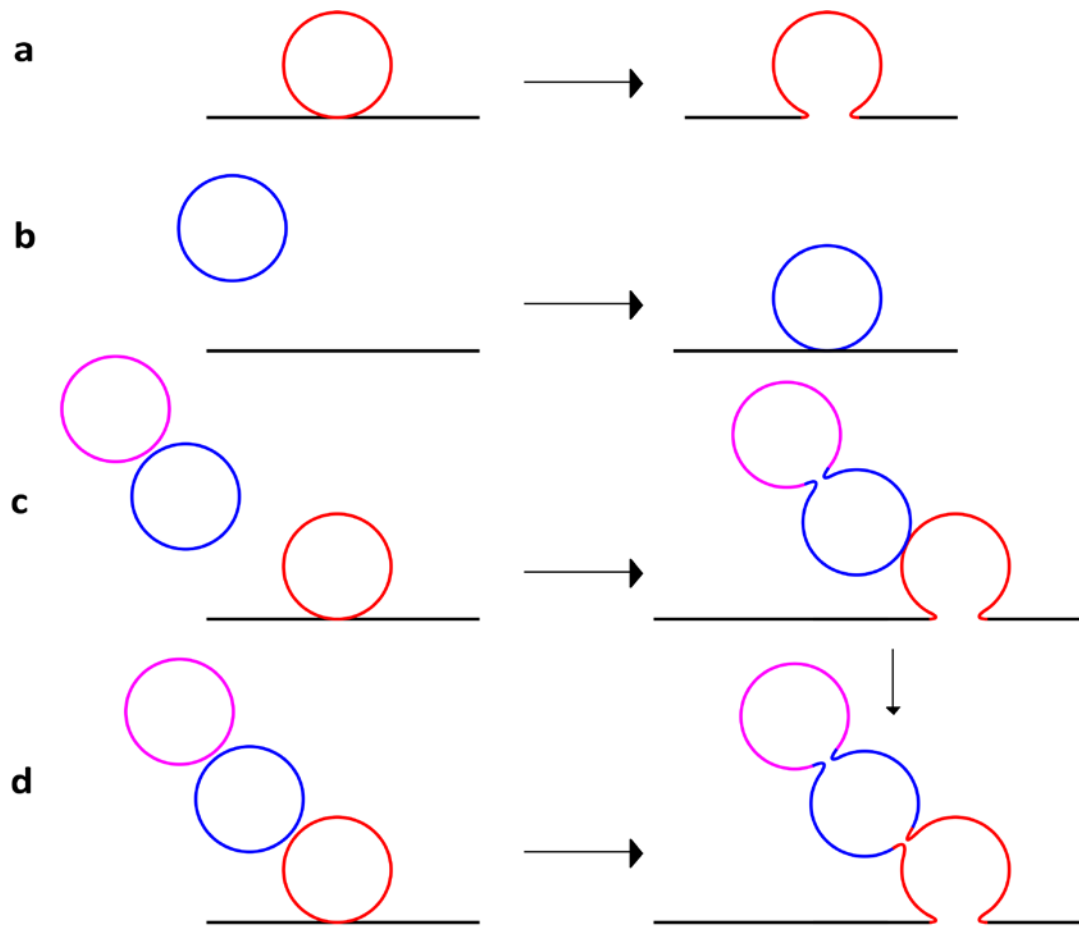
Figure 6.3. Different modes of granule fusion

The schematic presents the different modes of fusion. The arrows are directed towards the post-stimulus stage. A pre-docked granule can result in simple expedited fusion (**a**). A granule located in cytosol has to travel to site of fusion, post-stimulation (**b**). There might be inter-granule fusion followed by fusion with already docked vesicle (**c**). Sequential granule fusion (**d**) can result in release of cargo molecules from all the granules involved in the fusion process with the fusion pore being maintained by the initial vesicle.
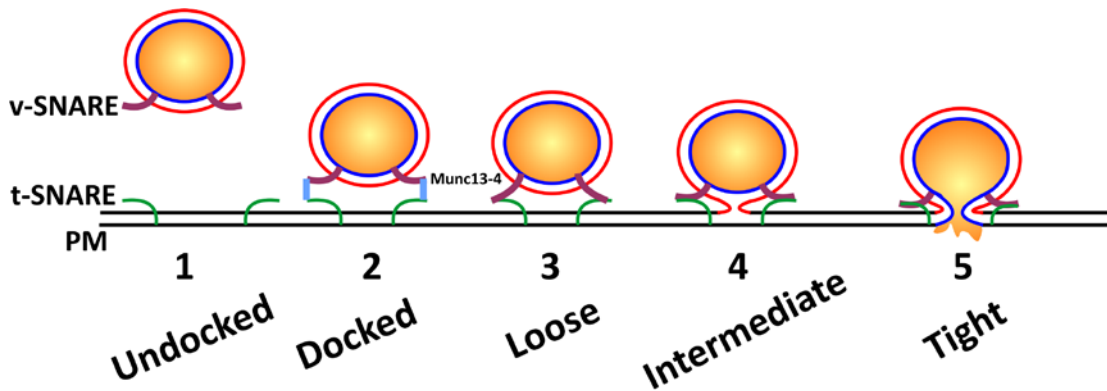
Figure 6.4. Influence of secretion machinery on granule fusion

Cognate v- and t-SNARE recognition ultimately leads to granule fusion upon platelet activation whether undocked (**1**) or docked (**2**). Munc 13-4 has been observed to be a regulatory molecule serving as an anchor to the docked vesicle for the fusion to reach completion. The concept of the extent of v- and t-SNARE interaction ultimately leading to the release of granule contents is depicted in **3**, **4** and **5** described as loose, intermediate and tight stages respectively. These stages represent the progression of granule fusion upon platelet activation.
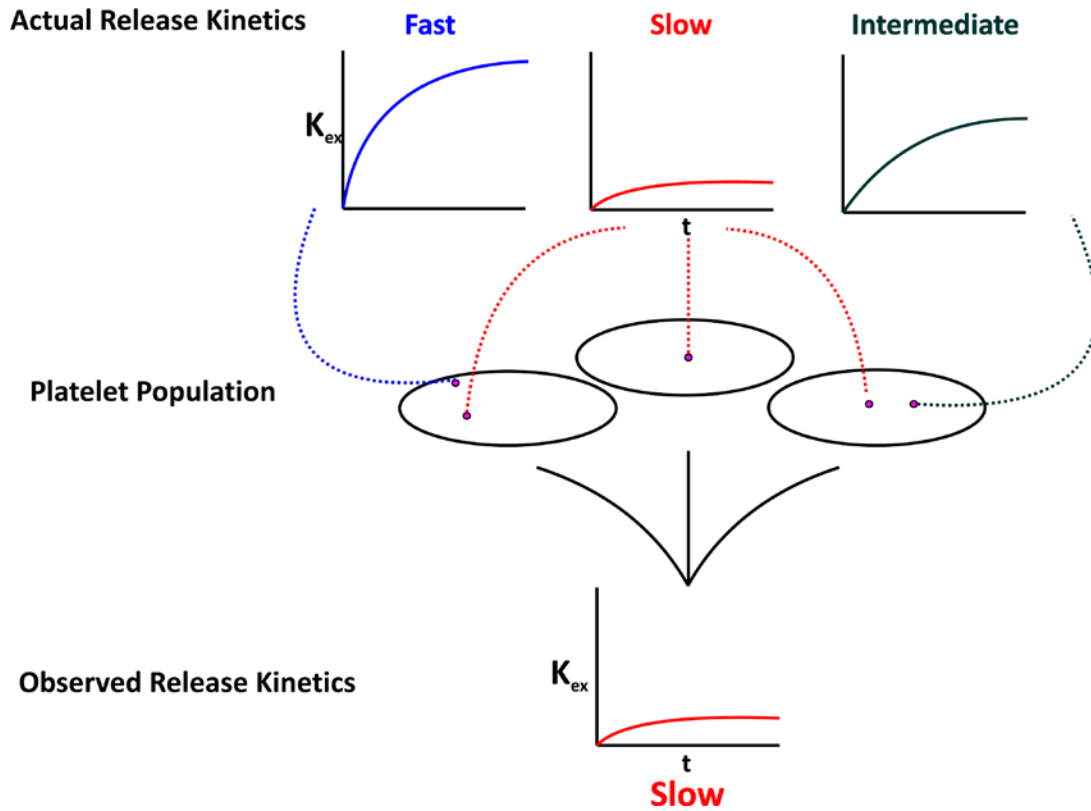
Figure 6.5. Explanation of the caveat of the study

Only three platelets with limited granules are depicted to maintain simplicity. Each platelet with a similar granule, differing in *locales,* can result in differential kinetics to varying degrees when studied individually. With the strategy employed in the present study, averages of multiple kinetic patterns is perceived as a final signal.
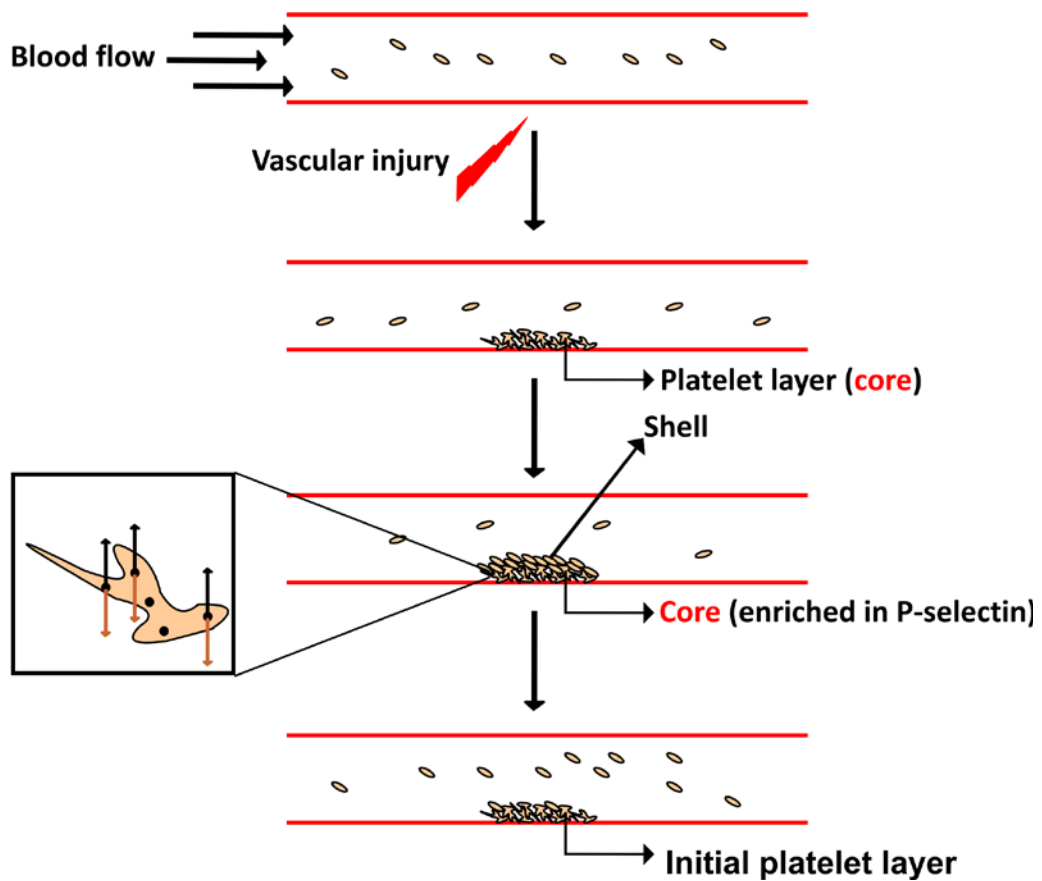
Figure 6.6. Hierarchical organization of the growing thrombus

Under shear flow of blood, platelets in circulation start to adhere to the injury site, undergo activation and release their contents. This forms the initial layer of platelets (core) which further recruits more platelets to form the shell. The platelets constituting shell are only tethered to the platelets in the 'core' and are hence, capable of returning to the circulation. The secondary agonists from the 'core' might contribute to the activation of platelets in the 'shell'. The inset shows a zoomed picture of an activated platelet depicting the granules as black dots. The black and the brown arrows represent the release of the cargo stored in these granules away or towards a lesion site upon fusion respectively.
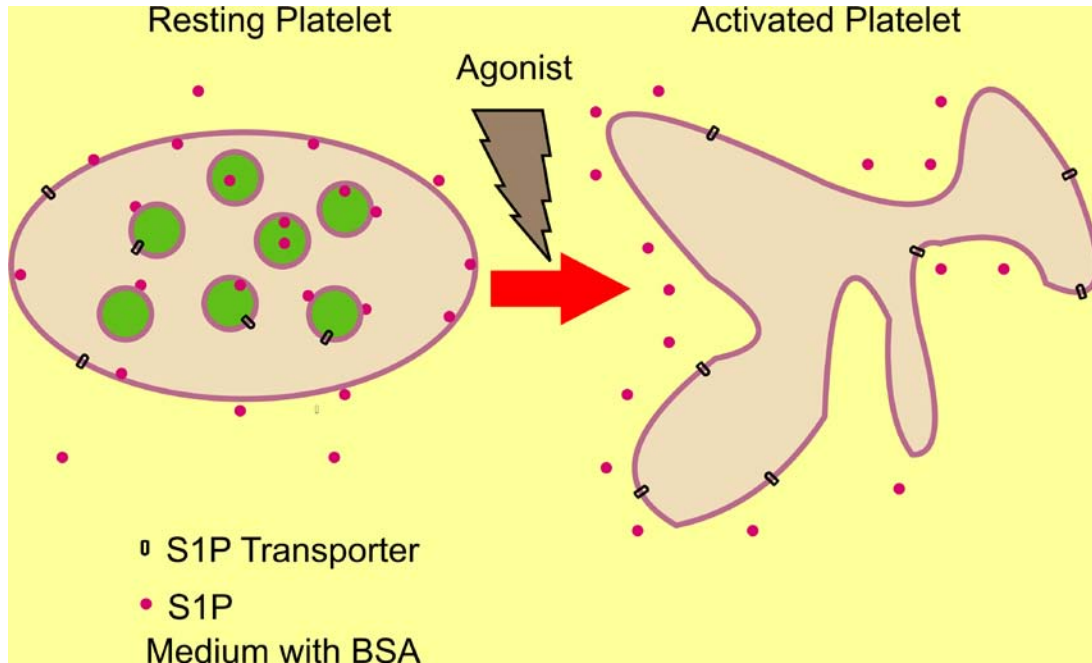
Figure 6.7. S1P in platelets

S1P exists in a granular pool and in an agranular pool. The agranular pool is extractable by BSA alone. The granular pool requires the granules to fuse to the plasma membrane. This might facilitate the exposure of S1P transporters present on granule membrane, thus allowing further release of S1P.

Abbreviations

$(Ca^{2+})_i$	Intracellular Calcium
ABC	ATP Binding Casette
ARC	Arthrogryposis, Renal Dysfunction, and Cholestasis
BEACH	Beige-Chediak/Higashi
BSS	Bernard Soulier Syndrome
C1P	Ceramide-1-Phosphate
cAMP	Cyclic Adenosine Mono Phosphate
cGMP	Cyclic Guanosine Mono Phosphate
CHS	Chediak Higashi Syndrome
CTAP	Connective Tissue Activation Peptide
CTL	Cytotoxic T Lymphocyte
DAG	Di Acyl Glycerol
DNA	Deoxy Ribonucleic Acid
DTS	Dense Tubular System
EDG	Endothelial Differentiation Gene
EGF	Epidermal Growth Factor
FGF	Fibroblast Growth Factor
FHL	Familial Hemophagocytic Lymphohistiocytosis
GP	Glycoprotein
GPCR	G-Protein Coupled Receptor
GPS	Gray Platelet Syndrome
GRO	Growth Releated Oncogene
HDL	High Density Lipoprotein
HGF	Hepatocyte Growth Factor
HPS	Hermansky Pudlak Syndrome
Hzf	Human Zinc Finger
IGF	Insulin like Growth Factor
IL	Interleukin
IP3	Inositol 1,4,5 tris phosphate
LAMP2	Lysosome Associated Membrane Protein
LDL	Low Density Lipoprotein
LPA	Lyso-Phosphatidic Acid
MIP	Macrophage Inhibitory Protein
MK	Megakaryocyte
MMP	Matrix Metallo Proteinase
Munc	Mouse Uncoordinated Mutants
MVB	Multi Vesicular Body
MYH	Myosin Heavy Chain
NBEAL	Neurobeachin-like 2
NO	Nitric Oxide
OCS	Open Canalicular System

PAR	Protease Activated Receptor
PDGF	Platelet Derived Growth Factor
PF4	Platelet Factor 4
PGI_2	Protaglandin I_2
PSGL	P-Selectin Glycoprotein Ligand
RANTES	Regulated and Normal T cell Expressed
RBC	Red Blood Cell
S1P	Sphingosine-1-Phosphate
$S1P_{1-5}$	S1P Receptors 1-5
SDF	Stromal Derived Growth Factor
Sec1	Secretion 1
SK	Sphingosine Kinase
SNAP	Synaptosomal Associated Protein
SNARE	Soluble N-ethyl maleimide Associated Protein Receptor
SPD	Storage Pool Disorder
TIMP	Tissue Inhibitor of MetalloProteinase
TNF	Tumor Necrosis Factor
TP	Thrombopoeitin
TSP	Thrombospondin
TxA_2	Thromboxane A_2
Unc	Uncoordinated Mutants
VAMP	Vesicle Associated Membrane Protein
VEGF	Vascular Endothelial Growth Factor
VPS33B	Vacuolar Protein Sorting 33B
vWF	von Willebrand Factor
α-Granule	Alpha Granule
β-TG	Beta-Thromboglobulin
δ-Granule	Delta-Granule

References

Al Hawas, R., Ren, Q., Ye, S., Karim, Z. A., Filipovich, A. H., and Whiteheart, S. W. (2012). Munc18b/STXBP2 is required for platelet secretion. *Blood 120*, 2493-2500.

Albrecht, C., and Viturro, E. (2007). The ABCA subfamily—gene and protein structures, functions and associated hereditary diseases. *Pflügers Archiv - European Journal of Physiology 453*, 581-589.

Alexander, J. S., Patton, W. F., Christman, B. W., Cuiper, L. L., and Haselton, F. R. (1998). Platelet-derived lysophosphatidic acid decreases endothelial permeability in vitro. *American Journal of Physiology - Heart and Circulatory Physiology 274*, H115-H122.

Anada, Y., Igarashi, Y., and Kihara, A. (2007). The immunomodulator FTY720 is phosphorylated and released from platelets. *European Journal of Pharmacology 568*, 106-111.

Andrews, N. W. (2000). Regulated secretion of conventional lysosomes. *Trends in Cell Biology 10*, 316-321.

Anitua, E., Andí, I., Sanchez, M., Azofra, J., del Mar Zalduendo, M., de la Fuente, M., Nurden, P., and Nurden, A. T. (2005). Autologous preparations rich in growth factors promote proliferation and induce VEGF and HGF production by human tendon cells in culture. *Journal of Orthopaedic Research 23*, 281-286.

Aoki, S., Yatomi, Y., Ohta, M., Osada, M., Kazama, F., Satoh, K., Nakahara, K., and Ozaki, Y. (2005). Sphingosine 1-Phosphate–Related Metabolism in the Blood Vessel. *Journal of Biochemistry 138*, 47-55.

Argraves, K. M., and Argraves, W. S. (2007). HDL serves as a S1P signaling platform mediating a multitude of cardiovascular effects. *Journal of Lipid Research 48*, 2325-2333.

Arisato, T., Hashiguchi, T., Sarker, K. P., Arimura, K., Asano, M., Matsuo, K., Osame, M., and Maruyama, I. (2003). Highly accumulated platelet vascular endothelial growth factor in coagulant thrombotic region. *Journal of Thrombosis and Haemostasis 1*, 2589-2593.

Aursnes, I. (1974). Increased permeability of capillaries to protein during thrombocytopenia an experimental study in the rabbit. *Microvascular Research 7*, 283-295.

Babich, V., Meli, A., Knipe, L., Dempster, J. E., Skehel, P., Hannah, M. J., and Carter, T. (2008). Selective release of molecules from Weibel-Palade bodies during a lingering kiss. *Blood 111*, 5282-5290.

Balduini, C., Iolascon, A., and Savoia, A. (2002). Inherited thrombocytopenias: from genes to therapy. *Haematologica 87*, 860-880.

Bandhuvula, P., and Saba, J. D. (2007). Sphingosine-1-phosphate lyase in immunity and cancer: silencing the siren. *Trends in Molecular Medicine 13*, 210-217.

Bartke, N., and Hannun, Y. A. (2009). Bioactive sphingolipids: metabolism and function. *Journal of Lipid Research 50*, S91-S96.

Baskova, I. P., Cherkesova, D. U., and Mosolov, V. V. (1983). Hirudin from leech heads and whole leeches and "pseudo-hirudin" from leech bodies. *Thrombosis Research 30*, 459-467.

Berger, G., Masse, J., and Cramer, E. (1996). Alpha-granule membrane mirrors the platelet plasma membrane and contains the glycoproteins Ib, IX, and V. *Blood 87*, 1385-1395.

Bernstein, A. M., and Whiteheart, S. W. (1999). Identification of a Cellubrevin/Vesicle Associated Membrane Protein 3 Homologue in Human Platelets. *Blood 93*, 571-579.

Bik, T., Sarov, I., and Livne, A. (1982). Interaction between vaccinia virus and human blood platelets. *Blood 59*, 482-487.

Bikfalvi, A. (2004). Recent developments in the inhibition of angiogenesis: examples from studies on platelet factor-4 and the VEGF/VEGFR system. *Biochemical Pharmacology 68*, 1017-1021.

Blair, P., and Flaumenhaft, R. (2009). Platelet α-granules: Basic biology and clinical correlates. *Blood Reviews 23*, 177-189.

Bonifacino, J. S. (2004). Insights into the Biogenesis of Lysosome-Related Organelles from the Study of the Hermansky-Pudlak Syndrome. *Annals of the New York Academy of Sciences 1038*, 103-114.

Boujaoude, L. C., Bradshaw-Wilder, C., Mao, C., Cohn, J., Ogretmen, B., Hannun, Y. A., and Obeid, L. M. (2001). Cystic Fibrosis Transmembrane Regulator Regulates Uptake of Sphingoid Base Phosphates and Lysophosphatidic Acid: MODULATION OF CELLULAR ACTIVITY OF SPHINGOSINE 1-PHOSPHATE. *Journal of Biological Chemistry 276*, 35258-35264.

Brass, L. (2010). Understanding and Evaluating Platelet Function. *ASH Education Program Book* 2010, 387-396.

Brass, L. F. (2003). Thrombin and Platelet Activation*. *CHEST Journal* 124, 18S-25S.

Bretscher, M. S. (1973). Membrane structure: some general principles. *Science* 181, 622-629.

Brill, A., Elinav, H., and Varon, D. (2004). Differential role of platelet granular mediators in angiogenesis. *Cardiovascular Research* 63, 226-235.

Brinkmann, V. (2007). Sphingosine 1-phosphate receptors in health and disease: Mechanistic insights from gene deletion studies and reverse pharmacology. *Pharmacology & Therapeutics* 115, 84-105.

Broekman, M. J. (1992). Homogenization by nitrogen cavitation technique applied to platelet subcellular fraction. In Methods in Enzymology, J.H. Jacek, ed. (Academic Press), pp. 21-32.

Burger, P. C., and Wagner, D. D. (2003). Platelet P-selectin facilitates atherosclerotic lesion development. *Blood* 101, 2661-2666.

Burkhart, J. M., Vaudel, M., Gambaryan, S., Radau, S., Walter, U., Martens, L., Geiger, J., Sickmann, A., and Zahedi, R. P. (2012). The first comprehensive and quantitative analysis of human platelet protein composition allows the comparative analysis of structural and functional pathways. *Blood* 120, e73-e82.

Buton, X., Morrot, G., Fellmann, P., and Seigneuret, M. (1996). Ultrafast Glycerophospholipid-selective Transbilayer Motion Mediated by a Protein in the Endoplasmic Reticulum Membrane. *Journal of Biological Chemistry* 271, 6651-6657.

Camerer, E., Regard, J. B., Cornelissen, I., Srinivasan, Y., Duong, D. N., Palmer, D., Pham, T. H., Wong, J. S., Pappu, R., and Coughlin, S. R. (2009). Sphingosine-1-phosphate in the plasma compartment regulates basal and inflammation-induced vascular leak in mice. *The Journal of Clinical Investigation* 119, 1871-1879.

Carr, C. M., and Rizo, J. (2010). At the junction of SNARE and SM protein function. *Current Opinion in Cell Biology* 22, 488-495.

Carty, S. E., Johnson, R. G., and Scarpa, A. (1981). Serotonin transport in isolated platelet granules. Coupling to the electrochemical proton gradient. *Journal of Biological Chemistry* 256, 11244-11250.

Chalfant, C. E., and Spiegel, S. (2005). Sphingosine 1-phosphate and ceramide 1-phosphate: expanding roles in cell signaling. *Journal of Cell Science 118*, 4605-4612.

Chang, J.-Y. (1983). The functional domain of hirudin, a thrombin-specific inhibitor. *FEBS Letters 164*, 307-313.

Chatterjee, M., Huang, Z., Zhang, W., Jiang, L., Hultenby, K., Zhu, L., Hu, H., Nilsson, G. P., and Li, N. (2011). Distinct platelet packaging, release, and surface expression of proangiogenic and antiangiogenic factors on different platelet stimuli. *Blood 117*, 3907-3911.

Chen, D., Bernstein, A. M., Lemons, P. P., and Whiteheart, S. W. (2000a). Molecular mechanisms of platelet exocytosis: role of SNAP-23 and syntaxin 2 in dense core granule release. *Blood 95*, 921-929.

Chen, D., Lemons, P. P., Schraw, T., and Whiteheart, S. W. (2000b). Molecular mechanisms of platelet exocytosis: role of SNAP-23 and syntaxin 2 and 4 in lysosome release. *Blood 96*, 1782-1788.

Chen, D., Minger, S. L., Honer, W. G., and Whiteheart, S. W. (1999). Organization of the secretory machinery in the rodent brain: distribution of the t-SNAREs, SNAP-25 and SNAP-23. *Brain Research 831*, 11-24.

Chen, J., Ishii, M., Wang, L., Ishii, K., and Coughlin, S. R. (1994). Thrombin receptor activation. Confirmation of the intramolecular tethered liganding hypothesis and discovery of an alternative intermolecular liganding mode. *Journal of Biological Chemistry 269*, 16041-16045.

Christoffersen, C., Obinata, H., Kumaraswamy, S. B., Galvani, S., Ahnström, J., Sevvana, M., Egerer-Sieber, C., Muller, Y. A., Hla, T., Nielsen, L. B., and Dahlbäck, B. (2011). Endothelium-protective sphingosine-1-phosphate provided by HDL-associated apolipoprotein M. *Proceedings of the National Academy of Sciences 108*, 9613-9618.

Chun, J., Goetzl, E. J., Hla, T., Igarashi, Y., Lynch, K. R., Moolenaar, W., Pyne, S., and Tigyi, G. (2002). International Union of Pharmacology. XXXIV. Lysophospholipid Receptor Nomenclature. *Pharmacological Reviews 54*, 265-269.

Clawson CC, R. G., White JG. (1975). Platelet interaction with bacteria. IV. Stimulation of the release reaction. *Am J Pathol 81*, 411-420.

Cleator, J. H., Zhu, W. Q., Vaughan, D. E., and Hamm, H. E. (2006). Differential regulation of endothelial exocytosis of P-selectin and von Willebrand factor by protease-activated receptors and cAMP. *Blood* 107, 2736-2744.

Cole, A. M., Ganz, T., Liese, A. M., Burdick, M. D., Liu, L., and Strieter, R. M. (2001). Cutting Edge: IFN-Inducible ELR– CXC Chemokines Display Defensin -Like Antimicrobial Activity. *The Journal of Immunology* 167, 623-627.

Coller, B., Seligsohn, U., West, S., Scudder, L., and Norton, K. (1991). Platelet fibrinogen and vitronectin in Glanzmann thrombasthenia: evidence consistent with specific roles for glycoprotein IIb/IIIA and alpha v beta 3 integrins in platelet protein trafficking [see comments]. *Blood* 78, 2603-2610.

Collins, R. G., Velji, R., Guevara, N. V., Hicks, M. J., Chan, L., and Beaudet, A. L. (2000). P-Selectin or Intercellular Adhesion Molecule (Icam)-1 Deficiency Substantially Protects against Atherosclerosis in Apolipoprotein E–Deficient Mice. *The Journal of Experimental Medicine* 191, 189-194.

Coppinger, J. A., Cagney, G., Toomey, S., Kislinger, T., Belton, O., McRedmond, J. P., Cahill, D. J., Emili, A., Fitzgerald, D. J., and Maguire, P. B. (2004). Characterization of the proteins released from activated platelets leads to localization of novel platelet proteins in human atherosclerotic lesions. *Blood* 103, 2096-2104.

Coughlin, S. R., Scarborough, R. M., Vu, T.-K. H., and Hung, D. T. (1992). Thrombin Receptor Structure and Function. *Cold Spring Harbor Symposia on Quantitative Biology* 57, 149-154.

Covic, L., Gresser, A. L., and Kuliopulos, A. (2000). Biphasic Kinetics of Activation and Signaling for PAR1 and PAR4 Thrombin Receptors in Platelets†. *Biochemistry* 39, 5458-5467.

Cramer, E., Vainchenker, W., Vinci, G., Guichard, J., and Breton-Gorius, J. (1985). Gray platelet syndrome: immunoelectron microscopic localization of fibrinogen and von Willebrand factor in platelets and megakaryocytes. *Blood* 66, 1309-1316.

Croce, K., and Libby, P. (2007). Intertwining of thrombosis and inflammation in atherosclerosis. *Current Opinion in Hematology* 14, 55-61.

Cuvillier, O. (2002). Sphingosine in apoptosis signaling. *Biochimica et Biophysica Acta (BBA) - Molecular and Cell Biology of Lipids* 1585, 153-162.

Danielli, J. F. (1940). Capillary permeability and oedema in the perfused frog. *The Journal of Physiology* *98*, 109-129.

De Clerck, F., Xhonneux, B., Leysen, J., and Janssen, P. A. J. (1984). Evidence for functional 5-HT2 receptor sites on human blood platelets. *Biochemical Pharmacology* *33*, 2807-2811.

Deeley, R. G., Westlake, C., and Cole, S. P. C. (2006). Transmembrane Transport of Endo- and Xenobiotics by Mammalian ATP-Binding Cassette Multidrug Resistance Proteins. *Physiological Reviews* *86*, 849-899.

Dekkers, D. W. C., Comfurius, P., Schroit, A. J., Bevers, E. M., and Zwaal, R. F. A. (1998). Transbilayer Movement of NBD-Labeled Phospholipids in Red Blood Cell Membranes: Outward-Directed Transport by the Multidrug Resistance Protein 1 (MRP1). *Biochemistry* *37*, 14833-14837.

Deutsch, V. R., and Tomer, A. (2006). Megakaryocyte development and platelet production. *British Journal of Haematology* *134*, 453-466.

Devi, S., Kuligowski, M. P., Kwan, R. Y. Q., Westein, E., Jackson, S. P., Kitching, A. R., and Hickey, M. J. (2010). Platelet Recruitment to the Inflamed Glomerulus Occurs via an αIIbβ3/GPVI-Dependent Pathway. *The American Journal of Pathology* *177*, 1131-1142.

Di Pietro, S. M., and Dell'Angelica, E. C. (2005). The Cell Biology of Hermansky–Pudlak Syndrome: Recent Advances. *Traffic* *6*, 525-533.

Dietrich, L. E. P., Boeddinghaus, C., LaGrassa, T. J., and Ungermann, C. (2003). Control of eukaryotic membrane fusion by N-terminal domains of SNARE proteins. *Biochimica et Biophysica Acta (BBA) - Molecular Cell Research* *1641*, 111-119.

Dong, Z. M., Brown, A. A., and Wagner, D. D. (2000). Prominent Role of P-Selectin in the Development of Advanced Atherosclerosis in ApoE-Deficient Mice. *Circulation* *101*, 2290-2295.

Eichholtz T, J. K., Fahrenfort I, Moolenaar WH. (1993). The bioactive phospholipid lysophosphatidic acid is released from activated platelets. *Biochem J* *291*, 677-680.

Escolar, G., Leistikow, E., and White, J. (1989). The fate of the open canalicular system in surface and suspension- activated platelets. *Blood* *74*, 1983-1988.

Fabbro, S., Kahr, W. H. A., Hinckley, J., Wang, K., Moseley, J., Ryu, G.-Y., Nixon, B., White, J. G., Bair, T., Schutte, B., and Di Paola, J. (2011). Homozygosity mapping with SNP arrays

confirms 3p21 as a recessive locus for gray platelet syndrome and narrows the interval significantly. *Blood 117*, 3430-3434.

Feng, D., Crane, K., Rozenvayn, N., Dvorak, A. M., and Flaumenhaft, R. (2002). Subcellular distribution of 3 functional platelet SNARE proteins: human cellubrevin, SNAP-23, and syntaxin 2. *Blood 99*, 4006-4014.

Flaumenhaft, R., Croce, K., Chen, E., Furie, B., and Furie, B. C. (1999). Proteins of the Exocytotic Core Complex Mediate Platelet α-Granule Secretion: ROLES OF VESICLE-ASSOCIATED MEMBRANE PROTEIN, SNAP-23, AND SYNTAXIN 4. *Journal of Biological Chemistry 274*, 2492-2501.

Folkman, J. (2007). Angiogenesis: an organizing principle for drug discovery? *Nat Rev Drug Discov 6*, 273-286.

Fosset, M., De Weille, J. R., Green, R. D., Schmid-Antomarchi, H., and Lazdunski, M. (1988). Antidiabetic sulfonylureas control action potential properties in heart cells via high affinity receptors that are linked to ATP-dependent K+ channels. *Journal of Biological Chemistry 263*, 7933-7936.

Foster, C. J., Prosser, D. M., Agans, J. M., Zhai, Y., Smith, M. D., Lachowicz, J. E., Zhang, F. L., Gustafson, E., Monsma, F. J., Wiekowski, M. T.*, et al.* (2001). Molecular identification and characterization of the platelet ADP receptor targeted by thienopyridine antithrombotic drugs. *The Journal of Clinical Investigation 107*, 1591-1598.

Franke, J. D., Dong, F., Rickoll, W. L., Kelley, M. J., and Kiehart, D. P. (2005). Rod mutations associated with MYH9-related disorders disrupt nonmuscle myosin-IIA assembly. *Blood 105*, 161-169.

Frenette, P. S., Johnson, R. C., Hynes, R. O., and Wagner, D. D. (1995). Platelets roll on stimulated endothelium in vivo: an interaction mediated by endothelial P-selectin. *Proceedings of the National Academy of Sciences 92*, 7450-7454.

Gahl, W. A., Brantly, M., Kaiser-Kupfer, M. I., Iwata, F., Hazelwood, S., Shotelersuk, V., Duffy, L. F., Kuehl, E. M., Troendle, J., and Bernardini, I. (1998). Genetic Defects and Clinical Characteristics of Patients with a Form of Oculocutaneous Albinism (Hermansky–Pudlak Syndrome). *New England Journal of Medicine 338*, 1258-1265.

Garcia, J. G. N., Liu, F., Verin, A. D., Birukova, A., Dechert, M. A., Gerthoffer, W. T., Bamberg, J. R., and English, D. (2001). Sphingosine 1-phosphate promotes endothelial cell barrier integrity by Edg-dependent cytoskeletal rearrangement. *The Journal of Clinical Investigation 108*, 689-701.

Gawaz, M., Langer, H., and May, A. E. (2005). Platelets in inflammation and atherogenesis. *The Journal of Clinical Investigation 115*, 3378-3384.

Ge, S., White, J. G., and Haynes, C. L. (2009). Quantal Release of Serotonin from Platelets. *Analytical Chemistry 81*, 2935-2943.

Gerrard, J. (1988). Platelet Aggregation: Cellular regulation and physiologic role. *Hospital Practice (Off Ed) 20*, 89-98.

Ghosh, T. K., Bian, J., and Gill, D. L. (1990). Intracellular Calcium Release Mediated by Sphingosine Derivatives Generated in Cells. *Science 248*, 1653-1656.

Ghosh, T. K., Bian, J., and Gill, D. L. (1994). Sphingosine 1-phosphate generated in the endoplasmic reticulum membrane activates release of stored calcium. *Journal of Biological Chemistry 269*, 22628-22635.

Gimbrone, M. A., Aster, R. H., Cotran, R. S., Corkery, J., Jandl, J. H., and Folkman, J. (1969). Preservation of Vascular Integrity in Organs perfused in vitro with a Platelet-rich Medium. *Nature 222*, 33-36.

Gissen, P., Johnson, C. A., Morgan, N. V., Stapelbroek, J. M., Forshew, T., Cooper, W. N., McKiernan, P. J., Klomp, L. W. J., Morris, A. A. M., Wraith, J. E*., et al.* (2004). Mutations in VPS33B, encoding a regulator of SNARE-dependent membrane fusion, cause arthrogryposis-renal dysfunction-cholestasis (ARC) syndrome. *Nat Genet 36*, 400-404.

Gleissner, C. A., von Hundelshausen, P., and Ley, K. (2008). Platelet Chemokines in Vascular Disease. *Arteriosclerosis, Thrombosis, and Vascular Biology 28*, 1920-1927.

Goerge, T., Ho-Tin-Noe, B., Carbo, C., Benarafa, C., Remold-O'Donnell, E., Zhao, B.-Q., Cifuni, S. M., and Wagner, D. D. (2008). Inflammation induces hemorrhage in thrombocytopenia. *Blood 111*, 4958-4964.

Golfier, S., Kondo, S., Schulze, T., Takeuchi, T., Vassileva, G., Achtman, A. H., Gräler, M. H., Abbondanzo, S. J., Wiekowski, M., Kremmer, E*., et al.* (2010). Shaping of terminal megakaryocyte differentiation and proplatelet development by sphingosine-1-phosphate receptor S1P4. *The FASEB Journal 24*, 4701-4710.

Graham, G. J., Ren, Q., Dilks, J. R., Blair, P., Whiteheart, S. W., and Flaumenhaft, R. (2009). Endobrevin/VAMP-8–dependent dense granule release mediates thrombus formation in vivo. *Blood 114*, 1083-1090.

Gunay-Aygun, M., Falik-Zaccai, T. C., Vilboux, T., Zivony-Elboum, Y., Gumruk, F., Cetin, M., Khayat, M., Boerkoel, C. F., Kfir, N., Huang, Y*., et al.* (2011). NBEAL2 is mutated in gray

platelet syndrome and is required for biogenesis of platelet [alpha]-granules. *Nat Genet 43*, 732-734.

Gunay-Aygun, M., Huizing, M., and Gahl, W. A. (2004). Molecular Defects that Affect Platelet Dense Granules. *Semin Thromb Hemost 30*, 537-547.

Gunay-Aygun, M., Zivony-Elboum, Y., Gumruk, F., Geiger, D., Cetin, M., Khayat, M., Kleta, R., Kfir, N., Anikster, Y., Chezar, J*., et al.* (2010). Gray platelet syndrome: natural history of a large patient cohort and locus assignment to chromosome 3p. *Blood 116*, 4990-5001.

Hait, N. C., Oskeritzian, C. A., Paugh, S. W., Milstien, S., and Spiegel, S. (2006). Sphingosine kinases, sphingosine 1-phosphate, apoptosis and diseases. *Biochimica et Biophysica Acta (BBA) - Biomembranes 1758*, 2016-2026.

Hamberg, M., Svensson, J., and Samuelsson, B. (1974). Prostaglandin Endoperoxides. A New Concept concerning the Mode of Action and Release of Prostaglandins. *Proceedings of the National Academy of Sciences of the United States of America 71*, 3824-3828.

Hamilton, J. A. (2003). Fast flip-flop of cholesterol and fatty acids in membranes: implications for membrane transport proteins. *Current Opinion in Lipidology 14*, 263-271.

Hamon, Y., Luciani, M.-F., Becq, F., Verrier, B., Rubartelli, A., and Chimini, G. (1997). Interleukin-1β Secretion Is Impaired by Inhibitors of the Atp Binding Cassette Transporter, ABC1. *Blood 90*, 2911-2915.

Hanada, K., Kumagai, K., Yasuda, S., Miura, Y., Kawano, M., Fukasawa, M., and Nishijima, M. (2003). Molecular machinery for non-vesicular trafficking of ceramide. *Nature 426*, 803-809.

Hänel, P., Andréani, P., and Gräler, M. H. (2007). Erythrocytes store and release sphingosine 1-phosphate in blood. *The FASEB Journal 21*, 1202-1209.

Hannun, Y. A., and Bell, R. M. (1989). Functions of Sphingolipids and Sphingolipid Breakdown Products in Cellular Regulation. *Science 243*, 500-507.

Hannun, Y. A., and Obeid, L. M. (2008). Principles of bioactive lipid signalling: lessons from sphingolipids. *Nat Rev Mol Cell Biol 9*, 139-150.

Harrison, P., Wilbourn, B., Debili, N., Vainchenker, W., Breton-Gorius, J., Lawrie, A. S., Masse, J. M., Savidge, G. F., and Cramer, E. M. (1989). Uptake of plasma fibrinogen into

the alpha granules of human megakaryocytes and platelets. *The Journal of Clinical Investigation 84*, 1320-1324.

Haskó, G., Deitch, E. A., Németh, Z. H., Kuhel, D. G., and Szabó, C. (2002). Inhibitors of ATP-Binding Cassette Transporters Suppress Interleukin-12 p40 Production and Major Histocompatibility Complex II Up-Regulation in Macrophages. *Journal of Pharmacology and Experimental Therapeutics 301*, 103-110.

Hayward, C. P. M., Furmaniak-Kazmierczak, E., Cieutat, A.-M., Moore, J. C., Bainton, D. F., Nesheim, M. E., Kelton, J. G., and Côté, G. (1995). Factor V Is Complexed with Multimerin in Resting Platelet Lysates and Colocalizes with Multimerin in Platelet -Granules. *Journal of Biological Chemistry 270*, 19217-19224.

Heijnen, H. F. G., Debili, N., Vainchencker, W., Breton-Gorius, J., Geuze, H. J., and Sixma, J. J. (1998). Multivesicular Bodies Are an Intermediate Stage in the Formation of Platelet α-Granules. *Blood 91*, 2313-2325.

Hermansky, F., and PUDLAK, P. (1959). Albinism Associated with Hemorrhagic Diathesis and Unusual Pigmented Reticular Cells in the Bone Marrow: Report of Two Cases with Histochemical Studies. *Blood 14*, 162-169.

Higashi, O. (1954). Congenital Gigantism of Peroxidase Granules

The First Case ever Reported of Qualitative Abnormity of Peroxidase. *The Tohoku Journal of Experimental Medicine 59*, 315-332.

Hisano, Y., Kobayashi, N., Kawahara, A., Yamaguchi, A., and Nishi, T. (2011). The Sphingosine 1-Phosphate Transporter, SPNS2, Functions as a Transporter of the Phosphorylated Form of the Immunomodulating Agent FTY720. *Journal of Biological Chemistry 286*, 1758-1766.

Hisano, Y., Kobayashi, N., Yamaguchi, A., and Nishi, T. (2012). Mouse SPNS2 Functions as a Sphingosine-1-Phosphate Transporter in Vascular Endothelial Cells. *PLoS ONE 7*, e38941.

Hla, T. (2004). Physiological and pathological actions of sphingosine 1-phosphate. *Seminars in Cell & Developmental Biology 15*, 513-520.

Hla, T., Venkataraman, K., and Michaud, J. (2008). The vascular S1P gradient—Cellular sources and biological significance. *Biochimica et Biophysica Acta (BBA) - Molecular and Cell Biology of Lipids 1781*, 477-482.

Ho-Tin-Noé, B., Demers, M., and Wagner, D. D. (2011). How platelets safeguard vascular integrity. *Journal of thrombosis and haemostasis : JTH 9 Suppl 1*, 56-65.

Hollopeter, G., Jantzen, H.-M., Vincent, D., Li, G., England, L., Ramakrishnan, V., Yang, R.-B., Nurden, P., Nurden, A., Julius, D., and Conley, P. B. (2001). Identification of the platelet ADP receptor targeted by antithrombotic drugs. *Nature 409*, 202-207.

Holmsen, H., and Weiss, H. J. (1979). SECRETABLE STORAGE POOLS IN PLATELETS. *Annual Review of Medicine 30*, 119-134.

Hu, C.-j., Baglia, F. A., Mills, D. C. B., Konkle, B. A., and Walsh, P. N. (1998). Tissue-Specific Expression of Functional Platelet Factor XI Is Independent of Plasma Factor XI Expression. *Blood 91*, 3800-3807.

Huang, R.-H., Wang, Y., Roth, R., Yu, X., Purvis, A. R., Heuser, J. E., Egelman, E. H., and Sadler, J. E. (2008). Assembly of Weibel–Palade body-like tubules from N-terminal domains of von Willebrand factor. *Proceedings of the National Academy of Sciences 105*, 482-487.

Iannacone, M., Sitia, G., Isogawa, M., Whitmire, J. K., Marchese, P., Chisari, F. V., Ruggeri, Z. M., and Guidotti, L. G. (2008). Platelets prevent IFN-α/β-induced lethal hemorrhage promoting CTL-dependent clearance of lymphocytic choriomeningitis virus. *Proceedings of the National Academy of Sciences 105*, 629-634.

Ichikawa, S., and Hirabayashi, Y. (1998). Glucosylceramide synthase and glycosphingolipid synthesis. *Trends in Cell Biology 8*, 198-202.

Israels, S., Gerrard, J., Jacques, Y., McNicol, A., Cham, B., Nishibori, M., and Bainton, D. (1992). Platelet dense granule membranes contain both granulophysin and P- selectin (GMP-140). *Blood 80*, 143-152.

Israels, S., mMcNicol, A., Robertson, C., and Gerrard, J. (1990). Platelet storage pool deficiency: Diagnosis in patients with prolonged bleeding times and normal platelet aggregation. *British Journal of Haematology 75*, 118-121.

Italiano, J. E., Lecine, P., Shivdasani, R. A., and Hartwig, J. H. (1999). Blood Platelets Are Assembled Principally at the Ends of Proplatelet Processes Produced by Differentiated Megakaryocytes. *The Journal of Cell Biology 147*, 1299-1312.

Italiano, J. E., Richardson, J. L., Patel-Hett, S., Battinelli, E., Zaslavsky, A., Short, S., Ryeom, S., Folkman, J., and Klement, G. L. (2008). Angiogenesis is regulated by a novel

mechanism: pro- and antiangiogenic proteins are organized into separate platelet α granules and differentially released. *Blood 111*, 1227-1233.

Italiano, J. E., and Shivdasani, R. A. (2003). Megakaryocytes and beyond: the birth of platelets. *Journal of Thrombosis and Haemostasis 1*, 1174-1182.

Jahn, R., and Südhof, T. C. (1999). MEMBRANE FUSION AND EXOCYTOSIS. *Annual Review of Biochemistry 68*, 863-911.

Jantzen, H.-M., Milstone, D. S., Gousset, L., Conley, P. B., and Mortensen, R. M. (2001). Impaired activation of murine platelets lacking Gαi2. *The Journal of Clinical Investigation 108*, 477-483.

Jedlitschky, G., Tirschmann, K., Lubenow, L. E., Nieuwenhuis, H. K., Akkerman, J. W. N., Greinacher, A., and Kroemer, H. K. (2004). The nucleotide transporter MRP4 (ABCC4) is highly expressed in human platelets and present in dense granules, indicating a role in mediator storage. *Blood 104*, 3603-3610.

Jimenez, B., Volpert, O. V., Crawford, S. E., Febbraio, M., Silverstein, R. L., and Bouck, N. (2000). Signals leading to apoptosis-dependent inhibition of neovascularization by thrombospondin-1. *Nat Med 6*, 41-48.

Johnson, K. R., Johnson, K. Y., Becker, K. P., Bielawski, J., Mao, C., and Obeid, L. M. (2003). Role of Human Sphingosine-1-phosphate Phosphatase 1 in the Regulation of Intra- and Extracellular Sphingosine-1-phosphate Levels and Cell Viability. *Journal of Biological Chemistry 278*, 34541-34547.

Jones, O. P. (1960). Origin of megakaryocyte granules from Golgi vesicles. *The Anatomical Record 138*, 105-113.

Kahn, M. L., Nakanishi-Matsui, M., Shapiro, M. J., Ishihara, H., and Coughlin, S. R. (1999). Protease-activated receptors 1 and 4 mediate activation of human platelets by thrombin. *The Journal of Clinical Investigation 103*, 879-887.

Kahr, W. H. A., Hinckley, J., Li, L., Schwertz, H., Christensen, H., Rowley, J. W., Pluthero, F. G., Urban, D., Fabbro, S., Nixon, B.*, et al.* (2011). Mutations in NBEAL2, encoding a BEACH protein, cause gray platelet syndrome. *Nat Genet 43*, 738-740.

Kamykowski, J., Carlton, P., Sehgal, S., and Storrie, B. (2011). Quantitative immunofluorescence mapping reveals little functional coclustering of proteins within platelet α-granules. *Blood 118*, 1370-1373.

Kark, L. R., Karp, J. M., and Davies, J. E. (2006). Platelet releasate increases the proliferation and migration of bone marrow-derived cells cultured under osteogenic conditions. *Clinical Oral Implants Research 17*, 321-327.

Kasai, H., Takahashi, N., and Tokumaru, H. (2012). Distinct Initial SNARE Configurations Underlying the Diversity of Exocytosis. *Physiological Reviews 92*, 1915-1964.

Kasper, B., Brandt, E., Brandau, S., and Petersen, F. (2007). Platelet Factor 4 (CXC Chemokine Ligand 4) Differentially Regulates Respiratory Burst, Survival, and Cytokine Expression of Human Monocytes by Using Distinct Signaling Pathways. *The Journal of Immunology 179*, 2584-2591.

Kasper, B., Brandt, E., Bulfone-Paus, S., and Petersen, F. (2004). Platelet factor 4 (PF-4)–induced neutrophil adhesion is controlled by src-kinases, whereas PF-4–mediated exocytosis requires the additional activation of p38 MAP kinase and phosphatidylinositol 3-kinase. *Blood 103*, 1602-1610.

Kawahara, A., Nishi, T., Hisano, Y., Fukui, H., Yamaguchi, A., and Mochizuki, N. (2009). The Sphingolipid Transporter Spns2 Functions in Migration of Zebrafish Myocardial Precursors. *Science 323*, 524-527.

Kiesselbach, T. H., and Wagner, R. H. (1972). DEMONSTRATION OF FACTOR XIII IN HUMAN MEGAKARYOCYTES BY A FLUORESCENT ANTIBODY TECHNIQUE*. *Annals of the New York Academy of Sciences 202*, 318-328.

Kihara, A., Mitsutake, S., Mizutani, Y., and Igarashi, Y. (2007). Metabolism and biological functions of two phosphorylated sphingolipids, sphingosine 1-phosphate and ceramide 1-phosphate. *Progress in Lipid Research 46*, 126-144.

Kimura, Y., Hart, A., Hirashima, M., Wang, C., Holmyard, D., Pittman, J., Pang, X.-L., Jackson, C. W., and Bernstein, A. (2002). Zinc Finger Protein, Hzf, Is Required for Megakaryocyte Development and Hemostasis. *The Journal of Experimental Medicine 195*, 941-952.

King, M., and Diamond, S. (2012). Multiscale Systems Biology: A Special Issue Devoted to Understanding Biology and Medicine Across Multiple Scales. *Annals of Biomedical Engineering 40*, 2293-2294.

Kisucka, J., Butterfield, C. E., Duda, D. G., Eichenberger, S. C., Saffaripour, S., Ware, J., Ruggeri, Z. M., Jain, R. K., Folkman, J., and Wagner, D. D. (2006). Platelets and platelet adhesion support angiogenesis while preventing excessive hemorrhage. *Proceedings of the National Academy of Sciences of the United States of America 103*, 855-860.

Knighton, D. R., HUNT, T. K., THAKRAL, K. K., and GOODSON, W. I. (1982). Role of Platelets and Fibrin in the Healing Sequence: An In Vivo Study of Angiogenesis and Collagen Synthesis. *Annals of Surgery 196*, 379-388.

Kobayashi, N., Nishi, T., Hirata, T., Kihara, A., Sano, T., Igarashi, Y., and Yamaguchi, A. (2006). Sphingosine 1-phosphate is released from the cytosol of rat platelets in a carrier-mediated manner. *Journal of Lipid Research 47*, 614-621.

Kohama, T., Olivera, A., Edsall, L., Nagiec, M. M., Dickson, R., and Spiegel, S. (1998). Molecular Cloning and Functional Characterization of Murine Sphingosine Kinase. *Journal of Biological Chemistry 273*, 23722-23728.

Kuligowski, M. P., Kitching, A. R., and Hickey, M. J. (2006). Leukocyte Recruitment to the Inflamed Glomerulus: A Critical Role for Platelet-Derived P-Selectin in the Absence of Rolling. *The Journal of Immunology 176*, 6991-6999.

Larsen, E., Celi, A., Gilbert, G. E., Furie, B. C., Erban, J. K., Bonfanti, R., Wagner, D. D., and Furie, B. (1989). PADGEM protein: A receptor that mediates the interaction of activated platelets with neutrophils and monocytes. *Cell 59*, 305-312.

Leclercq, T. M., and Pitson, S. M. (2006). Cellular signalling by sphingosine kinase and sphingosine 1-phosphate. *IUBMB Life 58*, 467-472.

Lee, M.-J., Thangada, S., Claffey, K. P., Ancellin, N., Liu, C. H., Kluk, M., Volpi, M., Sha'afi, R. I., and Hla, T. (1999). Vascular Endothelial Cell Adherens Junction Assembly and Morphogenesis Induced by Sphingosine-1-Phosphate. *Cell 99*, 301-312.

Lee, Y.-M., Venkataraman, K., Hwang, S.-I., Han, D. K., and Hla, T. (2007). A novel method to quantify sphingosine 1-phosphate by immobilized metal affinity chromatography (IMAC). *Prostaglandins & Other Lipid Mediators 84*, 154-162.

Leidl, K., Liebisch, G., Richter, D., and Schmitz, G. (2008). Mass spectrometric analysis of lipid species of human circulating blood cells. *Biochimica et Biophysica Acta (BBA) - Molecular and Cell Biology of Lipids 1781*, 655-664.

Lemons, P. P., Chen, D., Bernstein, A. M., Bennett, M. K., and Whiteheart, S. W. (1997). Regulated Secretion in Platelets: Identification of Elements of the Platelet Exocytosis Machinery. *Blood 90*, 1490-1500.

Lemons, P. P., Chen, D., and Whiteheart, S. W. (2000). Molecular Mechanisms of Platelet Exocytosis: Requirements for α-Granule Release. *Biochemical and Biophysical Research Communications 267*, 875-880.

Li, W., Rusiniak, M. E., Chintala, S., Gautam, R., Novak, E. K., and Swank, R. T. (2004). Murine Hermansky–Pudlak syndrome genes: regulators of lysosome-related organelles. *BioEssays 26*, 616-628.

Liu, Y., Wada, R., Yamashita, T., Mi, Y., Deng, C.-X., Hobson, J. P., Rosenfeldt, H. M., Nava, V. E., Chae, S.-S., Lee, M.-J*., et al.* (2000). Edg-1, the G protein–coupled receptor for sphingosine-1-phosphate, is essential for vascular maturation. *The Journal of Clinical Investigation 106*, 951-961.

Lo, B., Li, L., Gissen, P., Christensen, H., McKiernan, P. J., Ye, C., Abdelhaleem, M., Hayes, J. A., Williams, M. D., Chitayat, D., and Kahr, W. H. A. (2005). Requirement of VPS33B, a member of the Sec1/Munc18 protein family, in megakaryocyte and platelet α-granule biogenesis. *Blood 106*, 4159-4166.

Lo, S. K., Burhop, K. E., Kaplan, J. E., and Malik, A. B. (1988). Role of platelets in maintenance of pulmonary vascular permeability to protein. *American Journal of Physiology - Heart and Circulatory Physiology 254*, H763-H771.

Long, M. W. (1998). Megakaryocyte differentiation events. *Seminars in Hematology 35*, 192-199.

Louache, F., Debili, N., Cramer, E., Breton-Gorius, J., and Vainchenker, W. (1991). Fibrinogen is not synthesized by human megakaryocytes. *Blood 77*, 311-316.

Ma, L., Perini, R., McKnight, W., Dicay, M., Klein, A., Hollenberg, M. D., and Wallace, J. L. (2005). Proteinase-activated receptors 1 and 4 counter-regulate endostatin and VEGF release from human platelets. *Proceedings of the National Academy of Sciences of the United States of America 102*, 216-220.

Maisch, P. A., and Calderone, R. A. (1980). Adherence of Candida albicans to a fibrin-platelet matrix formed in vitro. *Infection and Immunity 27*, 650-656.

Mandon, E. C., Ehses, I., Rother, J., van Echten, G., and Sandhoff, K. (1992). Subcellular localization and membrane topology of serine palmitoyltransferase, 3-dehydrosphinganine reductase, and sphinganine N-acyltransferase in mouse liver. *Journal of Biological Chemistry 267*, 11144-11148.

Mao, C., and Obeid, L. M. (2008). Ceramidases: regulators of cellular responses mediated by ceramide, sphingosine, and sphingosine-1-phosphate. *Biochimica et Biophysica Acta (BBA) - Molecular and Cell Biology of Lipids 1781*, 424-434.

Marchesini, N., and Hannun, Y. A. (2004). Acid and neutral sphingomyelinases: roles and mechanisms of regulation. *Biochemistry and Cell Biology 82*, 27-44.

Masliah-Planchon, J., Darnige, L., and Bellucci, S. (2013). Molecular determinants of platelet delta storage pool deficiencies: an update. *British Journal of Haematology 160*, 5-11.

Massberg, S., Enders, G., Leiderer, R., Eisenmenger, S., Vestweber, D., Krombach, F., and Messmer, K. (1998). Platelet-Endothelial Cell Interactions During Ischemia/Reperfusion: The Role of P-Selectin. *Blood 92*, 507-515.

Mattie, M., Brooker, G., and Spiegel, S. (1994). Sphingosine-1-phosphate, a putative second messenger, mobilizes calcium from internal stores via an inositol trisphosphate-independent pathway. *Journal of Biological Chemistry 269*, 3181-3188.

May, A. E., Seizer, P., and Gawaz, M. (2008). Platelets: Inflammatory Firebugs of Vascular Walls. *Arteriosclerosis, Thrombosis, and Vascular Biology 28*, s5-s10.

Maynard, D. M., Heijnen, H. F. G., Gahl, W. A., and Gunay-Aygun, M. (2010). The α-granule proteome: novel proteins in normal and ghost granules in gray platelet syndrome. *Journal of Thrombosis and Haemostasis 8*, 1786-1796.

Maynard, D. M., Heijnen, H. F. G., Horne, M. K., White, J. G., and Gahl, W. A. (2007). Proteomic analysis of platelet α-granules using mass spectrometry. *Journal of Thrombosis and Haemostasis 5*, 1945-1955.

McConnell, H. M., and Kornberg, R. D. (1971). Inside-outside transitions of phospholipids in vesicle membranes. *Biochemistry 10*, 1111-1120.

McMorran, B. J., Marshall, V. M., de Graaf, C., Drysdale, K. E., Shabbar, M., Smyth, G. K., Corbin, J. E., Alexander, W. S., and Foote, S. J. (2009). Platelets Kill Intraerythrocytic Malarial Parasites and Mediate Survival to Infection. *Science 323*, 797-800.

McNicholas, C. M., Guggino, W. B., Schwiebert, E. M., Hebert, S. C., Giebisch, G., and Egan, M. E. (1996). Sensitivity of a renal K+ channel (ROMK2) to the inhibitory sulfonylurea compound glibenclamide is enhanced by coexpression with the ATP-binding cassette transporter cystic fibrosis transmembrane regulator. *Proceedings of the National Academy of Sciences 93*, 8083-8088.

McNicol, A., and Israels, S. J. (1999). Platelet Dense Granules: Structure, Function and Implications for Haemostasis. *Thrombosis Research 95*, 1-18.

Metzelaar, M., and Nieuwenhuis, H. (1991). Identity of Pltgp40 and lysomal integral membrane protein-CD63 [letter; comment]. *Blood 78*, 534-535.

Middelkoop, E., Van der Hoek, E. E., Bevers, E. M., Comfurius, P., Slotboom, A. J., Op den Kamp, J. A. F., Lubin, B. H., Zwaal, R. F. A., and Roelofsen, B. (1989). Involvement of ATP-dependent aminophospholipid translocation in maintaining phospholipid asymmetry in diamide-treated human erythrocytes. *Biochimica et Biophysica Acta (BBA) - Biomembranes 981*, 151-160.

Mitra, P., Oskeritzian, C. A., Payne, S. G., Beaven, M. A., Milstien, S., and Spiegel, S. (2006). Role of ABCC1 in export of sphingosine-1-phosphate from mast cells. *Proceedings of the National Academy of Sciences 103*, 16394-16399.

Mizugishi, K., Yamashita, T., Olivera, A., Miller, G. F., Spiegel, S., and Proia, R. L. (2005). Essential Role for Sphingosine Kinases in Neural and Vascular Development. *Molecular and Cellular Biology 25*, 11113-11121.

Mori, K., Suzuki, S., and Sugai, K. (1984). Electron Microscopic and Functional Studies on Platelets in Gray Platelet Syndrome. *The Tohoku Journal of Experimental Medicine 143*, 261-287.

Motohashi, K., Shibata, S., Ozaki, Y., Yatomi, Y., and Igarashi, Y. (2000). Identification of lysophospholipid receptors in human platelets: the relation of two agonists, lysophosphatidic acid and sphingosine 1-phosphate. *FEBS Letters 468*, 189-193.

Moulin, V., Lawny, F., Barritault, D., and Caruelle, J. P. (1998). Platelet releasate treatment improves skin healing in diabetic rats through endogenous growth factor secretion. *Cellular and molecular biology (Noisy-le-Grand, France) 44*, 961-971.

Murata, T., Ushikubi, F., Matsuoka, T., Hirata, M., Yamasaki, A., Sugimoto, Y., Ichikawa, A., Aze, Y., Tanaka, T., Yoshida, N*., et al.* (1997). Altered pain perception and inflammatory response in mice lacking prostacyclin receptor. *Nature 388*, 678-682.

Niiya, K., Hodson, E., Bader, R., Byers-Ward, V., Koziol, J., Plow, E., and Ruggeri, Z. (1987). Increased surface expression of the membrane glycoprotein IIb/IIIa complex induced by platelet activation. Relationship to the binding of fibrinogen and platelet aggregation. *Blood 70*, 475-483.

Nishibori, M., Cham, B., McNicol, A., Shalev, A., Jain, N., and Gerrard, J. M. (1993). The protein CD63 is in platelet dense granules, is deficient in a patient with Hermansky-Pudlak syndrome, and appears identical to granulophysin. *The Journal of Clinical Investigation 91*, 1775-1782.

Nishizuka, Y. (1992). Intracellular Signaling by Hydrolysis of Phospholipids and Activation of Protein Kinase C. *Science 258*, 607-614.

Nurden, A., and Nurden, P. (2011). Advances in our understanding of the molecular basis of disorders of platelet function. *Journal of Thrombosis and Haemostasis 9*, 76-91.

Nurden, A. T., and Nurden, P. (2007). The gray platelet syndrome: Clinical spectrum of the disease. *Blood Reviews 21*, 21-36.

Nurden, A. T., Nurden, P., Sanchez, M., Andia, I., and Anitua, E. (2008). Platelets and wound healing. *Frontiers in bioscience : a journal and virtual library 13*, 3532-3548.

Nurden, P., Jandrot-Perrus, M., Combrié, R., Winckler, J., Arocas, V., Lecut, C., Pasquet, J.-M., Kunicki, T. J., and Nurden, A. T. (2004). Severe deficiency of glycoprotein VI in a patient with gray platelet syndrome. *Blood 104*, 107-114.

Offermanns, S., Laugwitz, K. L., Spicher, K., and Schultz, G. (1994). G proteins of the G12 family are activated via thromboxane A2 and thrombin receptors in human platelets. *Proceedings of the National Academy of Sciences 91*, 504-508.

Offermanns, S., Toombs, C. F., Hu, Y.-H., and Simon, M. I. (1997). Defective platelet activation in G[alpha]q-deficient mice. *Nature 389*, 183-186.

Okajima, F. (2002). Plasma lipoproteins behave as carriers of extracellular sphingosine 1-phosphate: is this an atherogenic mediator or an anti-atherogenic mediator? *Biochimica et Biophysica Acta (BBA) - Molecular and Cell Biology of Lipids 1582*, 132-137.

Olivera, A., and Spiegel, S. (1993). Sphingosine-1-phosphate as second messenger in cell proliferation induced by PDGF and FCS mitogens. *Nature 365*, 557-560.

Osborne, N., Brand-Arzamendi, K., Ober, E. A., Jin, S.-W., Verkade, H., Holtzman, N. G., Yelon, D., and Stainier, D. Y. R. (2008). The Spinster Homolog, Two of Hearts, Is Required for Sphingosine 1-Phosphate Signaling in Zebrafish. *Current biology : CB 18*, 1882-1888.

Pappu, R., Schwab, S. R., Cornelissen, I., Pereira, J. P., Regard, J. B., Xu, Y., Camerer, E., Zheng, Y.-W., Huang, Y., Cyster, J. G., and Coughlin, S. R. (2007). Promotion of Lymphocyte Egress into Blood and Lymph by Distinct Sources of Sphingosine-1-Phosphate. *Science 316*, 295-298.

Patel, S. R., Hartwig, J. H., and Italiano, J. E. (2005). The biogenesis of platelets from megakaryocyte proplatelets. *The Journal of Clinical Investigation 115*, 3348-3354.

Paty, P. S., Sherman, P. F., Shepard, J. M., Malik, A. B., and Kaplan, J. E. (1992). Role of adenosine in platelet-mediated reduction in pulmonary vascular permeability. *American Journal of Physiology - Heart and Circulatory Physiology 262*, H771-H777.

Payen, L., Delugin, L., Courtois, A., Trinquart, Y., Guillouzo, A., and Fardel, O. (2001). The sulphonylurea glibenclamide inhibits multidrug resistance protein (MRP1) activity in human lung cancer cells. *British Journal of Pharmacology 132*, 778-784.

Perollet, C., Han, Z. C., Savona, C., Caen, J. P., and Bikfalvi, A. (1998). Platelet Factor 4 Modulates Fibroblast Growth Factor 2 (FGF-2) Activity and Inhibits FGF-2 Dimerization. *Blood 91*, 3289-3299.

Peters, C. G., Michelson, A. D., and Flaumenhaft, R. (2012). Granule exocytosis is required for platelet spreading: differential sorting of α-granules expressing VAMP-7. *Blood 120*, 199-206.

Pinedo, H. M., Verheul, H. M. W., D'Amato, R. J., and Folkman, J. (1998). Involvement of platelets in tumour angiogenesis? *The Lancet 352*, 1775-1777.

Polgár, J., Chung, S.-H., and Reed, G. L. (2002). Vesicle-associated membrane protein 3 (VAMP-3) and VAMP-8 are present in human platelets and are required for granule secretion. *Blood 100*, 1081-1083.

Polgár, J., Lane, W. S., Chung, S.-H., Houng, A. K., and Reed, G. L. (2003). Phosphorylation of SNAP-23 in Activated Human Platelets. *Journal of Biological Chemistry 278*, 44369-44376.

Pomorski, T., Holthuis, J. C. M., Herrmann, A., and van Meer, G. (2004). Tracking down lipid flippases and their biological functions. *Journal of Cell Science 117*, 805-813.

Pomorski, T., Hrafnsdóttir, S., Devaux, P. F., and Meer, G. v. (2001). Lipid distribution and transport across cellular membranes. *Seminars in Cell & Developmental Biology 12*, 139-148.

Qureshi, A. H., Chaoji, V., Maiguel, D., Faridi, M. H., Barth, C. J., Salem, S. M., Singhal, M., Stoub, D., Krastins, B., Ogihara, M.*, et al.* (2009). Proteomic and Phospho-Proteomic Profile of Human Platelets in Basal, Resting State: Insights into Integrin Signaling. *PLoS ONE 4*, e7627.

Redondo, P. C., Harper, A. G. S., Salido, G. M., Pariente, J. A., Sage, S. O., and Rosado, J. A. (2004). A role for SNAP-25 but not VAMPs in store-mediated Ca2+ entry in human platelets. *The Journal of Physiology 558*, 99-109.

Ren, Q., Barber, H. K., Crawford, G. L., Karim, Z. A., Zhao, C., Choi, W., Wang, C.-C., Hong, W., and Whiteheart, S. W. (2007). Endobrevin/VAMP-8 Is the Primary v-SNARE for the Platelet Release Reaction. *Molecular Biology of the Cell* 18, 24-33.

Ren, Q., Wimmer, C., Chicka, M. C., Ye, S., Ren, Y., Hughson, F. M., and Whiteheart, S. W. (2010). Munc13-4 is a limiting factor in the pathway required for platelet granule release and hemostasis. *Blood* 116, 869-877.

Ren, Q., Ye, S., and Whiteheart, S. W. (2008). The platelet release reaction: just when you thought platelet secretion was simple. *Current Opinion in Hematology* 15, 537-541 510.1097/MOH.1090b1013e328309ec328374.

Rendu, F., and Brohard-Bohn, B. (2001). The platelet release reaction: granules' constituents, secretion and functions. *Platelets* 12, 261-273.

Rosen, H., and Goetzl, E. J. (2005). Sphingosine 1-phosphate and its receptors: an autocrine and paracrine network. *Nat Rev Immunol* 5, 560-570.

Russel, F. G. M., Koenderink, J. B., and Masereeuw, R. (2008). Multidrug resistance protein 4 (MRP4/ABCC4): a versatile efflux transporter for drugs and signalling molecules. *Trends in Pharmacological Sciences* 29, 200-207.

Salazar, G., Falcon-Perez, J. M., Harrison, R., and Faundez, V. (2009). SLC30A3 (ZnT3) Oligomerization by Dityrosine Bonds Regulates Its Subcellular Localization and Metal Transport Capacity. *PLoS ONE* 4, e5896.

Sasaki, M., Shoji, A., Kubo, Y., Nada, S., and Yamaguchi, A. (2003). Cloning of rat ABCA7 and its preferential expression in platelets. *Biochemical and Biophysical Research Communications* 304, 777-782.

Sato, K., Malchinkhuu, E., Horiuchi, Y., Mogi, C., Tomura, H., Tosaka, M., Yoshimoto, Y., Kuwabara, A., and Okajima, F. (2007). Critical role of ABCA1 transporter in sphingosine 1-phosphate release from astrocytes. *Journal of Neurochemistry* 103, 2610-2619.

Schaphorst, K. L., Chiang, E., Jacobs, K. N., Zaiman, A., Natarajan, V., Wigley, F., and Garcia, J. G. N. (2003). Role of sphingosine-1 phosphate in the enhancement of endothelial barrier integrity by platelet-released products. *American Journal of Physiology - Lung Cellular and Molecular Physiology* 285, L258-L267.

Scheuerer, B., Ernst, M., Dürrbaum-Landmann, I., Fleischer, J., Grage-Griebenow, E., Brandt, E., Flad, H.-D., and Petersen, F. (2000). The CXC-chemokine platelet factor 4

promotes monocyte survival and induces monocyte differentiation into macrophages. **Blood** *95*, 1158-1166.

Schiavo, G., Matteoli, M., and Montecucco, C. (2000). Neurotoxins Affecting Neuroexocytosis. **Physiological Reviews** *80*, 717-766.

Schraw, T. D., Rutledge, T. W., Crawford, G. L., Bernstein, A. M., Kalen, A. L., Pessin, J. E., and Whiteheart, S. W. (2003). Granule stores from cellubrevin/VAMP-3 null mouse platelets exhibit normal stimulus-induced release. **Blood** *102*, 1716-1722.

Schwanstecher, M., Sieverding, C., Dorschner, H., Gross, I., Aguilar-Bryan, L., Schwanstecher, C., and Bryan, J. (1998). Potassium channel openers require ATP to bind to and act through sulfonylurea receptors. **EMBO J** *17*, 5529-5535.

Sehgal, S., and Storrie, B. (2007). Evidence that differential packaging of the major platelet granule proteins von Willebrand factor and fibrinogen can support their differential release. **Journal of Thrombosis and Haemostasis** *5*, 2009-2016.

Senis, Y., and García, Á. (2012). Platelet Proteomics: State of the Art and Future Perspective. In Platelets and Megakaryocytes, J.M. Gibbins, and M.P. Mahaut-Smith, eds. (Springer New York), pp. 367-399.

Senzel, L., Gnatenko, D. V., and Bahou, W. F. (2009). The platelet proteome. **Current Opinion in Hematology** *16*, 329-333 310.1097/MOH.1090b1013e32832e32839dc32836.

Serhan, C. N., and Savill, J. (2005). Resolution of inflammation: the beginning programs the end. **Nat Immunol** *6*, 1191-1197.

Shapiro, M. J., Weiss, E. J., Faruqi, T. R., and Coughlin, S. R. (2000). Protease-activated Receptors 1 and 4 Are Shut Off with Distinct Kinetics after Activation by Thrombin. **Journal of Biological Chemistry** *275*, 25216-25221.

Shepro, D., Welles, S. L., and Hechtman, H. B. (1984). Vasoactive agonists prevent erythrocyte extravasation in thrombocytopenic hamsters. **Thrombosis Research** *35*, 421-430.

Shirakawa, R., Higashi, T., Kondo, H., Yoshioka, A., Kita, T., and Horiuchi, H. (2005). Purification and Functional Analysis of a Rab27 Effector Munc13 Using a Semiintact Platelet Dense-Granule Secretion Assay. In Methods in Enzymology, C.J.D. William E. Balch, and H. Alan, eds. (Academic Press), pp. 778-788.

Simons, K., and Ikonen, E. (1997). Functional rafts in cell membranes. **Nature** *387*, 569-572.

Sollner, T., Whiteheart, S. W., Brunner, M., Erdjument-Bromage, H., Geromanos, S., Tempst, P., and Rothman, J. E. (1993). SNAP receptors implicated in vesicle targeting and fusion. *Nature 362*, 318-324.

Spiegel, S., and Milstien, S. (2002). Sphingosine 1-Phosphate, a Key Cell Signaling Molecule. *Journal of Biological Chemistry 277*, 25851-25854.

Spiegel, S., and Milstien, S. (2003). Sphingosine-1-phosphate: an enigmatic signalling lipid. *Nat Rev Mol Cell Biol 4*, 397-407.

Stalker, T. J., Traxler, E. A., Wu, J., Wannemacher, K. M., Cermignano, S. L., Voronov, R., Diamond, S. L., and Brass, L. F. (2013). Hierarchical organization in the hemostatic response and its relationship to the platelet-signaling network. *Blood 121*, 1875-1885.

Stenberg, P. E., Barrie, R. J., Pestina, T. I., Steward, S. A., Arnold, J. T., Murti, A. K., Hutson, N. K., and Jackson, C. W. (1998). Prolonged Bleeding Time With Defective Platelet Filopodia Formation in the Wistar Furth Rat. *Blood 91*, 1599-1608.

Stenberg, P. E., McEver, R. P., Shuman, M. A., Jacques, Y. V., and Bainton, D. F. (1985). A platelet alpha-granule membrane protein (GMP-140) is expressed on the plasma membrane after activation. *The Journal of Cell Biology 101*, 880-886.

Sutton, R. B., Fasshauer, D., Jahn, R., and Brunger, A. T. (1998). Crystal structure of a SNARE complex involved in synaptic exocytosis at 2.4[thinsp]A resolution. *Nature 395*, 347-353.

Suzuki, H., Murasaki, K., Kodama, K., and Takayama, H. (2003). Intracellular localization of glycoprotein VI in human platelets and its surface expression upon activation. *British Journal of Haematology 121*, 904-912.

Tafesse, F. G., Ternes, P., and Holthuis, J. C. M. (2006). The Multigenic Sphingomyelin Synthase Family. *Journal of Biological Chemistry 281*, 29421-29425.

Tang, Y.-Q., Yeaman, M. R., and Selsted, M. E. (2002). Antimicrobial Peptides from Human Platelets. *Infection and Immunity 70*, 6524-6533.

Tani, M., Sano, T., Ito, M., and Igarashi, Y. (2005). Mechanisms of sphingosine and sphingosine 1-phosphate generation in human platelets. *Journal of Lipid Research 46*, 2458-2467.

Thon, J., and Italiano, J. (2012). Platelets: Production, Morphology and Ultrastructure. In Antiplatelet Agents, P. Gresele, G.V.R. Born, C. Patrono, and C.P. Page, eds. (Springer Berlin Heidelberg), pp. 3-22.

Tomer, A., Harker, L., and Burstein, S. (1987). Purification of human megakaryocytes by fluorescence-activated cell sorting. *Blood 70*, 1735-1742.

Tomer, A., Harker, L., and Burstein, S. (1988). Flow cytometric analysis of normal human megakaryocytes. *Blood 71*, 1244-1252.

Tornhamre, S., Sjölinder, M., Lindberg, Å., Ericsson, I., Näsman-Glaser, B., Griffiths, W. J., and Lindgren, J. Å. (1998). Demonstration of leukotriene-C4 synthase in platelets and species distribution of the enzyme activity. *European Journal of Biochemistry 251*, 227-235.

Ulrych, T., BÖHm, A., Polzin, A., Daum, G., NÜSing, R. M., Geisslinger, G., Hohlfeld, T., SchrÖR, K., and Rauch, B. H. (2011). Release of sphingosine-1-phosphate from human platelets is dependent on thromboxane formation. *Journal of Thrombosis and Haemostasis 9*, 790-798.

Umezu-Goto, M., Kishi, Y., Taira, A., Hama, K., Dohmae, N., Takio, K., Yamori, T., Mills, G. B., Inoue, K., Aoki, J., and Arai, H. (2002). Autotaxin has lysophospholipase D activity leading to tumor cell growth and motility by lysophosphatidic acid production. *The Journal of Cell Biology 158*, 227-233.

Urban, D., Li, L., Christensen, H., Pluthero, F. G., Chen, S. Z., Puhacz, M., Garg, P. M., Lanka, K. K., Cummings, J. J., Kramer, H*., et al.* (2012). The VPS33B binding protein VPS16B is required in megakaryocyte and platelet α-granule biogenesis. *Blood*.

Valentijn, K. M., van Driel, L. F., Mourik, M. J., Hendriks, G.-J., Arends, T. J., Koster, A. J., and Valentijn, J. A. (2010). Multigranular exocytosis of Weibel-Palade bodies in vascular endothelial cells. *Blood 116*, 1807-1816.

van Nispen tot Pannerden, H., de Haas, F., Geerts, W., Posthuma, G., van Dijk, S., and Heijnen, H. F. G. (2010). The platelet interior revisited: electron tomography reveals tubular α-granule subtypes. *Blood 116*, 1147-1156.

Venkataraman, K., Lee, Y.-M., Michaud, J., Thangada, S., Ai, Y., Bonkovsky, H. L., Parikh, N. S., Habrukowich, C., and Hla, T. (2008). Vascular Endothelium As a Contributor of Plasma Sphingosine 1-Phosphate. *Circulation Research 102*, 669-676.

von Hundelshausen, P., and Weber, C. (2007). Platelets as Immune Cells: Bridging Inflammation and Cardiovascular Disease. *Circulation Research 100*, 27-40.

Vu, T.-K. H., Wheaton, V. I., Hung, D. T., Charo, I., and Coughlin, S. R. (1991). Domains specifying thrombin-receptor interaction. *Nature 353*, 674-677.

Weber, T., Zemelman, B. V., McNew, J. A., Westermann, B., Gmachl, M., Parlati, F., Söllner, T. H., and Rothman, J. E. (1998). SNAREpins: Minimal Machinery for Membrane Fusion. *Cell 92*, 759-772.

Weltermann, A., Wolzt, M., Petersmann, K., Czerni, C., Graselli, U., Lechner, K., and Kyrle, P. A. (1999). Large Amounts of Vascular Endothelial Growth Factor at the Site of Hemostatic Plug Formation In Vivo. *Arteriosclerosis, Thrombosis, and Vascular Biology 19*, 1757-1760.

White, J. G. (1968). The dense bodies of human platelets. Origin of serotonin storage particles from platelet granules. *The American Journal of Pathology 53*, 791-808.

White, J. G. (1969). The Dense Bodies of Human Platelets: Inherent Electron Opacity of the Serotonin Storage Particles. *Blood 33*, 598-606.

White, J. G., and Gerrard, J. M. (1976). Ultrastructural features of abnormal blood platelets. A review, Vol 83).

Woulfe, D., Jiang, H., Mortensen, R., Yang, J., and Brass, L. F. (2002). Activation of Rap1B by Gi Family Members in Platelets. *Journal of Biological Chemistry 277*, 23382-23390.

Yang, J., Wu, J., Jiang, H., Mortensen, R., Austin, S., Manning, D. R., Woulfe, D., and Brass, L. F. (2002). Signaling through Gi Family Members in Platelets: REDUNDANCY AND SPECIFICITY IN THE REGULATION OF ADENYLYL CYCLASE AND OTHER EFFECTORS. *Journal of Biological Chemistry 277*, 46035-46042.

Yang, J., Wu, J., Kowalska, M. A., Dalvi, A., Prevost, N., O'Brien, P. J., Manning, D., Poncz, M., Lucki, I., Blendy, J. A., and Brass, L. F. (2000). Loss of signaling through the G protein, Gz, results in abnormal platelet activation and altered responses to psychoactive drugs. *Proceedings of the National Academy of Sciences 97*, 9984-9989.

Yang, L., Yatomi, Y., Miura, Y., Satoh, K., and Ozaki, Y. (1999a). Metabolism and functional effects of sphingolipids in blood cells. *British Journal of Haematology 107*, 282-293.

Yang, L., Yatomi, Y., Satoh, K., Igarashi, Y., and Ozaki, Y. (1999b). Sphingosine 1-Phosphate Formation and Intracellular Ca2+ Mobilization in Human Platelets: Evaluation with Sphingosine Kinase Inhibitors. *Journal of Biochemistry 126*, 84-89.

Yatomi, Y., Ohmori, T., Rile, G., Kazama, F., Okamoto, H., Sano, T., Satoh, K., Kume, S., Tigyi, G., Igarashi, Y., and Ozaki, Y. (2000). Sphingosine 1-phosphate as a major bioactive lysophospholipid that is released from platelets and interacts with endothelial cells. *Blood 96*, 3431-3438.

Yatomi, Y., Ozaki, Y., Ohmori, T., and Igarashi, Y. (2001). Sphingosine 1-phosphate: synthesis and release. *Prostaglandins & Other Lipid Mediators* *64*, 107-122.

Yatomi, Y., Ruan, F., Hakomori, S., and Igarashi, Y. (1995). Sphingosine-1-phosphate: a platelet-activating sphingolipid released from agonist-stimulated human platelets. *Blood* *86*, 193-202.

Yatomi, Y., Yamamura, S., Ruan, F., and Igarashi, Y. (1997). Sphingosine 1-Phosphate Induces Platelet Activation through an Extracellular Action and Shares a Platelet Surface Receptor with Lysophosphatidic Acid. *Journal of Biological Chemistry* *272*, 5291-5297.

Ye, S., Karim, Z. A., Al Hawas, R., Pessin, J. E., Filipovich, A. H., and Whiteheart, S. W. (2012). Syntaxin-11, but not syntaxin-2 or syntaxin-4, is required for platelet secretion. *Blood* *120*, 2484-2492.

Zucker-Franklin, D., Seremetis, S., and Zheng, Z. (1990). Internalization of human immunodeficiency virus type I and other retroviruses by megakaryocytes and platelets. *Blood* *75*, 1920-1923.

Place of Birth: Hyderabad, Andhra Pradesh, India

Education

July 2008 – Present: Ph.D. Candidate in Molecular and Cellular Biochemistry, University of Kentucky College of Medicine, Lexington, Kentucky, USA.

August 2007 – June 2008: Ph.D. Candidate in Integrated Biomedical Sciences Program, University of Kentucky, Lexington, Kentucky, USA.

June 2004 – April 2006: M.Sc. in Biochemistry, University of Hyderabad, Hyderabad, India.

June 2001 – April 2004: B.Sc. (Biotechnology, Biochemistry and Chemistry), Aurora Degree College, Hyderabad, India.

Professional activities

May 2012 – Present: Member of Pain Journal Club, Pain research group, UK, Lexington, KY.

Fall 2010 – Spring 2012: Co-chair of the student-run data club, Department of Biochemistry, UK.

Fall 2008 – Spring 2009: Graduate Teaching Assistant in Department of Molecular and Cellular Biochemistry, University of Kentucky, Lexington, KY.

Fall 2008 – Present: Member of Blood Journal Club, Platelet Research Group, UK, Lexington, KY.

April 2006 – June 2006: Summer research volunteer in the lab of Dr. Krishnaveni Mishra, Department of Biochemistry, University of Hyderabad, Hyderabad, India.

April 2005 – June 2005: Summer research volunteer at Barawale Research Foundation, Hyderabad, India.

Awards

2012 Graduate Travel Award, University of Kentucky, Lexington, KY

2011 Max Steckler Award, University of Kentucky, Lexington, KY

2009 Graduate Travel Award, University of Kentucky, Lexington, KY

2009 Graduate Travel Award, the National Meeting of American Society of Biochemistry and Molecular Biology, New Orleans, LA

Peer reviewed publication

Jonnalagadda D, Izu L, and Whiteheart SW. Platelet Secretion is Kinetically Heterogeneous, but not Thematic (***Blood,*** *2012*)

Jonnalagadda D, Sunkara M, Morris AJ, and Whiteheart SW. (2012) Release of Sphingosine-1-Phosphate from Platelets (in preparation)

Abstracts and presentations

Jonnalagadda D, Sunkara M, Morris AJ, and Whiteheart SW. Platelet Secretion – Release of Sphingosine-1-Phosphate. Mid-West Platelet Conference, Case Western Reserve University, Cleveland, Ohio, October 2012.

Jonnalagadda D, Sunkara M, Morris AJ, and Whiteheart SW. Mechanism of S1P Release from Platelets. Gill Heart Cardiovascular Research Day, Lexington, KY, October 2012.

Jonnalagadda D, Sunkara M, Morris AJ, and Whiteheart SW. Mechanism of S1P Release from Platelets. Vasculata (NAVBO), Nashville, TN, July 2012.

Jonnalagadda D, Sunkara M, Morris AJ, and Whiteheart SW. Mechanism of S1P Release from Platelets. Gill Heart Cardiovascular Research Day, Lexington, KY, October 2011.

Jonnalagadda D, Izu L, and Whiteheart SW. Platelet Secretion is Kinetically Heterogeneous, Not Thematic. Molecular and Cellular Biochemistry Retreat, Corbin, KY, May 2011

Jonnalagadda D, Izu L, and Whiteheart SW. Heterogeneity in Platelet Secretion. Gill Heart Cardiovascular Research Day, Lexington, KY, October 2010

Jonnalagadda D, Izu L, and Whiteheart SW. Heterogeneity in Platelet Secretion. Mid-West Platelet Conference at Chapel Hill, UNC, October 2010

Jonnalagadda D, Izu L, and Whiteheart SW. Heterogeneity in Platelet Secretion. Molecular and Cellular Biochemistry Retreat, Corbin, KY, May 2009

Jonnalagadda D, Izu L, and Whiteheart SW. Heterogeneity in Platelet Secretion. ASBMB, New Orleans, LA, May 2009

Jonnalagadda D, Izu L, and Whiteheart SW. Heterogeneity in Platelet Secretion. Molecular and Cellular Biochemistry Retreat, Pineville, KY, July 2008

Jonnalagadda D, Izu L, and Whiteheart SW. Heterogeneity in Platelet Secretion. Gill Heart Cardiovascular Research Day, Lexington, KY, October 2008

Jonnalagadda D, Izu L, and Whiteheart SW. Heterogeneity in Platelet Secretion. Mid-West Platelet Conference, UK, Lexington, KY, October 2008

Jonnalagadda D and Mitra CK. Covalent coupling of glucose oxidase on gold nanoparticles. International symposium "Nano-Bio Interface". University of Kolkata, Kolkata, India, 2006

Deepa Jonnalagadda

04/30/2013